Maria do Carmo Castro Henriques de Castro Fraga

Mestre em Engenharia Química e Bioquímica

PILOT SCALE MEMBRANE FILTRATION AND DEVELOPMENT OF A PHOTOCATALYTIC MEMBRANE REACTOR FOR TREATMENT OF OLIVE MILL WASTEWATERS

Dissertação para obtenção do Grau de Doutor em
Engenharia Química e Bioquímica – Especialidade em
Engenharia Química

Orientadora: Doutora Vanessa Ranhada Pinto Jorge Pereira
Co-orientador: Professor Doutor João Paulo Serejo Goulão Crespo

Júri:

Presidente: Professora Doutora Maria Ascensão C.F. Miranda Reis
Arguentes: Doutora Lidietta Giorno
Professora Doutora Rosa Maria de Oliveira Quinta-Ferreira

Vogais: Professora Doutora Maria Ascensão C.F. Miranda Reis
Doutora Vanessa Ranhada Pinto Jorge Pereira
Engenheiro Paulo Garção Nunes

FACULDADE DE CIÊNCIAS E TECNOLOGIA
UNIVERSIDADE NOVA DE LISBOA

Setembro de 2018

Pilot scale membrane filtration and development of a photocatalytic membrane reactor for treatment of olive mill wastewaters

ACKNOWLEDGEMENTS

Ao finalizar esta etapa tão importante na minha vida queria, antes de mais, agradecer aos meus orientadores, a Doutora Vanessa Pereira e o Professor Doutor João Paulo Crespo. Obrigada pela oportunidade que me deram de fazer este Doutoramento, num tema que sempre gostei, e por toda a amizade que senti ao longo deste tempo. À Vanessa agradeço a presença e generosidade constante, o tantas vezes ter atrasado o seu trabalho para apoiar o meu, e sempre com um sorriso. Por me ter ensinado que, no trabalho e na vida, são as pequenas coisas que fazem a diferença. Agradeço todo o apoio científico, rigor, exigência e perfeccionismo, que me fizeram querer sempre fazer mais e melhor. Ao Professor João agradeço tudo o que me ensinou, desde os tempos das aulas faculdade. Foram essas aulas que suscitaram o meu interesse pela área das membranas. Não tenho palavras para agradecer todas as oportunidades que me deu e conhecimentos que me transmitiu, científicos e humanos. Apesar de ser uma referência na área de membranas, com uma enorme experiência e imensos conhecimentos, ouve sempre a perspetiva dos alunos com a maior simplicidade. Sou uma privilegiada por ter sido orientada por duas pessoas incríveis. Muito muito obrigada aos meus dois orientadores.

Muito obrigada à Grupeta do Almoço: à Mafalda Lopes, Rita Valério, Joana, Mafalda Cadima, Maria João e Jorge, com os quais partilhei ótimos momentos. É tão bom quando no trabalho temos amigos que partilham das nossas alegrias e nos ajudam nas inquietações. Muito obrigada a todo o grupo da FCT.

Agradeço à Teresa ter-me recebido tão bem no laboratório e a alegria que contagia quem está à sua volta. Obrigada a todo o grupo pela partilha de um dia-a-dia que foi sempre muito bom. Agradeço em especial à Sandra, que me introduziu nas dinâmicas do laboratório, e à Beatriz Oliveira, por fazer do laboratório um lugar tão bom (e arrumado!) para se trabalhar. Agradeço à Rosita toda a amizade e a disponibilidade que teve sempre para me ajudar com o meu trabalho. À minha amiga Bea, agradeço por animar os meus dias sempre com uma boa conversa e muita alegria!

Um enorme e especial obrigada à minha irmã Sofia e á minha amiga Inês. Fizemos o caminho juntas desde as aulas na faculdade, com tantos e tão bons momentos partilhados. Cada uma à sua maneira contribuiu de forma muito especial no meu percurso do doutoramento. Obrigada por terem estado e continuarem sempre presentes.

Muito obrigada à minha família, meus queridos Pais, Irmãos, Tios, Avó e Didi, pelo interesse que sempre demonstraram no meu trabalho, pela motivação que me deram e por estarem sempre presentes na minha vida. À minha Mãezinha muito obrigada pelo apoio, principalmente pelas vezes que ficou com os meus filhos para que eu pudesse trabalhar no meu doutoramento.

Ao Leonardo, meu marido, agradeço o apoio que me deu na decisão de fazer um Doutoramento e o muito interesse que sempre demonstrou naquilo que fiz. Por sempre me ter entusiasmado e

elogiado o meu trabalho. Obrigada principalmente por esta fase final, em que fez tudo o que conseguiu para que eu pudesse dedicar-me à escrita. Aos meus filhos queridos, Benedita, Salvador e Vicente, agradeço serem a minha motivação para fazer as coisas bem feitas e lhes dar um bom exemplo. Agradeço os sorrisos, gargalhadas e choros que me acompanharam nesta fase final enquanto trabalhava em casa e me serviram de verdadeira inspiração! Muito obrigada por fazerem de mim uma pessoa melhor.

Agradeço a Deus, porque sei que “tudo isto me é dado”.

ABSTRACT

The work developed in this thesis focused on optimizing membrane processes and in the development of a novel hybrid photocatalytic membrane reactor to treat olive mil wastewaters.

The traditional Mediterranean diet, known for being a rich and healthy diet, uses olive oil as its main source of fats. Therefore, in the Mediterranean region, there is an annual discharge of 30 million m^3 of the wastewaters produced by this industry into the environment. Olive mill wastewaters are a highly polluted effluent produced in olive oil industries, representing an environmental hazard if not treated properly. These effluents present low pH and a high concentration of solids, oil and organic compounds such as organic acids, lipids and alcohols. The presence of phenolic compounds hinders the biological treatment of these wastewaters.

Membrane separation processes stand out as promising treatment approaches and their application has expanded during recent decades for the treatment of wastewaters, as a result of increasingly stringent regulations in wastewater discharge and continuing improvements in membrane technology. However, wide acceptance of membrane processes by industries is limited by membrane fouling. Fouling is caused by the accumulation of rejected oil, suspended solids and other components of the wastewaters on the membrane surface and intrapore structure. Fouling results in flux decline and low membrane lifetime due to the need to perform frequent cleanings.

When compared with polymeric membranes, ceramic membranes present several advantages such as higher thermal stability, mechanical resistance and chemical resistance, and thus can be applied in extreme aggressive environmental conditions. These properties allow for a better control of membrane fouling since higher pressures can be employed during backpulse and backwash procedures, and cleanings can be performed with stronger chemicals, without compromising the membrane lifetime. In the present work, the treatment of the olive mill wastewaters was mostly performed with ultrafiltration ceramic membranes made of silicon carbide.

Different strategies to overcome the problem of fouling were studied: (a) the optimization of operating conditions, conducted under controlled pressure / controlled permeate flux, allowing for a sustainable performance, and the use of backpulse and backwash strategies at pilot scale and (b) the modification of the surface of the silicon carbide membranes to obtain a photocatalytic membrane with a lower molecular weight cut off and higher hydrophilicity.

The new photocatalytic membranes developed were obtained using a sol-gel process combining titanium dioxide, silicon dioxide and silicon carbide. These membranes proved to have photocatalytic activity and were thus tested in a new hybrid reactor. The extremely efficient removals of the compounds analyzed and the lower fouling potential observed, showed that the developed photocatalytic membranes and the novel hybrid reactor are highly promising solutions

to be used in the treatment of olive mill wastewaters, as well as in a variety of other wastewaters and water matrices.

Keywords: Olive mill wastewater, silicon carbide membranes, ultrafiltration, nanofiltration, titanium dioxide photocatalysis, submerged photocatalytic membrane reactor.

RESUMO

O trabalho desenvolvido nesta tese focou a otimização de processos de membranas e o desenvolvimento de um novo reator híbrido de membranas fotocatalíticas para o tratamento de águas ruças.

A dieta Mediterrânica, que é considerada rica e saudável, utiliza o azeite como principal fonte de gorduras. Consequentemente, na região do Mediterrâneo, há uma descarga anual de 30 milhões de m^3 do efluente produzido por esta indústria no meio ambiente. As águas ruças são um efluente altamente poluente produzido pela indústria do azeite, representando um risco ambiental se não forem tratados adequadamente. Estes efluentes apresentam baixo pH e alta concentração de sólidos, óleos e compostos orgânicos, como ácidos orgânicos, lípidos e álcoois. A presença de compostos fenólicos dificulta o tratamento biológico destas águas residuais.

Os processos de separação por membranas destacam-se como abordagens promissoras de tratamento e a sua aplicação expandiu-se durante as últimas décadas para o tratamento de águas residuais, como resultado de regulamentação cada vez mais rigorosa na descarga de efluentes e melhorias contínuas na tecnologia de membranas. No entanto, a aceitação dos processos de membrana é ainda limitada pelo risco de *fouling*, causado pela acumulação de óleo, sólidos suspensos e outros componentes das águas residuais na superfície da membrana e também na sua estrutura interna (intraporo). O *fouling* resulta num declínio de fluxo e reduz a vida útil da membrana, devido à necessidade de realizar lavagens químicas frequentes.

Quando comparadas com as membranas poliméricas, as membranas cerâmicas apresentam várias vantagens, tais como maior estabilidade térmica, resistência mecânica e resistência química, e, portanto, podem ser aplicadas em condições mais agressivas. Estas propriedades permitem um melhor controlo do *fouling* da membrana, uma vez que podem ser impostas pressões mais altas durante os procedimentos de *backpulse* e *backwash*, e as lavagens químicas podem ser realizadas com produtos químicos mais fortes, sem comprometer o tempo de vida da membrana. No presente trabalho, o tratamento dos efluentes do lagar de azeite foi realizado principalmente com membranas cerâmicas de ultrafiltração compostas por carboneto de silício.

Foram estudadas duas diferentes estratégias para minimizar o desenvolvimento de *fouling* na membrana: (a) a otimização das condições de operação, conduzidas sob pressão controlada / fluxo de permeado controlado, permitindo um desempenho sustentável e do uso de estratégias de *backpulse* e *backwash* à escala piloto e (b) a modificação da superfície das membranas de carboneto de silício para obter uma membrana fotocatalítica com um menor tamanho de poro e maior hidrofilicidade.

As novas membranas fotocatalíticas desenvolvidas foram produzidas utilizando um processo sol-gel combinando dióxido de titânio, dióxido de silício e carboneto de silício. Estas membranas

provaram ter atividade fotocatalítica e foram assim testadas num novo reator híbrido. As remoções extremamente eficientes dos compostos analisados e a menor formação de *fouling* observado mostraram que as membranas fotocatalíticas desenvolvidas e o novo reator híbrido são soluções altamente promissoras para o tratamento de águas ruças, bem como outros tipos de água residual e de consumo.

.

ABBREVIATIONS

AOPs – Advanced oxidation processes

BP - Backpulse

BW - Backwash

COD – Chemical oxygen demand

DAF – Dissolved air flotation

GG/MS – Gas chromatography–mass spectrometry

MF - Microfiltration

MWCO – Molecular weight cut-off

NaOH – Sodium hydroxide

NF – Nanofiltration

R_t – Total membrane resistance

R_m – Intrinsic membrane resistance

R_f – Resistance due to fouling

SEM – Scanning electron microscopy

SiO_2 – Silicon dioxide

SPME - Solid phase microextraction

TEOS - Tetraethyl orthosilicate

TiO_2 – Titanium dioxide

TTIP – *Titanium* (IV) *isopropoxide*

TMP – Transmembrane pressure

TOC – Total organic carbon

UF - Ultrafiltration

UV - Ultraviolet

VRF – Volume reduction factor

XPS - X-ray photoelectron spectroscopy

ZnO_2 – Zinc peroxide

CONTENTS

LIST OF FIGURES

LIST OF TABLES

1 INTRODUCTION

1.1 STATE OF THE ART

1.1.1 Mediterranean countries and olive oil production

The traditional Mediterranean diet, known for being a rich and healthy diet, uses olive oil as its main source of fats. Also olive oil is rich in specific phenolic compounds, that have been reported as very beneficial for human health [1]. Mediterranean Countries are responsible for 95% of the olive oil produced in the world, producing about 1.7 million tons of olive oil per year [2]. The production of olive oil employs a very significant number of people and is one of the main industrial activities in these Countries. Moreover, olive oil production has been expanding outside the Mediterranean area and is now an emerging activity in countries such as China, the USA, Australia and the Middle East [3].

1.1.2 Olive mill wastewaters

Due to the worldwide growth of the olive oil industry, the treatment and discharge of the produced wastewaters is becoming a global concern [4]. In the Mediterranean region, there is an annual discharge of 30 million m^3 olive mill wastewater into the environment [5, 6].

Olive mill wastewaters are highly charged effluents produced by olive oil industries [4], representing an environmental hazard if not treated properly. **Table 1.1** shows some of the main characteristics of olive mill wastewaters reported in the literature.

Table 1.1 *Composition of olive mill wastewaters*

Physico-chemical parameters	Literature Values
Total solids (mg/L)	99700 [7] 44000 [8] 63300 [9] 42400 – 101500 [10]
Total suspended solids (mg/L)	4520 [7] 2700 [8]
Total volatile solids (mg/L)	87200 [7] 33600 [8]
Total organic carbon (mg/L)	39800 [7] 34200 [11]
Chemical oxygen demand (mg/L O_2)	93000 [7] 67000 [8] 103000 [12] 178000 [13] 130000 [9] 89200 – 101500 [10]
Biochemical oxygen demand (mg/L O_2)	46000 [7] 55000 [8] 22800 – 23200 [10]
Total nitrogen (mg/L)	768 [7] 620 [8] 790 [12] 860 [9]
pH	4.8 [7] 4.93 [8] 4.8 [12] 5 [9] 5.4-5.5 [10]
Conductivity (mS/cm)	18 [7] 18 [8] 10 [9]
Carbohydrates (mg/L)	16100 [7] 4800 [8] 4700 [12]
Lipids (mg/L)	12000 [7] 2400 [13]
Polyphenols (mg/L)	10700 [7] 980 [8] 3800 [12]
Sodium (mg/L)	300 [7] 200 [13]
Calcium (mg/L)	270 [7] 200 [13]
Magnesium (mg/L)	44 [7] 92 [13]
Iron (mg/L)	120 [7] 18.3[13]
Copper (mg/L)	6 [7] 2.1 [13]
Manganese (mg/L)	12 [7] 1.5 [13]

These effluents present low pH and a high concentration of solids, oil and organic compounds such as organic acids, lipids and alcohols [5, 14].

Due to the high concentration of organic matter and phenolic compounds, that are responsible for the dark color and antimicrobial and phytotoxic effect of olive mill wastewaters, the traditional biological treatment becomes difficult [15-17], being necessary to study and develop new treatment processes.

1.1.3 Common practices and treatment processes

Land spreading and evaporation in lagoons are the most common practices of olive mill wastewater management [11, 18]. However, this practice may lead to serious impacts on environment due to the high acidity, antibacterial and phytotoxic properties of these effluents [19, 20]. On the other side, evaporation on lagoons has serious drawbacks such as low efficiency and sludge-disposal problems since it can only concentrate olive mill wastewater until 70-75% of its initial volume with no degradation of organic matter [21]. Moreover, this method requires a large area, produces bad odors, and may lead to pollutant infiltration to ground water and insect proliferation [22].

Conventional wastewater physical and chemical treatment approaches include coagulation, flocculation, sedimentation, and flotation. Coagulation and flocculation are commonly used treatment processes in water and wastewater treatment in which chemical compounds are added to the water in order to destabilize the colloidal materials/stable oil emulsified droplets and cause the small particles to agglomerate into larger settleable/floatable flocs that may be subsequently removed by sedimentation and flotation. This process was been studied to treat olive mill effluents with removals of chemical oxygen demand and phenolic compounds of 90% and 95%, respectively [18]. Flotation was also studied to integrate the treatment of olive mill wastewaters [10] and consists in increasing the density difference between the continuous and dispersed phases by adding a gas into the oily wastewater to promote the formation of air–solid or air–oil agglomerates with increased buoyancy, being used in the treatment of dispersed and emulsified oil in wastewaters.

Biodegradation is also an approach that has been studied for the treatment of olive mill effluents. However, the high concentration of organic matter and phenolic compounds has been described to hinder this process [15-17].

This problem and the need to achieve higher quality effluents have promoted the development of new processes for oily wastewater treatment such as membrane processes.

1.1.4 Pressure-driven membrane processes to treat olive mill wastewaters

The use of membrane processes for treatment of olive mill wastewater has been studied since the 1990s, having undergone a large increase at the beginning of this decade while the study of other simple processes tended to decrease [5].

It has gained interest due to more stringent regulations, translated into a demand for water with high quality as well as the increased awareness and need to reuse water [23, 24]. Membrane processes have been reported as highly efficient to treat stable emulsions, avoid chemical addition, produce a small amount of solids requiring disposal as well as achieve high chemical oxygen demand (COD) removal and overall higher quality of permeate produced. Moreover, these systems have a small footprint, easy operation and are easily combined with other treatment processes [25, 26].

Microfiltration, ultrafiltration and nanofiltration are widely studied as an integral part of the treatment of this effluent. Studies show that microfiltration can remove high extents of total suspended solids and oil and grease but the dissolved fraction of organic carbon needs a further treatment to be removed at satisfactory levels [27, 28]. Depending on the membrane characteristics, ultrafiltration can remove 20-50% of the total organic carbon [29, 30], 30-40% of chemical oxygen demand [31, 32] and can achieve removals near 50% of phenolic compounds [29]. If nanofiltration is used, removals higher than 80% of the mentioned parameters can be obtained [31, 32]. A work performed at industrial scale involving membrane processes allowed removals of 98% of organic load [33].

1.1.4.1 Ceramic membranes

The use of ceramic membranes recently increased, particularly in the treatment of industrial wastewaters, including food, pulp and paper, textile, petrochemicals and pharmaceutical industries [34]. Due to their advantages compared with polymeric membranes, such as better thermal stability, mechanical resistance and chemical resistance, ceramic membranes can be applied in extreme aggressive environmental conditions [35]. These properties allow for a better control of membrane fouling since higher pressures can be employed in backwashes and cleanings can be performed with stronger chemicals, without compromising the membrane lifetime [36].

Among several materials, alumina is often used as a support material for ceramic membranes due to its smooth surface, in contrast to other materials, and since it is fairly inert. On the other hand, it can be easily deposited in macroporous supports. However, alumina does not present high enough chemical or mechanical stability when subject to severe conditions. Silicon carbide (SiC) is a promising alternative material since it presents better resistance to chemicals, thus presenting advantages when strong and repeated cleanings are required [37, 38]. Even when

compared with polymeric and other ceramic membranes such as titania or zirconia, silicon carbide membranes present higher hydrophilicity and lower fouling tendency [39].

Ceramic membranes have been studied to treat olive mill wastewaters. Even though microfiltration using a TiO_2 membrane could not significantly remove phenolic compounds, a nanofiltration with a membrane made of the same material retained nearly 50% of phenolic compounds and 20% of the total organic carbon. However, this efficiency is low when compared with the results reported for polymeric membranes: in this case, polyphenols and total organic carbon can be removed in percentages higher than 90% [40]. On the other hand, microfiltration ceramic membranes can be extremely efficient for the removal of total suspended solids and oil and grease, achieving removals higher than 99% [27, 41, 42].

1.1.4.2 Membrane fouling

The development of fouling on the membrane is the main drawback of membrane processes, being a limiting factor in the use of this technology, particularly at industrial scale. Fouling is caused by the adsorption and accumulation of rejected oil, suspended solids and other components of the wastewaters on the membrane surface and within the intrapore structure [39]. The main consequence of fouling is flux decline, which leads to a decrease of permeate flux being higher pressures needed to maintain flux, with consequent higher energy consumption and operation costs [23].

1.1.4.2.1 Membrane cleaning and flux maintenance strategies

Although chemical cleaning methods are the most widely used in membrane cleaning, the chemical agents used may damage the membranes and reduce their lifetime. Furthermore, chemical cleaning methods generate waste solutions and have high costs associated [43].

The first approach that must be consider is to work below the critical flux which, minimizing the development of fouling [44]. Besides operating under optimum permeate flux conditions, different cleaning systems can be applied as flux maintenance strategies e.g. backpulses (BP), backwashes (BW), chemically enhanced backwashing (CEB) and cleaning in place (CIP). The goal of backpulses is to loosen membrane fouling through a negative transmembrane pressure (TMP) which is sufficient to penetrate into the inner channels. A great advantage of using backpulses is the low amount of permeate lost due to the short duration of the pulses. Frequent pulses are preferable because the initial impact of the pulse is considered determinant. When using ceramic membranes the backpulses are exceedingly efficient due to the low resistance in the porous matrix and due to the strength of the element. Nevertheless, frequent pulses need to be considered in the design of the membrane plant, as pressure oscillations may destabilize the

system. Backwashes use the shear from a reversed flowrate (the permeate is forced through the membrane towards the retentate side).

Some authors have already described the effect of backpulses and backwashes strategies in the development of fouling and, consequently, in the permeability of the membrane. The effect of backpulses and backwashes in the microfiltration of oil-in-water emulsions with ceramic membranes was already studied and reported. Results show that these strategies are efficient in fouling mitigation with no impact in the oil rejection [41, 42, 45]. From an economic point of view, a study comparing the microfiltration of emulsified crude oil with and without backpulses revealed that the process without backpulses is not economically viable when compared to conventional treatment methods. However, the same operation with regular backpulses resulted in lower costs of treated water when compared with conventional methods [46].

Despite the great advantages of performing backpulses and backwashes in order to minimize fouling, when the transmembrane pressure drops more than 15% compared to the initial transmembrane pressure after a backpulse or a backwash, chemical cleaning should be performed [47]. During the cleaning procedure, the filtration process is stopped and chemical solutions (e.g. sodium hydroxide, ultrasil® and citric acid solutions) are used to clean the membrane and remove chemically reversible fouling. While backpulses and backwashes are automatically carried out, chemical cleaning requires the presence of an operator and may take several hours. The frequency of cleanings and the type of chemicals to employ depend on the characteristics of the water but may vary between one time per week or per month [48, 49]. The composition of the cleaning solutions used should thus be defined in order to determine which chemicals and temperature levels should be employed to restore the permeability after filtration of different wastewaters. Pre-treatment of wastewater is often proposed to minimize the frequency of these procedures.

1.1.4.2.2 Modification of the membrane surface

Membrane performance, especially when treating wastewaters with high content of oil and grease, which is the case of olive mill wastewaters, is affected by surface hydrophilicity of the membrane. Hydrophobic solutes in the wastewater, such as emulsified oils, readily foul such membranes via strong hydrophobic interactions [50]. Therefore by improving the hydrophilicity of the membrane it is possible to reduce the development of fouling.

Several studies describe ways to increase the hydrophobicity of the membrane by modifying its surface, focusing on the use of nanoparticles. The use of nanoparticles enables the production of desired membrane structures and functionalities that allow a high degree of control over membrane fouling and achieving a high quality of permeate [51].

Among other materials, titanium dioxide (TiO_2) is the most studied due to its particular advantages, that includes its easy availability, low cost and high chemical stability in addition to its high oxidant capacity of the photogenerated holes, which gives a high photocatalytic activity to this nanoparticle [52]. Several publications report the superhydrophilic properties of membranes when TiO_2 is incorporated in their structure, especially in the presence of UV radiation [53-57]. In fact, TiO_2 surfaces become superhydrophilic with a contact angle of less than 5◦ when exposed to UV-light [58], originated by chemical composition changes on the surface [59].

The photocatalytic activity of TiO_2 has been also widely reported. TiO_2 is able to degrade a variety of organic compounds in the presence of UV radiation [52]. The photocatalytic process starts with the generation of conduction electrons and valence band holes as a consequence of the activation of TiO_2 by UV radiation with energy higher than its band gap energy. The photo induced hole can oxidize a donor molecule adsorbed on the TiO_2 surface and the electron in the conduction band can reduce an acceptor molecule. Thus, a variety of possible reactions can occur, that lead to the generation of superoxide and hydroxyl radicals. These radicals attack organic substrates initiating the process of photocatalytic oxidation [60, 61].

The use of TiO_2 photocatalysis to enhance the treatment of olive mill wastewaters has already been assessed. Badawy et al [62] studied the possibility of improving the biodegrability of this effluent for further treatment using TiO_2 photocatalysis obtaining positive results. The degradation of several phenolic compounds typically found in these wastewaters can also be achieved with TiO_2 photocatalysis [63], as well as the reduction of colored molecules and chemical oxygen demand [64].

1.1.4.3 Photocatalytic membrane reactors

Photocatalytic reactors have attracted attention for water and wastewater treatment since, using this technology, refractory organic and toxic pollutants present in water sources can be degraded into simple and harmless inorganic molecules, minimizing the use of chemicals and avoiding sludge production and its disposal. However, photocatalytic reactors present some drawbacks, including the catalyst-recovering step from the solution at the end of operation, that still need to be addressed before application at large scale [65-67]. Membrane technology can improve the implementation of photocatalysis by assuring the separation of the photocatalyst from the treated water [68].

TiO_2 photocatalysis can be performed in photocatalytic reactors with the photocatalyst in suspension or immobilized on a carrier and several schemes of photocatalytic membrane reactors have been described and extensively reviewed elsewhere [69, 70]. Regarding the membrane location, it can be placed outside in an external loop [71, 72] or submerged inside [73, 74] the photocatalytic reactor. In this case, the system is defined as submerged photocatalytic membrane

reactor. In the literature, most of the work published regarding the removal of organic compounds from water using submerged photocatalytic membrane reactors was performed with the photocatalyst in suspension.

When TiO_2 is in suspension, loss of TiO_2 due to adsorption to the system is expected [75]. Moreover, as previously mentioned, a further step is required in order to separate it from the treated water [69]. This step may also involve the use of a membrane. In addition, TiO_2 in suspension was reported to contribute to the fouling appearance on the membrane surface [76-78].

In this context, the immobilization of TiO_2 on the membrane surface is the best solution to combine the two processes, photocatalysis and membrane separation. Moreover, the immobilization of TiO_2 on the membrane surface showed to be useful in the mitigation of fouling [79-83].

The immobilization of TiO_2 on the membrane surface may be achieved by using a sol-gel technique. The sol-gel process consists of a chemical process (hydrolysis-condensation) involving a metal alkoxide (or semi metal) precursor with itself creating a three-dimensional continuous solid linkage, through a basic or acid catalysis process [84]. This process has been proposed to synthetize TiO_2-based photocatalysts with high oxidation efficiency as well as for TiO_2 immobilization in a large number of supports to control their porosity [85, 86].

1.2 OBJECTIVES

The main objectives of the work developed and presented in this thesis was: 1 - to enhance the treatment of olive mill wastewaters using different membrane processes and; 2 - the development of a novel hybrid photocatalytic membrane reactor.

A silicon carbide ultrafiltration ceramic membrane was chosen to perform this work due to the particular advantages of this material. This ceramic membrane was thoroughly characterized in terms of surface composition and morphology.

Two strategies were followed to improve the removal of the dissolved compounds to values acceptable by legislation [87] and minimize fouling: (a) pilot scale treatment by ultrafiltration after optimization of backpulses and backwashes, followed by nanofiltration and (b) development of photocatalytic membranes by sol-gel.

The final goal of this work was to develop a novel submerged photocatalytic membrane reactor that can be easily scaled up to test the photocatalytic membranes developed.

1.3 THESIS OUTLINE

The present work is, thus, organized in seven chapters.

Chapter 1 consists in a brief revision of the state-of-the-art, focused in the problem of olive mill wastewater treatment. Membrane processes (described in **Chapters 2 to 4**) and the development of hybrid systems combining membrane filtration with TiO_2 photocatalysis (described in **Chapters 5 and 6**) were addressed as these processes are an important part of the solution to overcome this problem.

Chapter 2 describes the exhaustive characterization and comparison in terms of surface composition, morphology and filtration performance of a commercially available membrane with a novel silicon carbide membrane produced by LiqTech with a single top layer. In this work, this membrane was validated to treat oily wastewater and proved to be extremely promising at laboratory scale to remove oil and grease and total suspended solids.

Chapter 3 presents the work developed at pilot scale using a tubular silicon carbide membrane to treat olive mill wastewaters under controlled constant permeate flux. The filtration conditions were evaluated and optimized in terms of the selection of the permeate flux and flux maintenance strategies employed—backpulses and backwashes—in order to reduce fouling formation. Membrane filtration using silicon carbide membranes was proven to be an effective alternative to dissolved air flotation and can be applied efficiently to remove total suspended solids and oil and grease from olive mill wastewaters. However, and even though good percent removals were obtained, the concentration of chemical oxygen demand was considerably above the legislated limit (125 mg O_2 L^{-1}) [87].

To overcome this problem, two different strategies were used: (a) further processing by nanofiltration using the polymeric membrane Desal 5DK (**Chapter 4**) and (b) a treatment using a hybrid photocatalytic membrane reactor (**Chapter 6**) after the development of effective and reproducible photocatalytic membranes (**Chapter 5**).

Chapter 4 presents the results obtained when nanofiltration was performed at pilot scale to treat an effluent similar to the permeate resultant from ultrafiltration. Considerably high rejections of total suspended solids, total organic carbon, chemical oxygen demand, as well as oil and grease were attained. Only the concentration of total phenols and chemical oxygen demand in the permeates produced could not comply with European legislation [87] for discharge into water courses.

In **Chapter 5**, novel coatings comprising titanium dioxide (TiO_2), silicon dioxide (SiO_2) and silicon carbide (SiC) semiconductors, were deposited over silicon-carbide substrates to develop photocatalytic membranes. The most promising membrane in terms of photocatalytic effectiveness and reusability was modified with SiO_2 obtained by sol-gel combined with Degussa TiO_2 nanoparticles. This membrane was used in a dead-end filtration system combined with UV

light. Results confirmed the photocatalytic activity of the membrane combined with filtration, showing that the modified membranes have a high potential to degrade organic contaminants.

The work presented in **Chapter 6** consists in the olive mill wastewater treatment using the photocatalytic membrane developed in **Chapter 5** in a new conceived and assembled submerged membrane photocatalytic reactor that can be easily scaled up. Results proved the photocatalytic activity of the membrane and the effectiveness of the new proposed treatment process.

Chapter 7 summarizes the main results obtained in the studies presented in this thesis and provides a discussion integrating the results obtained in the different developed works. Future work and perspectives are also discussed.

2 MORPHOLOGICAL, CHEMICAL SURFACE AND FILTRATION CHARACTERIZATION OF A NEW SILICON CARBIDE MEMBRANE

Published as: ***M.C. Fraga****, S. Sanches, V.J. Pereira, J.G. Crespo, L. Yuan, J. Marcher, M.V.M. de Yuso, E. Rodríguez-Castellón, J. Benavente, Morphological, chemical surface and filtration characterization of a new silicon carbide membrane, Journal of the European Ceramic Society 37(3) (2017) 899-905.*
The author M.C. Fraga was directly involved in planning and executing the study of the morphology of the membrane and the filtration tests, as well as on the data analysis, discussion and interpretation and manuscript elaboration.

2.1 SUMMARY

A new silicon carbide ceramic membrane consisting of a unique top layer on a silicon carbide support for application in oily wastewaters filtration was produced and characterized in terms of morphology and chemical surface composition by scanning electron microscopy and X-ray photoelectron spectroscopy measurements. The manufacturing process of this new membrane allows time and economic savings when compared with a two layers membrane previously obtained. The new membrane has a smooth top layer with controlled porosity and a higher permeability compared to already developed commercial membranes. Moreover, it is extremely efficient to remove total suspended solids as well as oil and grease and, consequently, it can be applied to effective treatment of industrial oily wastewaters.

2.2 INTRODUCTION

Oily wastewaters are generated by different industries. In particular, vegetable oil wastewater from the food industry shows high content in solids, chemical oxygen demand as well as oil and grease components [88-90]. Numerous techniques can be employed for the removal of emulsions: conventional physical and chemical treatment approaches include gravity separation and skimming, coagulation, flocculation, sedimentation, and flotation. However, these methods present disadvantages such as low efficiency in the treatment of stable emulsions, high sludge production, high operation costs and need of chemical addition [91].

Membrane processes such as microfiltration, ultrafiltration, nanofiltration and reverse osmosis are increasingly being applied for treating oily wastewaters, metal polluted waters and desalting processes [91]. Among other advantages, membrane filtration processes present high efficiency for oil removal, moderate energy cost and compact design compared with the conventional treatment methods [42]. However, membrane fouling caused by the deposition (or adsorption) of

solution particles and solutes on the membrane surface and pore walls, is the main factor limiting the application of membranes filtration processes, since it reduces the permeate flux and impairs separation properties [92]. Consequently, frequent membrane cleaning protocols need to be applied sequentially which partially affects the selection of a particular membrane.

Commercial synthetic membranes are produced from two distinct classes of material: polymers consisting of organic material (e.g. polysulfone, regenerated cellulose, poliamide and polyvynilfluoride) or inorganic materials (mainly ceramics) [93]. Ceramic membranes have advantageous properties when compared to polymeric membranes such as higher mechanical, chemical and thermal stability, which are basic requirements for adequate cleaning protocols and, consequently, higher membrane lifetime [9-10]. Furthermore, depending on the used materials, they can present a higher hydrophilicity [39, 94, 95].

The improvement of membrane hydrophilicity and fouling reduction through the use of membrane coatings with nanoparticles are currently a challenge [96]. Silicon carbide (SiC) ultrafiltration (UF) membranes exhibit high hydrophilic membrane surface, high porosity, and rather uniform pore size distribution [97, 98]. Higher membrane fluxes, lower fouling, and longer membrane lifetime are, therefore, expected using these membranes [39]. Further membrane structure modifications could still be tested to reduce production time and costs, while maintaining the membrane efficiency.

In this work, a new silicon carbide ceramic membrane (with a single retentive layer above the substrate) was developed (referred in this work as 2nd generation membrane) and compared with a previously developed and commercialized silicon carbide membrane with two layers above the substrate (1st generation membrane). These membranes were characterized in terms of morphology and chemical composition by scanning electron microscopy and X-ray photoelectron spectroscopy measurements. Both membranes were also tested with respect to their possible application in the treatment of vegetable (sunflower) oil wastewaters. Their efficiency was evaluated in terms of their effectiveness to remove solids, chemical oxygen demand and oil and grease.

2.3 MATERIAL AND METHODS

2.3.1 Silicon carbide membranes

Two different 100% silicon carbide membranes (1st generation and 2nd generation) were manufactured by LiqTech. The membranes were prepared in tubular configuration and were used for surface characterization and to perform filtration tests of sunflower oily wastewater.

The 1st generation membrane consists of a highly porous silicon carbide substrate, prepared by extrusion, and two top layers applied by push-pull-coating. The first membrane layer was sintered

on the substrate by high temperature thermal treatment (T > 2000^{0}C) in an argon atmosphere, followed by an oxidation step. Subsequently, the final selective layer is coated on the top of this layer and a second sintering takes place (T > 1800^{0}C) to achieve the appropriate pore size.

Considerable evidence suggested that the surface properties of the support (roughness, inhomogeneity and defect density) influence the uniformity and the integrity of the coated membrane. Therefore, a new procedure was developed to produce a new membrane (2nd generation membrane), in which a single top layer is applied directly on the substrate (without the intermediate membrane layer present in the 1st generation membrane). The advantage of this new procedure is the fact that one firing step can be eliminated in the production process, reducing significantly both the production time and the manufacturing costs (approximately 30%). Since sintering the membrane layer is the manufacturing bottleneck, this process change may increase a factory capacity by 100%. Moreover, the microstructure and the surface of the substrate is better controlled, since the whole process has one less high temperature firing, thus, making the final layer smoother and with less defects.

2.3.2 Scanning electron microscopy (SEM)

The surface and cross section of 1st and 2nd generation membranes were characterized by scanning electron microscopy (SEM) using a field emission gun scanning Electron Microscope (FEG-SEM from JEOL) model JSM7001F with an acceleration voltage of 15kV. The samples were placed in a sample holder with carbon double sided adhesive tape and were then coated with a film of chromium using a Quorum Technologies Q150T ES.

The SEM images were processed using the ImageJ software developed by Wayne Rasband (http://rsb.info.nih.gov/ij/docs/intro.html), a public domain Java image processing program that superseded the Image Macintosh software developed by the National Institute of Health (USA).

2.3.3 X-ray photoelectron spectroscopy (XPS)

The chemical characterisation of the surface of the studied membranes was performed by XPS. A Physical Electronics spectrometer (PHI 5700) with X-ray Mg K_α radiation (300W, 15 kV, 1253.6 eV) as the excitation source was used for these measurements. High-resolution spectra were recorded at a given take-off angle of 45º by concentric hemispherical analyser operating in the constant pass energy mode at 29.35 eV, using a 720 μm diameter analysis area. Under these conditions, the Au $4f_{7/2}$ line was recorded with 1.16 eV FWHM at a binding energy of 84.0 eV. Each spectral region was scanned several sweeps until a good signal to noise ratio was observed. The pressure in the analysis chamber was maintained lower than 5×10^{-6} Pa. The software package PHI ACCESS ESCA-V6.0 F was used for data acquisition and analysis. A Shirley-type

background was subtracted from the signals. The recorded spectra were fitted using Gauss–Lorentz curves according to the methodology described in detail elsewhere [18], in order to determine more accurately the binding energy (BE) of the different element core levels. Atomic concentration percentages of the characteristic elements on the sample surfaces were determined taking into account the corresponding area sensitivity factor [18] for the different measured spectral regions.

In order to eliminate possible surface contamination (sample manufacture or environmental contamination), measurements using a non-invasive technique such as angle resolved XPS (ARXPS) using five values of the take-off angle ($15° \leq \alpha \leq 75°$) were also performed, which provide chemical information for depth ranging, approximately, between 2.5 nm and 9.5 nm [99].

2.3.4 Membrane filtration: Experimental set-up and ultrafiltration procedure

A comparison of the performance of 1st and 2nd generation membranes was carried out using a laboratory scale filtration unit operated with total recirculation of permeate and retentate due to volume constrains. **Figure 2.1** shows a scheme of the filtration system while the characteristics of the membranes used are indicated in Table 2.1.

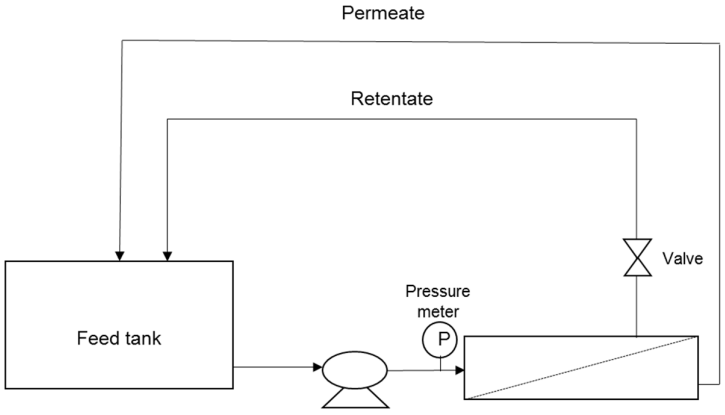

Figure 2.1 *Experimental set-up used for the ultrafiltration experiments*

The filtration unit is composed of a feed vessel, a high-pressure pump, a valve to regulate pressure on the retentate side, three pressure sensors and the membrane housing (LiqTech, Denmark). Pressure readings of permeate, feed, and retentate were acquired in real-time and used for the determination of transmembrane pressure (TMP).

Table 2.1 Characteristics of the tubular SiC membranes tested

Length (mm)	305
Number of channels	31
Channel diameter (mm)	3
Cross-section area of each channel (m^2)	7.1×10^{-6}
Total cross-section area (m^2)	2.2×10^{-4}
Filtration area (m^2)	0.089

The hydraulic permeability of the 1st and 2nd generation membranes was determined by setting different permeate fluxes and reading the corresponding pressure values to further calculate transmembrane pressure. For both membranes, five measurements were performed for each permeate flux set to obtain an average value. Five liters of real sunflower oil wastewater sample were then filtered using 1st and 2nd generation membranes. The experiments were carried out with a constant transmembrane pressure of 1.5 bar and a cross flow velocity of 0.5 m/s.

Samples of feed were taken in the beginning and in the end of each experiment while samples of retentate and permeate were taken in the end of the experiments to quantify total solids, chemical oxygen demand as well as oil and grease concentrations using the methods detailed below. Samples were stored at 4°C until analysis.

2.3.5 Analytical methods

Permeate, feed, and retentate samples from cross-flow filtration experiments were characterized in terms of the following parameters using well established methods [100]: total solids (Standard Method 2540B), total suspended solids (Standard Method 2540D), chemical oxygen demand (Standard Method 5220) and oil and grease (Standard Method 5520C).

2.4 RESULTS AND DISCUSSION

2.4.1 Membrane characterization

Cross sections and surfaces of 1st and 2nd generation membranes were analyzed by scanning electron microscopy (SEM). **Figure 2.2** shows the cross-section of both samples where the presence of two different layers on the support structure can be observed for the 1st generation membrane (**Figure 2.2** a), while a single layer of 60 µm exists in the case of the 2nd generation membrane (**Figure 2.2** b). This difference could affect the solution flow across the membranes, depending on the layers' structure.

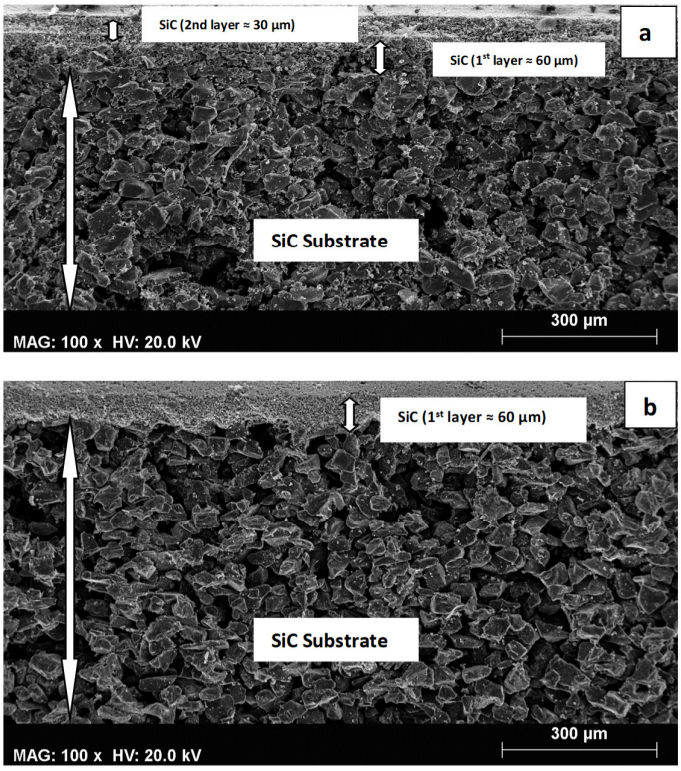

***Figure 2.2** Cross section view coated (a) 1st generation and (b) 2nd generation membranes*

Figure 2.3 shows that even though the size of silicon carbide nanoparticles is varied, different sections of the same membrane are very similar. Two different membrane sections of each membrane were processed using the ImageJ software for the ×1000 images magnifications obtained. The original SEM images composed of 256 grey levels were analysed using ImageJ, spatially scaled, their total membrane surface area was calculated and the images were then binarized.

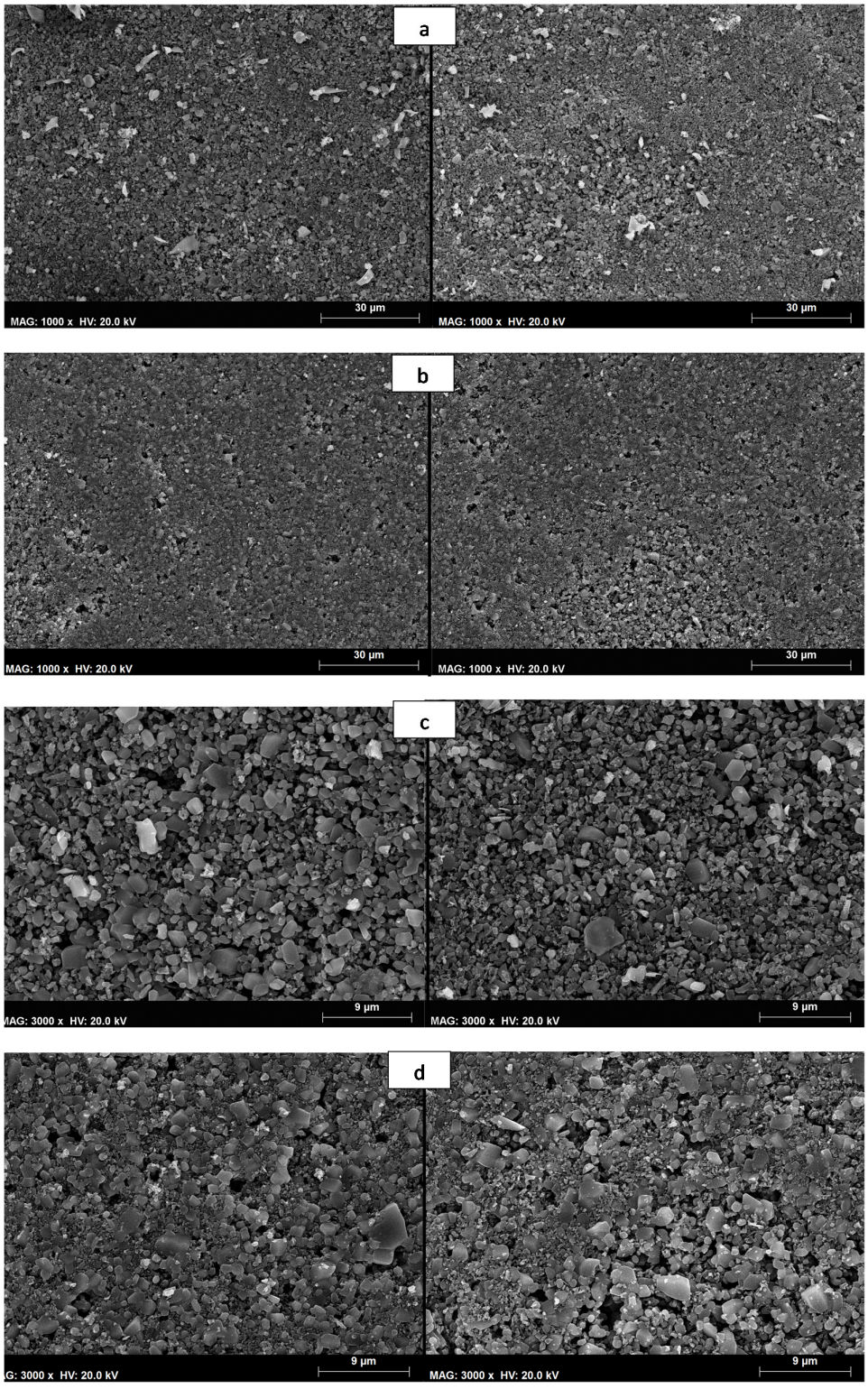

Figure 2.3 *Comparison between two different membrane surface sections; Top view of the 1st generation membrane (a and c) and 2nd generation membranes (b and d) at 1000 and 3000 magnifications.*

The area measurements obtained, calculated pore density (number of pores divided by area of membrane), porosity (area of pores divided by area of membrane), circularity (equation 2.1), and Feret's diameter (the longest distance between any two points along the selection boundary) [101] are presented in **Table 2.2** for the 1st (a) and 2nd (b) generation membranes.

$$Circularity = 4\,\pi\,\frac{Area}{Perimeter^2} \qquad \text{(Equation 2.1)}$$

Table 2.2 *Predicted measurements for two sections (S1 and S2) of the 1st generation and 2nd generation membranes obtained based on the SEM magnification of 1000*

Predicted parameters	**1st Generation**		**2nd Generation**	
Porosity (%)	3.274	2.740	2.536	2.844
Number of pores	8872	8340	8329	8506
Pore density (μm^{-2})	0.687	0.646	0.645	0.659
Mean Pore Area ± Standard Deviation (μm^2)	0.048 ± 0.088	0.042 ± 0.074	0.040 ± 0.114	0.043 ± 0.109
Minimum Pore Area (μm^2)	0.009	0.009	0.009	0.009
Maximum Pore Area (μm^2)	1.661	1.458	3.884	1.996
Total Pore Area (μm^2)	422.762	353.780	327.508	367.177
Average Circularity	0.869 ± 0.203	0.885 ± 0.189	0.903 ± 0.188	0.902 ± 0.190
Average Feret's diameter (µm)	0.325 ± 0.276	0.305 ± 0.250	0.269 ± 0.269	0.282 ± 0.291
Maximum Feret's diameter (µm)	3.233	1.000	3.487	3.478
Minimum Feret's diameter (µm)	0.133	0.121	0.131	0.132

The results obtained show similar average pore density, total pore area and porosity in different sections of the first and second generation membranes. Feret's diameters [101] up to 3.5 µm were detected. The average circularity value was approximately 0.9 in all the measurements with values obtained that varied between 0.5 and 1 (perfect circles).

Chemical composition of the surfaces of 1st generation and 2nd generation membranes were obtained by analysing the XPS spectra. Survey spectra at 45º take off angle showed the presence of characteristic material elements (carbon and silicon) as well as oxygen and other elements (Na, N or Ca), which are attributed to contamination (environmental/manufacturing contamination). **Figure 2.4** shows the C 1s and Si 2p core level spectra for both membranes, and chemical differences between them can be observed. Both membranes show a peak at a binding energy (B.E.) of 284.8-285.0 eV, associated to C-C and C-H links [102] and attributed to contamination, while the two shoulders at higher B.E. values (286.0 eV and 280.0 eV) are

attributed to oxidized carbons. The peak at the lowest B.E. (282.0 eV) corresponds to the Si-C link [103] and this contribution increases in the spectrum obtained for the 2nd generation sample. The analysis of the Si core level spectra in Fig. 4b shows that both membranes presents a clear peak at 100.0 eV, corresponding to the Si-C link [103], but another peak at a B.E. of 102.5 eV, assigned to the Si-O link [103], was also obtained for both membranes. Moreover, the higher relative intensity between both peaks exhibited by the spectrum of the 1st generation membrane when comparing with the 2nd generation indicates higher SiO_2 formation for this sample than for the 2nd generation membrane.

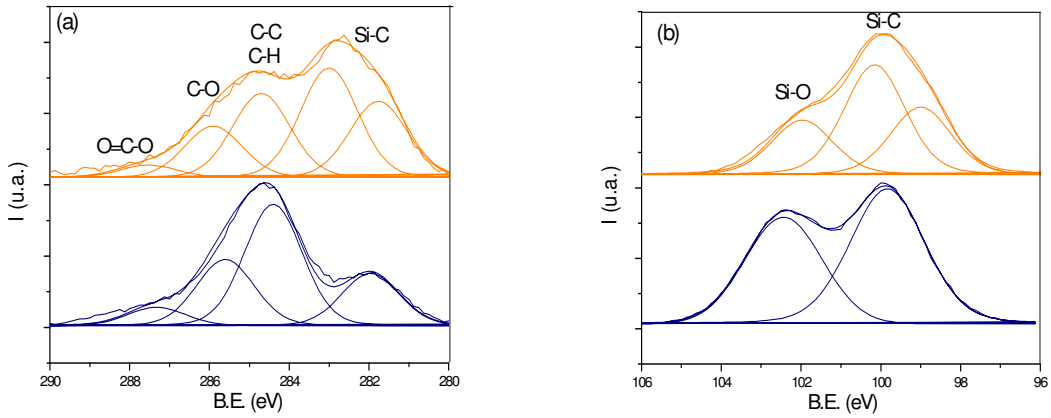

Figure 2.4 *C 1s (a) and Si 2p (b) core level spectra for 1st generation (blue) and 2nd generation (orange) membranes*

The fit of the area under the spectra allows the determination of the atomic concentration percentage (A.C. %) of the principal elements found on the surfaces of both membranes and their values are indicated in **Table 2.3**; small percentages of non-constituent elements (Na, N, S, Al, Cu, Ca) were also obtained but they are not indicated in **Table 2.3**. The C/Si correlation obtained for each membrane is also shown in **Table 2.3**, and its comparison with the theoretical value for the membranes material (C/Si = 1) gives also information on the superficial contamination of the samples.

Table 2.3 *Atomic concentration percentages of the characteristic elements found on the surface of the analyzed samples and C/Si ratio*

Sample	C (%)	Si (%)	O (%)	C/Si
1st generation	41.5	20.1	30.6	2.1
2nd generation	35.1	31.6	30.5	1.1

In order to discriminate between environmental contamination and that associated to membrane fabrication, XPS spectra at different depths (between 2.3 and 9.6 nm) for both samples were recorded and analysed. The fit of these spectra allows us to determine the A.C. (%) of the characteristic elements, and the values obtained for each sample at a specific depth are shown in **Figure 2.5**a in the case of carbon and **Figure 2.5**b for silicon. As it can be observed, the C (%) slightly decreases with depth in both samples (around 4 % with respect to surface value for 1st generation and 6% for 2nd generation samples), while the Si (%) increases in similar percentages.

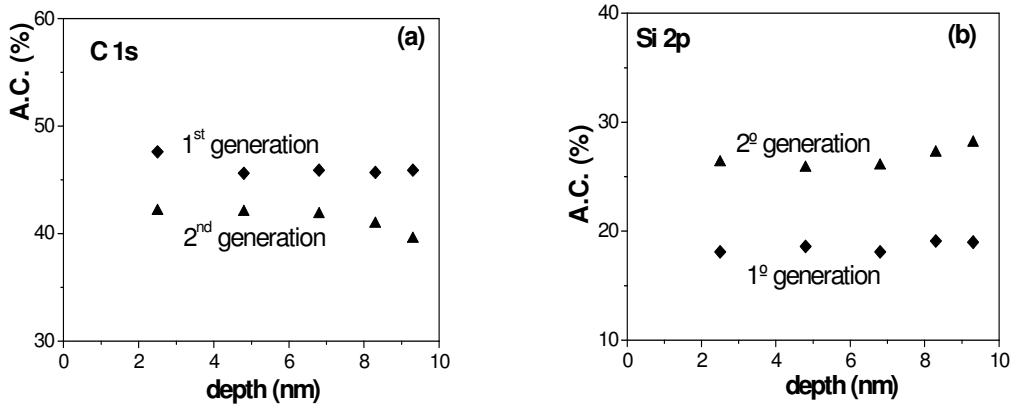

Figure 2.5 *Depth variation of: (a) carbon A.C. (%) and (b) silicon A.C. (%) for 1st generation membrane (♦) and 2nd generation membrane (▲).*

These results seem to indicate the decrease of contamination contribution when moving from the surface towards the bulk sample, in concordance with that expected from environmental contamination, but they also show the higher richness in SiC on the top layer of the 2nd generation, that is, the sample obtained eliminating one firing step.

2.4.2 Membrane filtration

Filtration measurements give information on the membrane behaviour under typical experimental conditions. Values obtained for the hydraulic permeability (volume flow/applied pressure difference ratio, Jv/ΔP) are shown in **Table 2.4**, while **Figure 2.6** shows a comparison of water quality obtained using 1st and 2nd generation membranes. According to the results indicated in **Table 2.4**, the 1st generation membrane exhibits lower permeability (~ 20 %) than the 2nd generation one.

Table 2.4 *Hydraulic permeability of 1st and 2nd generation membranes*

Jv/ΔP ($Lh^{-1}m^{-2}bar^{-1}$)	
1st generation	2nd generation
1677 ± 214	2083 ± 127

The lower differences of permeability in the 2nd generation membranes may be due to a better control of the thickness of the selective layer. These membranes will thus provide benefits in terms of quality control and improving the process yield.

Figure 2.6 shows a comparison of the quality of the water obtained before and after filtration of sunflower wastewater using the two membranes in terms of total solids (**Figure 2.6**a), total suspended solids (**Figure 2.6**b), chemical oxygen demand (**Figure 2.6**c) and oil and grease (**Figure 2.6**d).

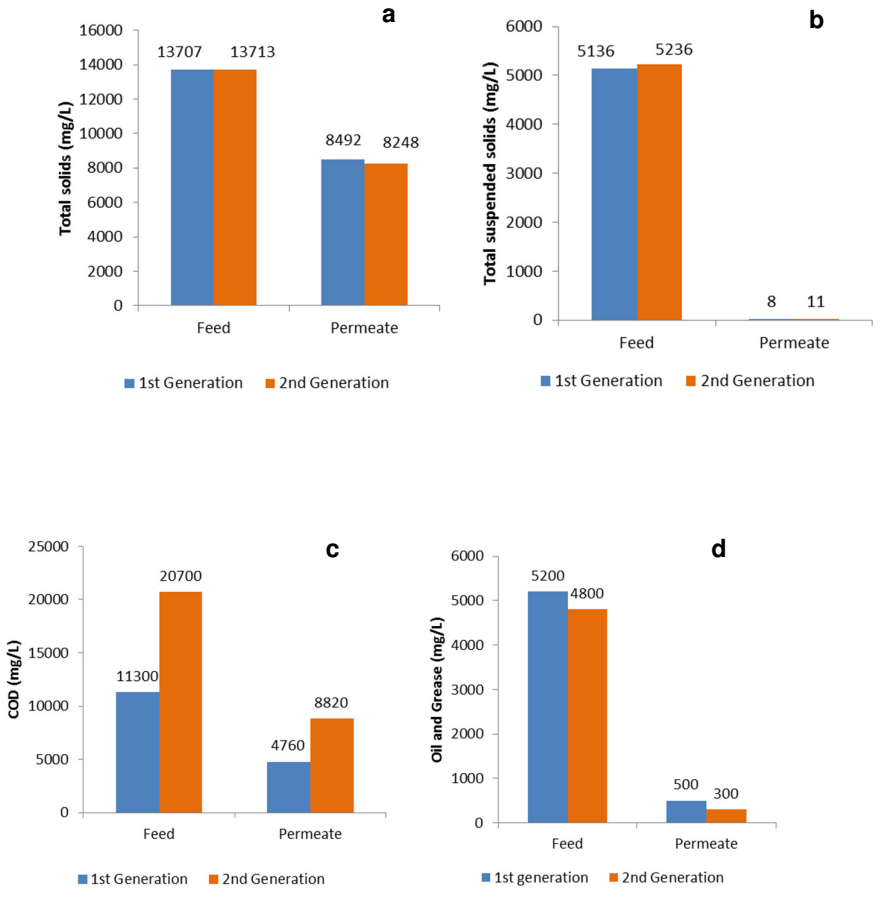

Figure 2.6 *Characterization of the feed and permeate samples taken during with the filtration experiments of sunflower oil wastewater using 1st and 2nd generation membranes in terms of (a) total solids, (b) total suspended solids, (c) chemical oxygen demand (COD) and (d) oil and grease*

Table 2.5 shows the percent removal of total solids, total suspended solids, chemical oxygen demand (COD) and oil and grease obtained using 1st and 2nd generation membranes. Similar removals of the quantified parameters were obtained using both membranes as expected due to their similar average pore density, total pore area and porosity determined. Almost all total suspended solids as well as the oil and grease present on the sunflower oil wastewater were removed. Moreover, the membranes also eliminate 40% of the total solids and approximately 60% of the chemical oxygen demand.

Table 2.5 *Percentage removal of the quantified parameters obtained by membrane filtration of sunflower oil wastewater using 1st and 2nd generation membranes*

Membrane	% Removal			
	Total solids	**Total suspended solids**	**COD**	**Oil and grease**
1st generation	38.0	99.8	57.9	90.4
2nd generation	39.9	99.7	57.4	93.8

These results indicate that both membranes are able to remove effectively particles and oil droplets from the wastewater, wherein the soluble fraction is not completely removed.

2.5 CONCLUSIONS

In this study, a new silicon carbide membrane with a single top layer fabricated by only one firing step (2nd generation membrane) was developed and characterized. This new membrane shows similar structural, chemical and removal efficiency characteristics, but higher permeability than a silicon carbide membrane previously developed with two layers and firing processes (1st generation membrane). Consequently, the results obtained show advantage in the replacement of the current membrane manufacture procedure in terms of economics and time savings, without affecting separation performance.

Taking into account the higher permeability of the 2nd generation membrane, its application will increase the production of treated water. Furthermore, given the extremely high removals determined for total suspended solids as well as oil and grease, this membrane is appropriate for the treatment of oily wastewaters such as sunflower oil.

2.6 ACKNOWLEDGMENTS

Financial support from the EU FP7/SME theme [SME-2013-1] through the project O-WaR (grant agreement no: 605641) as well as from FCT through the post-doc fellowship SFRH/BPD/94303/2013 are gratefully acknowledged. iNOVA4Health - UID/Multi/04462/2013, a program financially supported by Fundação para a Ciência e Tecnologia/Ministério da Educação e Ciência, through national funds and co-funded by FEDER under the PT2020 Partnership Agreement is also acknowledged. This work was also supported by the Associate Laboratory for Green Chemistry LAQV which is financed by national funds from FCT/MEC (UID/QUI/50006/2013) and co-financed by the ERDF under the PT2020 Partnership Agreement (POCI-01-0145-FEDER - 007265).

3 ASSESSMENT OF A NEW SILICON CARBIDE TUBULAR HONEYCOMB MEMBRANE FOR TREATMENT OF OLIVE MILL WASTEWATERS

Published as: ***C.M. Fraga****, S. Sanches, G.J. Crespo, J.V. Pereira, Assessment of a New Silicon Carbide Tubular Honeycomb Membrane for Treatment of Olive Mill Wastewaters, Membranes 7(1) (2017).*
The author M. C. Fraga was involved in planning all the filtration experiments, on the sample and data analysis, discussion and interpretation and manuscript elaboration.

3.1 SUMMARY

Extremely high removals of total suspended solids and oil and grease were obtained when olive mill wastewaters were filtered using new silicon carbide tubular membranes. These new membranes were used at constant permeate flux to treat real olive mill wastewaters at pilot scale. The filtration conditions were evaluated and optimized in terms of the selection of the permeate flux and flux maintenance strategies employed—backpulses and backwashes—in order to reduce fouling formation. The results obtained reveal that the combination of backpulses and backwashes helps to maintain the permeate flux, avoids transmembrane pressure increase and decreases the cake resistance. Moreover, membrane cleaning procedures were compared and the main agents responsible for fouling formation identified. Results also show that, under total recirculation, despite an increased concentration of pollutants in the feed stream, the quality of the permeate is maintained. Membrane filtration using silicon carbide membranes is an effective alternative to dissolved air flotation and can be applied efficiently to remove total suspended solids and oil and grease from olive mill wastewaters.

3.2 INTRODUCTION

Oily wastewaters are one of the main pollutants of the aquatic environment that, due to its hazardous nature, can cause serious environmental problems [91]. A large volume of these wastewaters is generated from various industrial processes, such as olive oil production, and needs to be treated before being discharged in the aquatic environment. The annual world production of olive oil, estimated in 2.5×10^6 tons, is one of the most important agricultural activities in the Mediterranean countries, which are responsible for the production of 97% of the total world's olive oil [104, 105]. However, such a high production of olive oil also results in an extremely high production of wastewaters characterized by a high concentration of total suspended solids and organic compounds (polysaccharides, phenols, polyalcohols, proteins, organic acids and oil) [106-109]. The physical and chemical composition of olive mill wastewaters

depend on several factors such as olive extraction processes and olive maturation as well as climatic and agronomic conditions [110, 111].

Due to the presence of phytotoxic and antibacterial phenolic substances, these wastewaters are often resistant to biological degradation [2, 111]. Traditional treatment methods, including skimming, coagulation, flocculation, sedimentation and flotation, present disadvantages such as low efficiency in the treatment of stable emulsions, high sludge production, high operation costs or need to add chemicals. In this context, membrane technology has become a significant separation process over the last years [95, 112-115], being efficient in treating stable emulsions, allowing high quality of permeate produced (the variation in feed water quality will have a minimal impact on permeate quality) and generating a small volume of waste requiring further treatment [25, 91]. Moreover, membranes require small implementation areas and the use of chemicals is avoided. Regarding the costs, membrane processes present low investment and maintenance costs, high efficiency and low energy consumption [116]. The use of membrane technology can therefore be compared to conventional processes for different wastewater applications.

Membrane fouling and its consequent flux decline (when the filtration process is performed under constant transmembrane pressure) or transmembrane pressure increase (when the filtration process is performed under constant permeate flux conditions) is the main drawback of pressure-driven membrane separation processes. Even though most studies in the literature operate at constant transmembrane pressure, most industrial water purification membrane installations operate at constant flux [117]. Working at constant permeate flux seems to be a valid strategy to reduce the fouling occurrence rather than working at constant-pressure operation [44] [18]. Miller et al. [50] compared membrane fouling in the filtration of oily wastewater with polysulfone membranes with 20 kDa molecular weight cut off. They observed that, working below a specific threshold flux, a constant flux operation minimizes fouling appearance and membrane resistance.

It is important to define the permeate flux at which fouling is first observed for a given feed concentration to optimize the membrane process and minimize fouling [118, 119]. Besides defining an optimum operating permeate flux, different cleaning systems can be applied as flux maintenance strategies such as backpulse (BP), backwash (BW), chemically enhanced backwash (CEB) and cleaning in place (CIP) [119]. The effect of backpulses and backwashes in the microfiltration of oil-in-water emulsions with ceramic membranes was already studied and reported. Results show that these strategies are efficient in fouling prevention without decreasing the oil rejection [41, 42, 45]. From an economic point of view, a study comparing the microfiltration of emulsified crude oil with and without backpulses revealed that the process without backpulses is not economically viable when compared to conventional treatment methods. However, the same operation with regular backpulses resulted in lower costs of treated water when compared with conventional methods [46].

The use of ceramic membranes recently increased, mainly for application in industrial processes [120]. Due to their advantages compared with polymeric membranes—including better thermal

stability, mechanical resistance and chemical resistance—ceramic membranes can be applied in extremely aggressive environmental conditions [121]. These properties allow for better control of membrane fouling since higher pressures can be employed in backwashes and cleanings can be performed with stronger chemicals, while extending the membrane lifetime [122]. Satisfactory results in the treatment of oily wastewaters were reported when microfiltration ceramic membranes were used [41, 42, 123]. γ-alumina is often used as a support material for ultrafiltration membranes due to its smooth surface, in contrast to other materials, and since it is fairly inert. On the other hand, it can be easily deposited in macroporous supports. Nevertheless, γ-alumina do not present high enough chemical or mechanical stability when subject to severe conditions. A promising material for ceramic membranes is silicon carbide (SiC) since it presents better resistance to chemicals, and thus presents advantages when strong and repeated cleanings are required [37, 38]. Moreover, when compared with polymeric and other ceramic membranes such as titania or zirconia, silicon carbide membranes present higher hydrophilicity and lower fouling tendency [39] and thus allow higher permeate fluxes in wastewater treatment.

In the present work, a new silicon carbide tubular ceramic membrane [124], with a single retentive layer on top of the substrate was tested, for the first time, to treat real olive mill wastewaters at pilot scale. This work focused in the optimization of constant flux filtration conditions. Backpulses and backwashes were studied in order to reduce the fouling formation and consequently avoid transmembrane pressure increase. The filtration studies were performed under total recirculation conditions and a final concentration test was conducted under optimized conditions. Different cleaning protocols were also tested in order to optimize the chemical cleaning of the membrane.

3.3 MATERIAL AND METHODS

3.3.1 Characterization of pilot scale unit, membranes and wastewater

Olive mill wastewater, collected after the sedimentation process at a real wastewater treatment plant, was processed in a pilot scale membrane filtration unit (LabBrain unit, depicted in **Figure 3.1**), with cleaning devices (backpulse and backwash) incorporated and automatic data acquisition of transmembrane pressure (TMP) and permeate flux.

The characteristics of the new tubular honeycomb silicon carbide membranes (produced by LiqTech, Ballerup, Denmark) used in this study are detailed in **Table 3.1**. These membranes were developed in the scope of a joint project, previously characterized in terms of morphology, chemical surface composition and effectiveness to treat a different matrix (sunflower oil wastewater) [33]. The manufacturing process of these new membranes allows time and economic savings when compared with commercially available membranes with two layers (a top and an intermediate layer). It is extremely interesting to observe that, in spite of the relatively low membrane porosity (**Table 3.1**), this membrane presents a high hydraulic permeability, possibly

as a result of its high hydrophilic character. In this study, contact angle measurements were performed (KSV Instruments LTD, CAM 100, Helsinki, Finland, with the software KSV CAM2008) to further characterize the new membrane (**Table 3.1**). However, a stable contact angle could not be determined because the coating of the membrane is extremely hydrophilic and the water drop was readily absorbed by the membrane. For nine different zones of the membrane, the average first contact angle value was determined. In addition, since the water drop was readily absorbed by the membrane, the contact angle decrease was also followed over time in the nine different zones. The measurements were performed with frame intervals of 100 ms. The contact angle values measured over time adjusted to a linear regression and the average of all the slopes obtained (velocity of decreasing contact angle) are also presented in **Table 3.1**.

The pilot scale installation is built in stainless steel (AISI-304) and all components in contact with liquids are stainless steel AISI-316 with Teflon-coated components or Viton/EPDM/Nitrile sealing gaskets. The LabBrain Unit (LiqTech, Ballerup, Denmark) is equipped with a feed pump (Grundfos CRN 1-3, Bjerringbro, Denmark) and a recirculation pump which generates the crossflow (Grundfos CRN 3-4, Bjerringbro, Denmark). The unit can be operated both under crossflow and semi-dead-end mode; in this work the filtration was performed in crossflow mode. The pressure and flow rate inside the system are controlled by adjusting the position of the regulating valves and the pump speed. All data from pressure transmitters, flow transmitters, temperature transmitters, pump settings and valve positions are stored in the internal memory of the unit.

In addition, the unit is equipped with a Back Pulse Hammer (BPH). The BPH system is a pulse generator delivering high frequency “block” pulses from the permeate side, back through the membrane in order to keep the membrane clean and free of foulants. Backwash controlled by compressed air is also integrated in the unit. Both backpulses and backwashes can be performed manually or automatically. Various terminologies are applied in the literature regarding cleaning devices. In this work, the term “backpulse” will refer to very short air pulses generated from the permeate side, whose function is to loosen foulants, which are then removed by the crossflow. The term “backwash” will refer to the reversion of the permeate flow by means of a pump. In this case, the foulants on the membrane surface are washed away by the reversed permeate flow and removed by the crossflow.

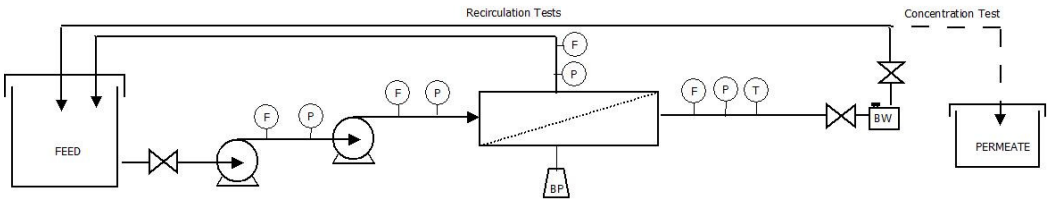

Figure 3.1 *Scheme of the pilot filtration unit with cleaning devices (BP—Backpulse and BW—Backwash) used to treat the real olive mill wastewater in different operation modes (recirculation and concentration tests).*

Table 3.1 *Characteristics of the silicon carbide (SiC) membrane module used.*

Configuration	Cylindrical with round channels
Element Dimensions (mm)	Length: 305 ± 1; Diameter: 25± 1
Area (m^2)	0.09
Number of Channels	31
Channel Diameter (mm)	3
Manufacture Nominal Pore Size (μm)	0.04
Maximum Operation Pressure (bar)	10
Temperature Tolerance (°C)	Up to 800
pH Tolerance	0–14
Hydraulic Permeability (Experimentally Determined) ($L \cdot m^{-2}\ h^{-1} \cdot bar^{-1}$) [a]	2083 ± 127
Porosity (%) [a,b]	2.7 ± 0.2
First contact angle (°) [c]	19 ± 4
Velocity of decreasing contact angle ($°s^{-1}$) [c]	35 ± 6

a: reference [124] b: average of the values determined in two zones of the membrane; c: average of the values determined in nine zones of the membrane.

Table 3.2 presents an average of the parameters analysed (total solids—Standard Method 2540B [100], total suspended solids—Standard Method 2540D [100], chemical oxygen demand (COD)—Standard Method 5220 [100], total organic carbon (TOC)—Standard Method 5310B and oil and grease—Standard Method 5520C [100]) of the wastewater samples collected in six different sampling events corresponding to the six tests performed, showing that concentration of the five parameters analysed are highly superior to the limits imposed by the legislation for direct discharge in watercourses.

Table 3.2 *Characterization of the real olive mill wastewater samples collected and limits imposed by legislation*

Parameter	**Average Concentration**	**Portuguese Legislation (DL 236/98) Concentration**	**European Legislation (91/271/EEC) Concentration**
Total solids (mg/L)	6260 ± 770	n.d.	n.d.
Total suspended solids (mg/L)	2010 ± 1105	60	35
COD (mg O_2/L)	8720 ± 1148	150	125
TOC (mg/L)	2555 ± 301	n.d	n.d.
Oil and grease (mg/L)	275 ± 60	15	n.d.

n.d.: not defined.

3.3.2 Membrane filtration tests

3.3.2.1 Determination of optimal permeate flux conditions

To define the best operating flux that minimizes fouling for further application in long-term filtration assays, a preliminary study was carried out using the pretreated wastewater samples by assessing transmembrane pressure (TMP) variations under different constant permeate flowrates set during five-minute intervals. The selected permeate flux to conduct the experiments was the one at which a lower TMP variation was observed.

3.3.2.2 Total recirculation tests

Table 3.3 summarizes the operating conditions set in each filtration test. Four 24 h assays (tests 1–4) were conducted in total recirculation mode with a crossflow velocity set at 2 $m \cdot s^{-1}$ and the previously determined optimum permeate flux value.

During the 24 h long assays, the variation of transmembrane pressure was followed and the effect of backpulse (every 10 min) and backwash (every 2 and 1h), employed as flux maintenance strategies, were studied. The permeate flux and pressure data acquisition in the LabBrain unit was automatically stored. A first test without cleaning strategies was performed (test 1). In order to study the effect of backpulses, a second test was carried out employing backpulses every 10 min (test 2). In tests 3 and 4, besides backpulses every 10 min, backwashes were also employed every two hours (test 3) and every hour (test 4) to study the effect of the combined flux maintenance strategies. These intervals were set based on experience of the manufacturer with other emulsified wastewaters and several assays performed with the unit and different wastewater qualities (data not shown).

Table 3.3 *Permeate flux and flux maintenance strategies applied in the different filtration tests.*

Conditions	test 1	test 2	test 3	test 4
Imposed constant permeate flux ($L \cdot m^{-2} \cdot h^{-1}$)	67	67	67	67
Flux maintenance strategy	No	Backpulse each 10 min (duration: 0.8 s; TMP = –3 bar)	Backpulse each 10 min + Backwash each 2h (duration: 2 s; Jb = 1 $m^3 \cdot h^{-1} \cdot m^{-2}$)	Backpulse each 10 min + Backwash each 1 h (duration: 2 s; Jb = $m^3 \cdot h^{-1} \cdot m^{-2}$)

The effectiveness of the membrane filtration assays was evaluated by monitoring TMP variation over time at the different imposed permeate fluxes and calculating the consequent membrane resistance levels as well as by determining the percent rejection and adsorption/deposition to the

silicon carbide membranes of different water quality parameters (total solids, total suspended solids, chemical oxygen demand, total organic carbon and oil and grease). Samples were stored at 4 ºC until analysis.

3.3.2.3 Optimization of membrane cleaning

In order to find out the best cleaning strategy to recover the permeability of the membrane, the effect of using different cleaning solutions and temperatures (25 ºC and 65 ± 5 ºC) was studied. Solutions of NaOH 4% (w/v) and citric acid 2% (w/v) were tested. The recovery of the permeability achieved in each cleaning step was determined to understand the efficiency of each cleaning. The permeability of the membrane was considered to be restored when 90% of its hydraulic permeability was recovered. A mass balance was performed to compare the concentrations of different water quality parameters detected in the cleaning solutions with the levels of adsorption calculated in the filtration assays, to gain further knowledge about the efficiency of the different cleaning steps.

3.3.2.4 Concentration test

In order to test conditions that best simulate the real conditions, a final concentration test was performed in the same unit. A quantity of 58 L of a pretreated olive mill wastewater was filtered with total recirculation of the retentate and total recovery of the permeate. Several samples were taken during the assay in order to evaluate the effectiveness of the membrane filtration in terms of the target parameters.

The starting conditions of the concentration test were set according to the optimum conditions selected in the total recirculation tests. Nevertheless, and due to a better quality of the wastewater received, no significant variation of TMP was observed after one hour of filtration; therefore, the permeate flux was incremented to 100 $L \cdot m^{-2} \cdot h^{-1}$ to increase the water production. During the entire filtration assay, backpulses (every 10 min) and backwashes (every hour) were applied. After the 7h assay, a volume reduction factor of 5.2 was achieved.

3.4 RESULTS AND DISCUSSION

3.4.1 Membrane filtration tests

3.4.1.1 Determination of controlled permeate flux operating conditions

In order to determine the optimum permeate flux for the 24 h filtration assays, different controlled permeate fluxes were set for 5 min and the corresponding TMP values recorded. The chosen flux was the one for which a lower increase in TMP was observed, in order to ensure a minimal fouling under long-term operation.

Figure 3.2 shows the TMP increasing with the permeate flux variation. Due to limitations of the system used, it was not possible to test fluxes lower than 67 $L \cdot m^{-2} \cdot h^{-1}$. Although some fouling was observed in each step, resulting in TMP increase in all of them, the value of 67 $L \cdot m^{-2} \cdot h^{-1}$ was the chosen permeate flux to initiate the tests since at this permeate flux the lowest TMP increase was observed.

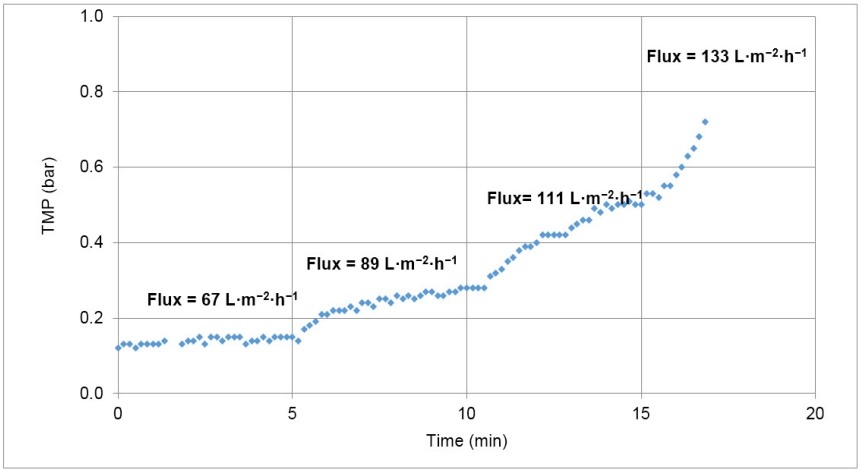

Figure 3.2 *Variation of transmembrane pressure (TMP) with increase of controlled permeate flux.*

3.4.1.2 Total recirculation tests

Figure 3.3 shows the TMP variation in the different 24 h assays conducted with the chosen permeate flux (67 $L \cdot m^{-2} \cdot h^{-1}$) and different flux maintenance strategies (detailed in **Table 3.3**).

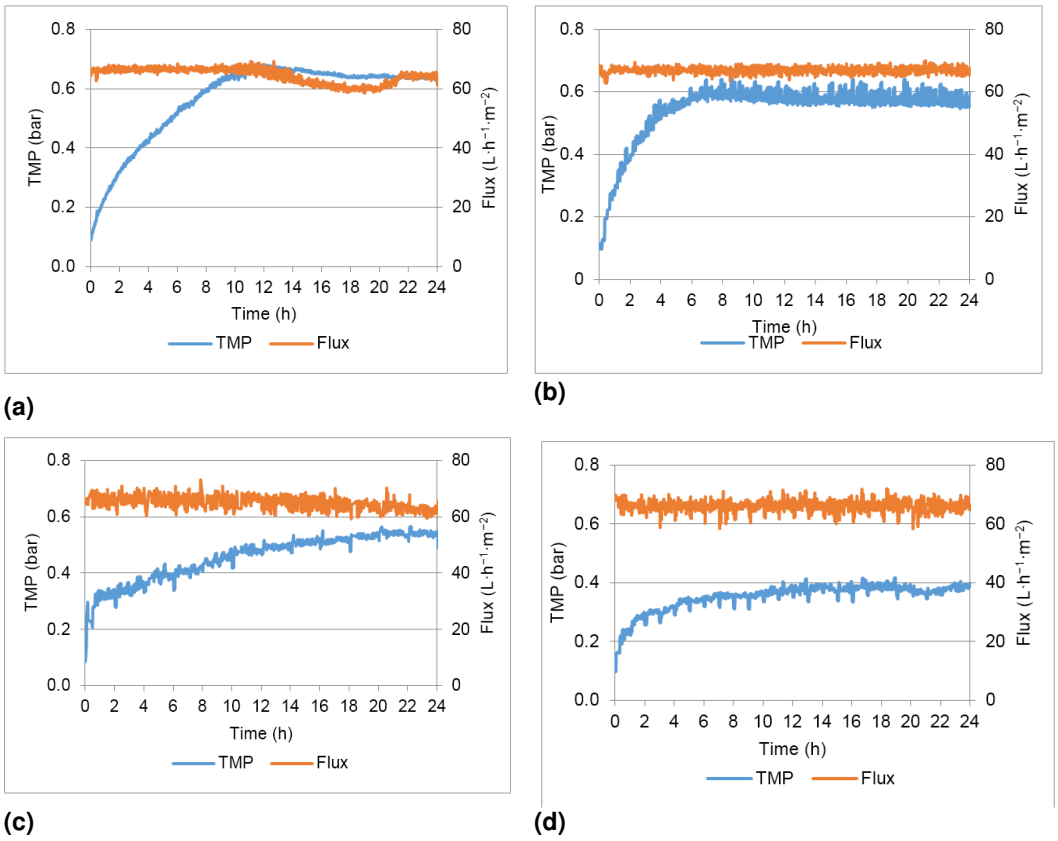

Figure 3.3 *TMP and flux profiles obtained in the different assays: (a) test 1; (b) test 2; (c) test 3;(d) test 4*

The effectiveness of the different flux maintenance strategies was calculated using Equation 3.1, where ΔTMP_{T1} is the total variation of the TMP in the 24 h of test without flux maintenance strategy (test 1) and ΔTMP_{test} refers to the variation of TMP in each test.

$$\eta(\%) = 100x\frac{(\Delta TMP_{T1} - \Delta TMP_{test})}{\Delta TMP_{T1}} \qquad \text{(Equation 3.1)}$$

In tests 2 and 3 a positive effect of backpulse (test 2) and backpulse combined with backwashing each 2 h (test 3) was observed compared with test 1 (no flux maintenance strategies and a TMP variation of 0.53 bar in the 24 h of assay). A transmembrane pressure variation of 0.48 and 0.43 bar in the 24h was observed in tests 2 and 3, respectively. When the filtration assay was performed with backpulses each 10 min and backwashing each hour (test 4), a transmembrane pressure variation of 0.28 bar was obtained, nearly half the variation of transmembrane pressure observed when no flux maintenance strategies were applied, indicating that these strategies are rather efficient for fouling mitigation.

The higher effectiveness (**η**) value presented in **Table 3.4** indicates a lower fouling potential when the combined flux maintenance strategies were applied in test 4. The trend observed was expected: as the flux maintenance strategies are intensified, the effectiveness increases.

Table 3.4 *Comparison of ΔTMP and effectiveness (**η**) of backpulses (test 2) and backwashings (test 3 and test 4) as flux maintenance strategies.*

Column Heading	test 1	test 2	test 3	test 4
ΔTMP_{test}	0.53	0.48	0.43	0.28
η	0%	9%	19%	47%

After test 4, in order to improve the permeate production, a new test was performed increasing 50% of the controlled permeate flux (100 $L \cdot m^{-2} \cdot h^{-1}$). However, under these conditions, a flux decrease of 55% was observed in the 24 hour assay which indicated that, for the oily wastewater tested, it was not possible to maintain this higher flux even when the flux maintenance systems are applied.

Using the optimal conditions (test 4), that allowed operation at a lower transmembrane pressure variation, a fouling rate was calculated using the TMP values recorded between 10 and 24 h. The fouling rate obtained (6×10^{-4} bar/h) was used to estimate the time needed to achieve 0.64 bar (the TMP obtained without flux maintenance strategies). The result obtained estimates an operation of 19 days using the optimal conditions proposed and shows that a long term continuous operation (without the need to stop the process and perform chemical cleanings) can be expected using these conditions.

Table 3.5 summarizes the percent rejection and adsorption/deposition related with the different parameters—total solids, total suspended solids, chemical oxygen demand, total organic carbon and oil and grease. The apparent rejection of the different parameters was calculated according to the following equation:

$$\%Apparent\ rejection = \frac{C_f - C_p}{C_f} \times 100 \qquad \text{(Equation 3.2)}$$

where C_f is the concentration of the different parameters in the feed water, C_p is the concentration of the different parameters in the permeate stream (**Table 3.6**). The percent adsorption or deposition of the different parameters in the total recirculation tests was calculated according to Equation 3.3.

$$\%Adsorption/Deposition = \frac{C_{f0} \times V_{f0} - C_{f24} \times V_{f24}}{C_{f0} \times V_{f0}} \times 100 \quad \text{(Equation 3.3)}$$

where C_{f0} and C_{f24} are the concentrations of the parameters in the feed tank at t = 0 and 24, respectively and V_{f0} and V_{f24} are the volumes of feed at t = 0 and 24 h, respectively.

Table 3.5 *Percent total rejection and adsorption/deposition of total solids, total suspended solids, chemical oxygen demand (COD), total organic carbon (TOC) and oil and grease*

Parameter	test 1		test 2		test 3		test 4	
	% Rejection	% Ads/Dep	% Rejection	% Ads/Dep	% Rejection	% Ads/Dep	% Rejection	% Ads/Dep
Total solids	37	12	29	2	49	0	56	12
Total suspended solids	>99.9	49	>99.9	24	99	19	>99.9	22
COD	57	30	37	0	64	1	69	3
TOC	49	26	60	23	68	0	64	0
Oil and grease	97	89	97	76	99	74	99	46

Extremely high percent removals of total suspended solids (>99%) and oil and grease (>97%) were observed in tests 1–4. **Table 3.6** shows that membrane filtration ensures removals of these parameters until values lower than the legislation discharge limits. Removal of oil and grease is significantly due to adsorption/deposition on the membrane surface. The high adsorption/deposition of oil and grease was minimized by 48% using the optimized flux maintenance strategy (test 4).

Yang et al. [125] prepared a ZrO_2/α-Al_2O_3 microfiltration membrane to treat oil-in-water emulsions, obtaining removals higher than 99% of oil. However, the hydraulic permeability of the microfiltration membranes were much lower than the hydraulic permeability of the silicon carbide membranes used in this work. Cui et al [41] also reported removals higher than 99% of oil when using NaA/α-Al_2O_3 membranes to treat oil-in-water emulsions. In this case, the permeate fluxes were only 5 and 18 $L \cdot m^{-2} \cdot h^{-1}$, with a filtration time of 600 min. Regarding polymeric membranes, good oil and grease removals were also reported but with higher transmembrane pressures [126, 127]. Ochando-Pulido et al. [128] achieved extremely high removals of total suspended solids from olive mill wastewaters by an ultrafiltration process using polymeric membranes but, once again, with fluxes not higher than 10 $L \cdot m^{-2} \cdot h^{-1}$. The silicon carbide membranes tested in this study ensure extremely high removals of oil and grease and total suspended solids allowing high permeate fluxes with low transmembrane pressure.

Lower removals of total solids, chemical oxygen demand and total organic carbon were observed, achieving up to 69% of chemical oxygen demand rejection in test 4 and 68% of total organic

carbon rejection in test 3. Using the optimized conditions, higher values of rejection of all the tested parameters, except TOC, were obtained by ultrafiltration (this study, **Table 3.5**, test 4) compared to the removal values obtained by dissolved air flotation reported in a previous study (Total solids: 27%, total suspended solids: 98%, COD: 67%, TOC: 72%, Oil and grease: 77% [129]). Ultrafiltration can therefore be applied instead of flotation for the treatment of olive mill wastewaters. COD removal was not enough to achieve values under the limit legislated. However, good percent removals were achieved when compared with other studied membrane processes: Coskun et al. [32] achieved the same range of removals combining ultrafiltration and nanofiltration to treat olive mill wastewaters. A previous study [130] obtained a maximum removal of 15% of COD from an olive mill wastewater using a regenerated cellulose membrane in dead-end configuration. The results obtained in this study are extremely promising since tests were performed using robust ceramic membranes and in conditions closer to reality in terms of flow dynamics. The membranes tested can achieve good removals with only one membrane step, maintaining a high permeate flux, during prolonged operation periods, with a low transmembrane pressure increase.

Higher percent adsorption/deposition values were reported in the assay without flux maintenance strategies (test 1) compared to the assays conducted with backpulse (test 2) and the tests conducted with backpulse and backwash (tests 3 and 4). These results were expected since backpulse and backwash are used to release the fouling components from the membrane surface.

Table 3.6 *Characterization of feed and permeate in terms of total solids, total suspended solids (TSS), chemical oxygen demand (COD), total organic carbon (TOC) and oil and grease in tests 1–4.*

Concentration (mg/L)	test 1			test 2			test 3			test 4		
	Feed 0 h	Feed 24 h	Permeate 24 h	Feed 0 h	Feed 24 h	Permeate 24 h	Feed 0 h	Feed 24 h	Permeate 24 h	Feed 0 h	Feed 24 h	Permeate 24 h
Total solids	7012	5664	4416	5232	4692	3728	6148	6072	3108	6644	5168	2944
TSS	1525	770	1.7	843	640	1.8	2233	1813	12	3432	2460	5.6
COD	8824	5752	3756	7085	6715	4465	9708	9264	3516	9264	8468	2832
TOC	2247	1530	1152	2812	2031	1120	2813	3126	904	2346	2623	856
Oil and grease	270	30	7.6	250	58	8.5	360	93	4	220	89	3

The total membrane resistance (R_t), corresponding to the sum of the membrane resistance (R_m) and the resistance due to fouling (R_f) in tests 1 to 4 was calculated at t = 24 h using Equation 3.4:

$$R_t = R_m + R_f = \frac{TMP}{\mu_t \times J} \qquad \text{(Equation 3.4)}$$

where *TMP* refers to the transmembrane pressure, *J* to the permeate flux and μ_t to the fluid viscosity corrected to the working temperature, according to Equation (3.5) [49]:

$$\mu_t = 1.784 - (0.0575 \times T) + (0.0011 \times T^2) - (10^{-5} \times T^3) \quad \text{(Equation 3.5)}$$

The value of the membrane resistance was determined (R_m = 1.58 × 10^{11} m^{-1}) using the value of the hydraulic permeability determined during clean water flux measurements. In order to analyse the effect of the cleaning strategies in the fouling formation, the values of resistance due to fouling of tests 1–4 were calculated and results clearly show the effect of backpulse and backwash strategies in the total resistance of the membrane. In test 1, conducted without flux maintenance strategies, the resistance of the membrane due to fouling at the end of the test was 4.14 × 10^{12} m^{-1}. The use of backpulses each 10 min resulted in a decrease of the resistance of the membrane due to fouling to 3.75 × 10^{12} m^{-1}. With backwashes each two hours in addition to the backpulses (R_f = 3.54 × 10^{12} m^{-1}) the difference was minor but when backwashes were performed each hour an accentuated decrease in membrane resistance due to fouling was observed (2.29 × 10^{12} $m^{-1)}$. The considerable reduction in the resistance due to fouling, observed in test 4, may be interpreted taking into consideration the results presented in **Table 3.5**. The only parameter that could justify this difference taking into account the deposition/adsorption results is oil and grease. Therefore, it can be concluded that the reduction of the fouling resistance can be due to an effective release of oil and grease from the surface of the membrane when backpulses each 10 min are combined with backwashes every hour. The conditions employed in test 4 were therefore applied in a final concentration study, that better simulates real filtration conditions, conducted with total recirculation of the retentate and total recovery of the permeate.

3.4.1.3 Optimization of membrane cleaning

In order to optimize the cleaning protocol of the membrane, different cleaning solutions were tested and analysed in terms of total suspended solids and oil and grease—the contaminants considered to be the most important in fouling formation. In all tests, the first cleaning step was a rinsing step with hot water (60 ± 5 ºC). Alkaline and acid solutions were tested after the rinsing step, and the effect of the temperature of the cleaning solutions was studied.

The first approach included the use of a 4% NaOH solution, recommended by the membrane manufacturer since it has a low cost, is easily available and can efficiently remove the oil and grease adsorbed on the surface of the membrane [47]

Figure 3.4a shows the permeability of the membrane recovered after each cleaning step in test 1. Results show that rinsing and using NaOH at controlled temperature (60 ± 5 ºC) was not enough to recover the permeability of the membrane. A solution of 2% citric acid was therefore

employed. The results obtained show that the permeability was totally restored. It was thus concluded that the use of an acid solution may also be important to recover the permeability of the membrane with this wastewater.

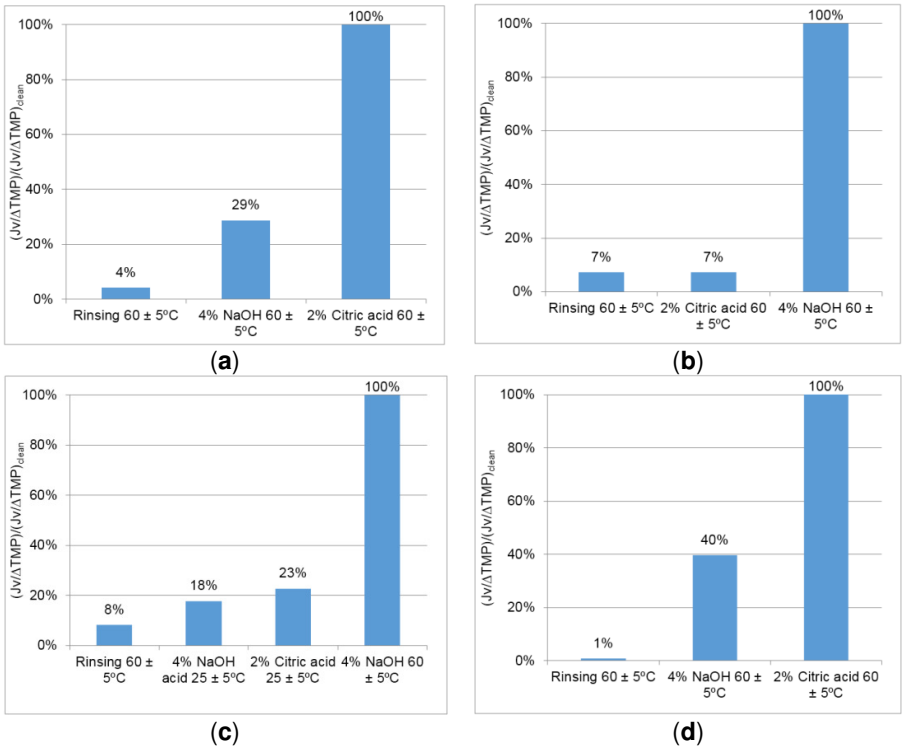

Figure 3.4 *Percent recovery of the permeate flux per transmembrane pressure applied* $(J_v/\Delta TMP)/(J_v/\Delta TMP)_{clean}$ *with different cleaning protocols performed after the membrane filtration assays: (**a**) test 1; (**b**) test 2; (**c**) test 3; (**d**) test 4.*

After test 2 (**Figure 3.4**b), the strategy to clean the membrane was therefore the use of both acid and alkaline solutions at 60 ± 5 ℃ after an initial rinsing step. In this protocol, the sequence of steps was inverted, with the acid cleaning performed before the alkaline cleaning. The acid solution by itself was not enough to recover the permeability and only 6.5% of the adsorbed total suspended solids were recovered in this step. Even though total suspended solids and oil and grease were not detected after the acid cleaning step, a quick recovery of permeability was obtained using the consecutive acid and basic cleaning agents.

To understand if the use of a high temperature was really needed, cleaning after test 3 was performed with acid and alkaline solutions at room temperature—25 ℃ after rinsing with hot water (**Figure 3.4**c). The cleanings performed at 25 ℃ were not enough to restore the membrane permeability. After cleaning with NaOH at 60 ± 5 ℃, the permeability was totally restored, so it was concluded that it is necessary to increase the temperature at least in one step of the chemical

cleaning. A total of 100% of the suspended solids and 23% of the oil and grease adsorbed on the membrane were detected after analysing the cleaning solutions. Again, rinsing with hot water proved to be the most important step in the removal of total suspended solids (57%) and oil and grease (100%); 4% of the adsorbed total suspended solids was detected in the acid solution.

To study if the sequence of the chemical cleanings was important, in test 4 (**Figure 3.4**d) this procedure was performed after rinsing with an alkaline cleaning followed by an acid cleaning both at 60 ± 5 ºC. It was observed that the permeability was totally restored after a sequence of basic and acid cleaning steps, indicating that the sequence does not seem to be important (compared with **Figure 3.4**b). Nevertheless, alternating alkaline and acid cleanings seems to be important in addition to the temperature: results indicate that the first chemical cleaning contributes to the destructuring of the existent fouling facilitating the subsequent cleaning. Furthermore, 75% of the total suspended solids removed using this cleaning protocol were recovered in the rinsing step, 21% in the alkaline cleaning and 4% in the acid cleaning. In sum, 82% of the total suspended solids adsorbed on the membrane surface were recovered in the cleaning procedure. All the adsorbed oil and grease were recovered in the rinsing step. Since the permeate flux was totally restored after the proposed cleaning procedure, the results indicate that total suspended solids, oil and grease and inorganic matter are important agents involved in fouling formation during the filtration of these wastewaters.

3.4.1.4 Concentration test

Figure 3.5 shows the TMP variation during the concentration test. During the first hour, the flux was set at 67 $L \cdot m^{-2} \cdot h^{-1}$ and backpulses every 10 min were performed in addition to backwashes every hour; the optimized conditions were determined in the total recirculation tests. The transmembrane pressure variation during the first hour was only 0.02 bar, very low compared to 0.15 bar variation obtained in the same period in the total recirculation assay—**Figure 3.3**d. In order to increase the process efficiency, the controlled permeate flux was therefore increased 50% in relation to the initial permeate flux, to 100 $L \cdot m^{-2} \cdot h^{-1}$, while keeping the flux maintenance strategies previously optimized.

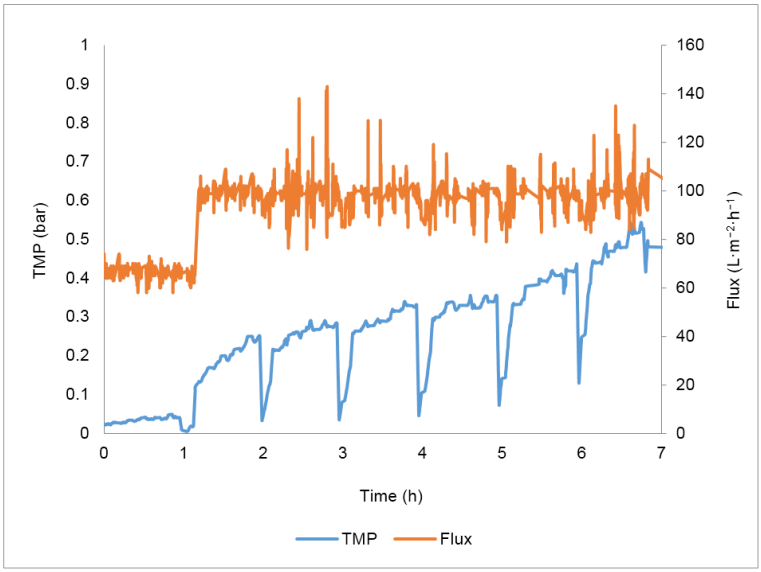

Figure 3.5 *Transmembrane pressure (TMP) and permeate flux profiles obtained in the concentration test.*

The lower transmembrane pressure variation in this assay was due to a better quality of the large volume of oily wastewater received for the concentration study (**Table 3.7**), that was much less concentrated in terms of the water quality parameters analysed.

$$Concentration\ factor = \frac{Volume\ feed}{Volume\ feed - Volume\ permeate} \qquad \text{Equation 6.6}$$

In these conditions, a final concentration factor (Equation 6.6) of 5.2 was achieved, corresponding to a permeate recovery of 81%.

Table 3.7 Characterization of the olive mill wastewater used in the concentration test in terms of total solids, total suspended solids, chemical oxygen demand (COD), total organic carbon (TOC) and oil and grease.

Parameter	Concentration (mg/L)
Total solids	1946
Total suspended solids	438
COD	1850
TOC	305

Figure 3.6 presents the percent rejection of the different parameters obtained in samples collected during the concentration assay.

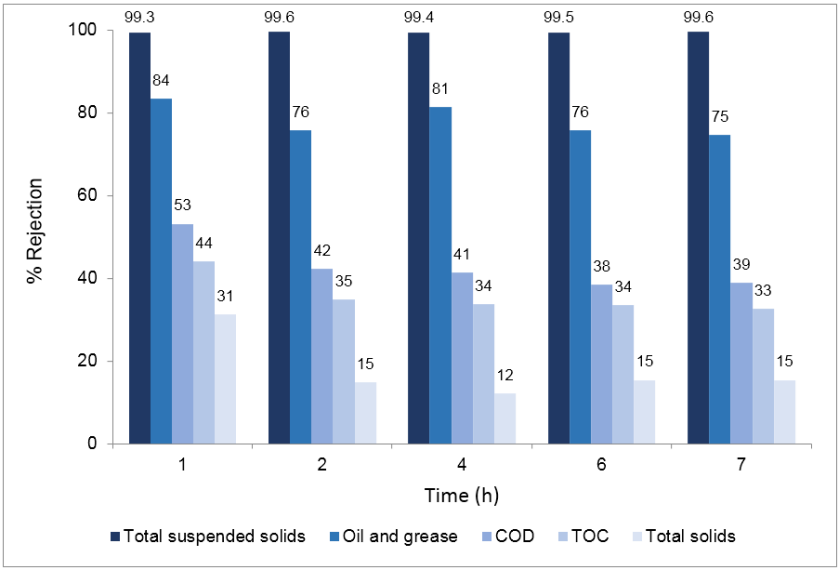

Figure 3.6 *Percent rejection of total suspended solids, oil and grease, chemical oxygen demand (COD), total organic carbon (TOC) and total solids—Concentration test.*

Results show that the rejections of the different parameters monitored were maintained during the 7 h concentration study, evidencing that the quality of the permeate over time was not deteriorated despite the increasing concentration of the different components in the feed wastewater due to the total recirculation of the retentate. The results obtained in terms of rejection were consistent with the results previously obtained in the 24 h total recirculation test. The silicon carbide membranes used ensure high removals of total suspended solids and oil and grease. The value of membrane resistance at working temperature due to fouling at the end of this test was 2.31×10^{12} m^{-1}.

Huang et al. [131] adapted the Hermia's model [132] to describe fouling mechanisms in membrane processes performed at constant TMP and developed a similar one for membrane processes conducted at controlled permeate flux. This model was applied to the results obtained in the concentration test in order to identify the different fouling mechanisms involved. The results obtained indicate that the main fouling mechanism involved in this process is cake formation, since it presents the best coefficient of determination (0.92). This result is in accordance with other published studies, where the fouling formation during the ultrafiltration of oily wastewaters is mainly attributed to cake formation [133, 134]. This fouling mechanism is attributed to the deposit of large molecules on the membrane surface. Results are thus in accordance with the

assumption that total suspended solids and oil and grease are important parameters in fouling formation [135].

Figure 3.7 relates the maximum TMP achieved before backwashes with the concentration of total suspended solids present in the feed at the same time. A linear regression with a coefficient of determination (R^2) of 0.99 was obtained, indicating a strong relationship between these two variables and confirming the influence of the concentration of total suspended solids present in the feed in the cake formation.

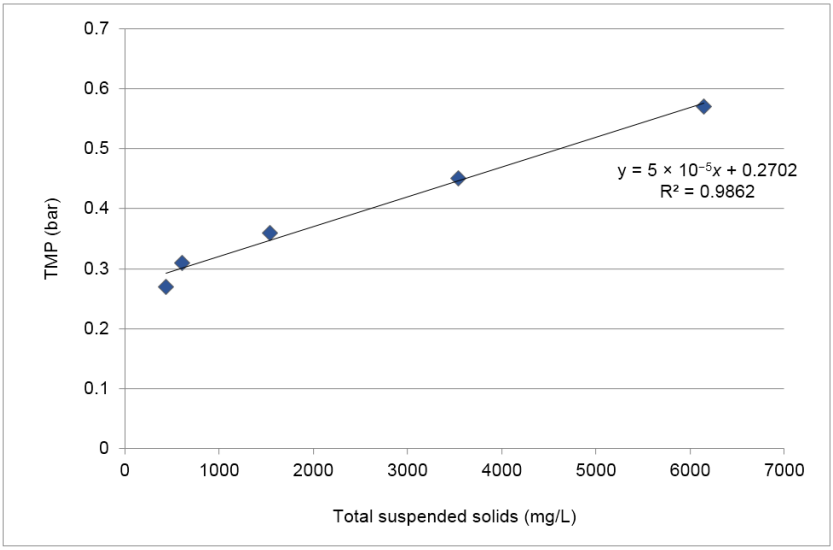

Figure 3.7 *Impact of total suspended solids present in the feed in TMP—Concentration test.*

The optimized cleaning procedure was applied after the concentration test to restore the membrane permeability. In this case, after the alkaline step, the permeability was totally restored and the acid cleaning step was therefore not needed. This may be due to the better quality of the wastewater. All the adsorbed total suspended solids and oil and grease were recovered.

3.5 CONCLUSIONS

This work shows that a new generation of silicon carbide membranes can be used to ensure extremely high removals of total suspended solids and oil and grease and moderate removals of chemical oxygen demand (COD) and total organic carbon (TOC) from olive mill wastewaters. Removal of oil and grease was largely due to adsorption/deposition of the compounds on the surface of the membrane and harder to remove using the flux maintenance strategies compared with other fouling agents.

The employment of backpulses every 10 min is an effective strategy to achieve a reduction of the fouling formation at the surface of the membrane since it enables a release of the adsorbed compounds. When the backpulses are combined with backwashes, the percent of adsorption/deposition of the analysed compounds is further reduced. The combination of backpulses every 10 min and backwash every 1 h helps minimize fouling, maintain flux and avoid high TMP increase. A high reduction of adsorption/deposition of oil and grease in the membrane surface was observed. This result can explain the decrease of the resistance due to the fouling observed when working under the determined optimum constant permeate flux (67 $L \cdot m^{-2} \cdot h^{-1}$) together with backpulses every 10 min and backwashes every hour, indicating that oil and grease is an important component of fouling.

To recover the membrane permeability, the simplest and most effective strategy is to rinse and alternate a basic and an acid cleaning solution. All these steps must be performed at controlled temperature, between 60 and 65 ºC. Rinsing at 60–65 ºC seems to be the step that most contributes to the removal of oil and grease and total suspended solids, followed by the basic cleaning with 4% NaOH.

Results demonstrate that membrane filtration using this new generation of silicon carbide membranes is extremely effective to remove total suspended solids and oil and grease from different real olive mill effluents and thus constitute a promising alternative to conventional wastewater treatment processes.

This process allowed us to obtain water with concentrations of total suspended solids and oil and grease below the maximum levels legislated for direct discharge in the environment. However, high contents of dissolved organic components are still present and must be further removed. Processes such as nanofiltration [129] or advanced oxidation processes [104, 110, 136] may be good options to reduce it and to guarantee the production of high quality water.

3.6 ACKNOWLEDGEMENTS

The authors thank Adventech for supplying the wastewater matrices and Liqtech for supplying the silicon carbide membranes used in this study, in the frame of EC project O-WaR. Financial support from the EU FP7/SME theme [SME-2013-1] through the project O-WaR (grant agreement no: 605641) as well as from FCT through the post-doc fellowship SFRH/BPD/94303/2013 are gratefully acknowledged. iNOVA4Health-UID/Multi/04462/2013, a program financially supported by Fundação para a Ciência e Tecnologia/Ministério da Educação e Ciência, through national funds and co-funded by FEDER under the PT2020 Partnership Agreement, is also gratefully acknowledged. This work was also supported by the Associate Laboratory for Green Chemistry LAQV which is financed by national funds from FCT/MEC (UID/QUI/50006/2013) and co-financed by the ERDF under the PT2020 Partnership Agreement (POCI-01-0145-FEDER-007265).

4 PILOT SCALE NANOFILTRATION TREATMENT OF OLIVE MILL WASTEWATER: A TECHNICAL AND ECONOMICAL EVALUATION

*Published as: S. Sanches, **M.C. Fraga**, N.A. Silva, P. Nunes, J.G. Crespo, V.J. Pereira, Pilot scale nanofiltration treatment of olive mill wastewater: a technical and economical evaluation, Environmental Science and Pollution Research 24(4) (2017) 3506-3518.*
The author M.C. Fraga was involved in planning all the filtration experiments, assembly of the pilot scale system tested and on the sample analysis

4.1 SUMMARY

The treatment of large volumes of olive mill wastewater is presently a challenge. This study reports the technical and economic feasibility of a sequential treatment of olive mill wastewater comprising a dissolved air flotation pre-treatment and nanofiltration. Different pilot nanofiltration assays were conducted in a concentration mode up to different volume reduction factors (29, 45, 58, and 81). Data attained demonstrated that nanofiltration can be operated at considerably high volume reduction factors and still be effective towards the removal of several components. A flux decline of approximately 50% was observed at the highest volume reduction factor, mainly due to increase of the osmotic pressure. Considerably high rejections were obtained across all experiments for total suspended solids (83 to >99%), total organic carbon (64 to 99%), chemical oxygen demand (53 to 77%), and oil and grease (67 to >82%). Treated water was in compliance with European legal limits for discharge regarding total suspended solids and oil and grease. The potential recovery of phenolic compounds was evaluated and found not relevant. It was demonstrated that nanofiltration is economically feasible, involving operation costs of approximately 2.56-3.08 €/m^3, depending on the working plan schedule and volume reduction factor, and requiring a footprint of approximately 52 m^2 to treat 1000 m^3 of olive mill wastewater.

4.2 INTRODUCTION

The world olive oil production in 2013/2014 was 3.27 million tons [137]. Since 0.5-1.5 m^3 of wastewater is produced per ton of olives [18], the effectiveness and cost of olive mill wastewater treatment that enables the compliance with legal discharge limits into water bodies or municipal wastewater treatment plants is a serious issue. This is particularly important in Mediterranean countries, where the olive oil production is more significant.

As revised by Zirehpour et al. [138], these wastewaters are characterized by high chemical oxygen demand (35-200 g/L), suspended solids (6-69 g/L), and total phenols (2-15 g/L). Evaporation in open-air lagoons is the most common treatment of olive mill wastewater [139,

140]. However, concerns arise due to hazardous underground leakages and emission of volatile organic compounds [141] that can significantly impact ecological balance [142, 143]. Alternative treatments have been proposed such as biological processes [144], advanced oxidation processes (AOPs) [145-147], and physico-chemical processes such as lime and clay treatment [12], coagulation-flocculation [10, 148], and electrocoagulation [149]. However, effectiveness as well as capital and operating costs are drawbacks for their application [150].

A benchmark analysis from Zagklis et al. [151] regarding olive mill wastewater treatments pointed out membrane filtration among the most promising processes taking into account the resulting treated water quality and treatment cost. Furthermore, membrane processes have gained interest for the treatment of these type of wastewater given the following characteristics: no need for chemicals addition, small footprint and simple industrial scaling, easy operation and integration with other treatment processes [25, 152]. Another advantage is the fact that permeate quality might be controlled by selecting a membrane with adequate retentive properties. For instance, membranes with specific molecular weight cut-off (MWCO) can be selected to allow the breakthrough of high added value by-products that may be further recovered for food, pharmaceutical or cosmetic industries. This is the case of phenols such as hydroxytyrosol, tyrosol, and oleuropein [27, 153, 154], which interest in fractionation and recovery relies on their anti-oxidant, anti-microbial, anti-inflammatory, and anti-carcinogenic properties [155].

Microfiltration (MF) and/or ultrafiltration (UF) may be used as primary treatment while nanofiltration (NF) and/or reverse osmosis (RO) may be used for final treatment. The sequential use of membrane processes has been proposed for olive mill wastewater treatment to attain water with acceptable quality for discharge into water bodies [27, 30-32, 138, 156]. Although RO is more effective than NF for COD removal (e.g. [146, 157], application of RO membranes demands more energy and yields lower permeate fluxes, resulting in higher costs than NF.

Different combinations of UF and MF pre-treatments with nanofiltration rendered COD removals between 50 and 90% [138, 150] while coagulation was found to positively impact NF membrane permeability and COD rejection [158]. Near-zero fouling with COD removals up to 58.9% was observed by using Fenton-like AOP, flocculation-sedimentation, and filtration through olive stones followed by nanofiltration [146]. Despite the lack of data regarding the combination of dissolved air flotation (DAF) with membrane filtration for the treatment of olive mill wastewaters, this process has been successfully applied to treat oily wastewaters from other industries [159, 160].

Despite the increasing number of publications assessing the technical use of membrane processes for the treatment of olive mill wastewater, an economic feasibility evaluation for further industrial application is lacking. This is required given the fact that there are plenty of small-sized olive mill factories that cannot afford high treatment costs and complex operation systems to ensure compliance with regulations.

The aim of this work is to address the technical and economic feasibility of using nanofiltration to treat on-site real olive mill wastewaters pre-treated by dissolved air flotation. Membrane flux decline as well as membrane efficiency towards the removal of relevant components (total suspended solids, total solids, total organic carbon, chemical oxygen demand, oil and grease, and total phenols) was evaluated when the real wastewater was treated and the volume of concentrated waste was reduced (volume reduction factors, VRF, up to 81). The potential recovery of valuable phenolic compounds was also evaluated aiming at the enhancement of process economics.

4.3 MATERIAL AND METHODS

4.3.1 Chemical reagents

P3-Ultrasil 11® (Henkel-ecolab GmbH Co.) was used to clean the membrane after nanofiltration experiments. Sodium carbonate (Sigma Aldrich, Germany) and Folin Ciocalteu reagent (Merck, Germany) were used for the determination of total phenols in the nanofiltration samples. The LCI 400 Kit (Hach GmbH, Germany), which has been developed in agreement with ISO 15705, was used for the determination of chemical oxygen demand. Milli-Q water used for the analysis of samples was produced by a Milli-Q water system (Millipore, CA, USA).

4.3.2 Olive mill wastewaters

Real dissolved air flotation pre-treated wastewaters from an olive oil production plant, located in Spain, were used to assess nanofiltration potential for their treatment. The characteristics of the wastewater prior to dissolved air flotation treatment are provided in **Table 4.1**.

Table 4.1 *Physico-chemical characterization of the raw olive mill wastewater*

Physico-chemical parameter	Concentration (mg/L)
Total suspended solids	642
Total solids	2700
Total organic carbon	827
Chemical oxygen demand	3000
Oil and grease	91

In this industrial plant, 700-1000 m^3 of wastewater are produced annually from November to March during olive oil extraction by a two-and-a-half-phase system, consisting in the employment of two distinct and sequential centrifugation phases, with or without additional water, in order to enhance the extraction process efficiency.

4.3.3 Experimental setup

Olive mill wastewater pre-treatment was conducted by a DAF Nikuni unit, using PAX-18 (coagulant) and Flochtech ADV C58 (cationic flocculant composed of a mixture of adipic acid and polymer aluminum hydroxychloride). DAF operating conditions were optimized and reported elsewhere [161]. The characteristics of the effluents pre-treated by DAF were fairly constant and are presented in **Table 4.2**.

Table 4.2 *Comparison of concentration values determined for the parameters addressed in the feed and permeate with regulated maximum allowed values*

Assay	NF stream	Total suspended solids (mg/L)	Total solids (mg/L)	Total organic carbon (mg/L)	Chemical oxygen demand (mg O_2/L)	Oil and grease (mg/L)	Total phenols (mg/L)
NF1	Feed	16.0	1964	229	996	21.0	154
	Permeate	< 0.2	1346	36	325	3.9	114
NF2	Feed	7.2	2116	266	1082	16.0	179
	Permeate	< 0.2	1816	95	506	5.3	153
NF3	Feed	26.5	3504	284	1240	15.3	202
	Permeate	2.0	3058	2	288	<2.7	150
NF4	Feed	10.3	2284	256	1106	14.0	162
	Permeate	1.8	1556	77	455	< 2.7	145
EU limit emission values for discharge of wastewater		35-60*	-	-	125*	15*	0.5*

*91/271/EEC

The pilot scale unit used to carry out nanofiltration experiments (**Figure 4.1**) was equipped with permeate and feed tanks (0.125 - 1 m^3), a high pressure diaphragm pump (Hydra-Cell, Wanner Engineering, USA), a permeate flow meter, a 70 µm metallic pre-filter cartridge (Atlas Filter, Italy) to remove larger particles from the nanofiltration feed stream, a valve to regulate pressure, and a spiral-wound Desal DK membrane (model DK2540F1072, GE Water & Process Technologies, USA).

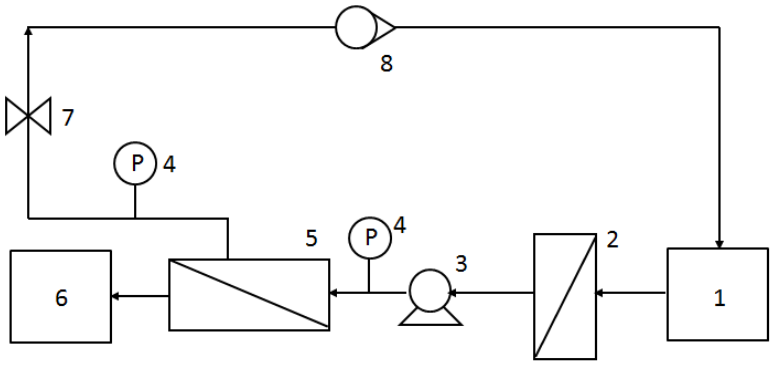

Figure 4.1 *Schematic representation of the experimental setup; 1, feed tank; 2, pre-filter; 3, high pressure pump; 4, pressure gauge; 5, spiral-wound membrane element; 6, permeate tank; 7, retentate valve; 8, flowmeter*

The nanofiltration membrane used has a molecular weight cut-off of 150-300 Da, an effective filtration area of 2.6 m2 and a minimum MgSO4 rejection of 98% (data provided by the manufacturer). An hydraulic permeability of 5.5 ± 0.1 L/ (h.m^2.bar) was determined experimentally at 25 ℃ for this membrane. The filtration pressure was adjusted on the retentate side with a brass ball valve and measured by pressure gauges. The tubing of the system was made of polyvinylidene difluoride to minimize the adsorption of organic compounds.

4.3.4 Nanofiltration assays

The pilot scale unit was operated at the wastewater treatment plant of an olive oil Spanish producer. Four olive mill wastewaters, pre-treated by dissolved air flotation, were treated by nanofiltration up to different volume reduction factors (defined as the ratio between the initial volume of feed and the volume of retentate) as described in **Table 4.3**, where the volume of treated water varied from 131 L to 593 L. Volume reduction factor values were progressively increased (from assay NF1 to assay NF4) to take the system to the limit while maintaining the quality of the effluent. This is the rationale behind the selection of the VRF values.

Table 4.3 *Volumes of feed and retentate, respective volume reduction factors (VRFs) as well as initial fluxes obtained in the different nanofiltration studies carried out*

Assay	Volume reduction factor (VRF)	Volume of Feed (L)	Volume of Retentate (L)	$J_{v,0}$ (L/h.m^2)
NF1	29	136	4.7	47
NF2	45	207	4.6	39
NF3	58	208	3.6	40
NF4	81	600	7.4	38

All nanofiltration studies were carried out at a constant transmembrane pressure (10 bar) and feed flow rate (370 L/h). These conditions were set based on previous work in the research group using the same system and a similar matrix (data not published). These studies were conducted in concentration mode, where permeate was collected over time into a clean tank and the retentate was recirculated back to the feed tank. Membrane permeability was determined throughout all experiments using flow rate permeate measurements. Since the assays were carried out outdoors, there were significant variations in temperature among the different assays and even throughout the same assay. Permeate temperature was, therefore, measured using a thermometer and all permeability values provided in this manuscript are corrected for a temperature of 25 ºC (viscosity correction) so that comparison of flux values throughout the different experiments would be possible.

Samples of permeate, feed, and retentate were taken and analyzed to determine the concentration of the following parameters: total solids, total suspended solids, total organic carbon, chemical oxygen demand, oil and grease, and total phenols. The nanofiltration removal efficiency (rejection) of each parameter was determined based on their concentrations in the global permeate (C_p) as well as in the initial feed concentrations (C_f) as follows:

$$R(\%) = 100 \times \left(1 - \frac{C_p}{C_f} \right) \qquad \text{(Equation 4.1)}$$

Although the determination of rejection using the initial feed concentration instead of using the concentrations in the retentate along time underestimates membrane effective rejection at each instant, this approach is more informative in terms of process performance.

For the longest nanofiltration experiment, samples of permeate were also taken throughout the assay to address the variation of permeate quality over time. Rejections were determined taking into account the concentration in permeate samples taken at each sampling time as well as the initial feed concentration.

The percentage of rejection due to adsorption (A) on the membrane was determined using Equation 4.2:

$$A(\%) = 100 \times \left(1 - \frac{C_p V_p + C_r V_r}{C_f V_f} \right) \qquad \text{(Equation 4.2)}$$

Where C_p, C_r, and C_f are the concentration of a given compound in the permeate, retentate, and feed, respectively, whereas V_p, V_r, and V_f are the volume of permeate, retentate, and feed, respectively.

When operating in concentration mode, the osmotic pressure difference ($\Delta\pi$) between the retentate and the permeate streams may have an impact in the permeate flux (Jv) profile because of the decrease in the driving force, according with Equation 4.3:

$$J_v = L_p(\Delta P - \Delta\pi) \quad \text{(Equation 4.3)}$$

where L_p is the membrane permeability and ΔP is the transmembrane pressure. The impact of the partial retention of low molecular weight molecules on the driving force was, thus, evaluated. For that, it was assumed (see Van't Hoff equation below) that molecules with high molecular weight do not significantly contribute to the osmotic pressure difference, even when retained, and only molecules with low molecular weight were considered relevant: small phenols and salts. From the Van't Hoff equation it can be seen that the osmotic pressure is directly proportional to the molar concentration of solutes and, therefore, solutes with a low molecular weight may reach relatively high molar concentrations even if their mass concentration is modest (while the opposite applies to large molecular weight solutes).

For both organic and inorganic molecules, the respective molar concentrations in the retentate were determined through a mass balance using the molar concentrations in the feed and permeate streams as well as the volume of these streams. Molar concentrations in the feed and permeate streams were determined using the mass concentrations obtained experimentally. The osmotic pressure difference between the retentate and the permeate side was, then, determined using the Van't Hoff equation, which can be applied in the range of the molar concentrations determined in this study:

$$\Delta\pi = RT(C_R - C_P) \quad \text{(Equation 4.4)}$$

where R is the gas constant, T is the absolute temperature, C_R is the molar concentration of solutes in the retentate stream, and C_P is their molar concentration in the permeate stream. As the molar concentrations were determined in the bulk solutions, the osmotic pressure difference calculated may be slightly underestimated since the local concentration of rejected molecules at the membrane surface was not considered.

For filtration volumes up to approximately 200 L/m^2, rinsing with tap water during 5 minutes was enough to recover membrane hydraulic permeability. Whenever a higher volume of wastewater was filtered per unit membrane area, a cleaning in place (CIP) was conducted using alkaline P3-

Ultrasil 11® (0.2%) during 45 min, followed by rinsing with tap water during 15 min. All CIP procedures were carried out at ambient temperature.

4.3.5 Analytical methods

The effectiveness of nanofiltration to treat the pre-treated olive mill wastewaters was evaluated by determining the following parameters using well established methods: total suspended solids (Standard Method 2540D [100]), total solids (Standard Method 2540B [100]), total organic carbon (Standard Method 5310B [100]), chemical oxygen demand (ISO 15705), oil and grease (Standard Method 5520C [100]), and total phenols [162]. The uncertainties associated with the analytical methodologies are as follows: 3% (total suspended solids and total solids), 1% (total organic carbon), 5% (chemical oxygen demand), 1% (oil and grease), and 10% (total phenols).

The quantification of the phenolic compounds tyrosol, hydroxytyrosol, and oleuropein was conducted by ionic chromatography using a Dionex ICS3000 system coupled to a photodiode array detector (DIONEX ICS series) as well as a Nova-Pak C18 column (60 Å, 4 µm, 3.9 mm x 150 mm). Gradient conditions were applied using 10% MeOH + 2% acetic acid (A) and 90% MeOH + 2% acetic acid (B) as follows: 100% A (0-10 min), 85% A and 15% B (10-15 min), 50% A and 50% B (15-25 min), 30% A and 70% B (25-30 min). The mobile phase flow rate was 0.5 mL/min and the oven temperature was 30 ºC. The phenolic compounds were monitored at 280 nm. The following detection limits were determined: tyrosol (35 mg/L), hydroxytyrosol (30 mg/L), and oleuropein (60 mg/L).

The presence of volatile compounds was determined in permeate and feed samples from the longest assay (NF 4) by solid phase microextraction (SPME) gas chromatography/mass spectrometry (GC/MS). The SPME procedure was conducted with a divinylbenzene/carboxen/polydimethylsiloxane fiber (DVB/CAR/PDMS; d_f 50/30 µm; needle size: 23ga; from Supelco). The incubation temperature and stirring speed were set to 40 ºC and 100 rpm, respectively. Extraction took 40 min while desorption took 3 min. A Shimadzu QP 2010 GC/MS with a Varian VF-5ms (30m x 0.25mm x 0.25µm) analytical column were used to detect the volatile compounds. The column temperature was held at 40 ºC for 5 min, increased to 170 ºC at a 5º C/min rate, then increased to 230 ºC at a 30 ºC/min rate and held for 4 min (splitless injection; ion source and interface temperatures set at 250 ºC).

4.4 RESULTS AND DISCUSSION

The disposal of large volumes of retentate streams is presently a challenge and needs to be taken into consideration when the technical feasibility of a membrane process is evaluated. Operating membrane systems up to high volume reduction factors leads to the generation of very low

volumes of retentate to dispose. In the present study, the highest volume reduction factors possible were attained by ensuring the minimum retentate volume, which was set according with the dead volume of the nanofiltration set-up. The performance of nanofiltration under such conditions is discussed below.

4.4.1 Membrane flux decline

Table 4.3 shows the initial permeate fluxes determined in the different experiments and **Figure 4.2** depicts the variation of membrane flux throughout the nanofiltration studies carried out up to different volume reduction factors.

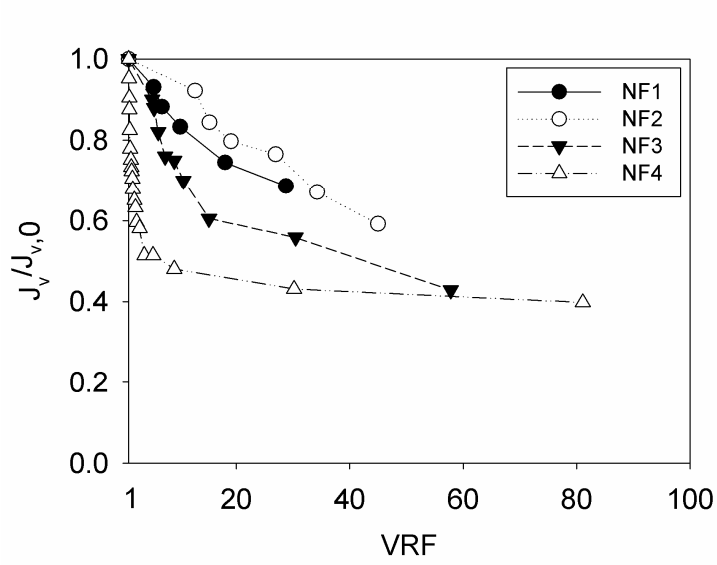

Figure 4.2 *Variation of normalized permeate flux (Jv/Jv, 0) with the volume reduction factor (VRF) throughout nanofiltration assays NF1 (VRF-29), NF2 (VRF-45), NF3 (VRF-58), and NF4 (VRF-81)*

Similar permeate flux profiles were observed in the studies carried out at the lowest VRF values of 29 (NF1) and 45 (NF2), with a total flux decline of 31% and 40%, respectively. A sharper flux decay is initially observed in the longest assay (NF4; VRF-81) until a VRF-10 is achieved. Beyond a VRF-33 value, the permeate flux decreased slightly. This trend was previously reported by other authors [141, 150, 163]. A similar pattern was observed in the assay NF3 (VRF-58), except for the fact that a steady flux was not achieved. Despite the fairly similar composition of the feed wastewaters in all the assays (**Table 4.2**), the slightly higher concentrations of solids determined for NF3 and NF4 may support the initial sharper flux decline comparatively to the NF1 and NF2 assays.

Since nanofiltration rejects dissolved salts as well as small organic molecules, the osmotic pressure difference, which acts against the transport of the water through the membrane, must also be taken into account. The osmotic pressure difference was determined by considering only low molecular weight compounds: low molecular weight phenols and salts. Low molecular weight phenols were selected for these calculation since phenols were generally poorly retained (see section 4.4.2), suggesting that the majority of these molecules possess molecular weights lower than the membrane molecular weight cut-off (150-300 Da). Larger phenols (even if retained) are not relevant in terms of osmotic pressure difference, because their molar concentration is low (even if their mass concentration is not negligible). An average molecular weight of 150 Da was, then, assumed for the small phenolic compounds [164] in the calculation of osmotic pressure difference. In the case of ions, calcium, magnesium, sodium and chloride were used as reference ions, and their concentrations were determined by inductively coupled plasma-atomic emission spectrometry. The final osmotic pressure difference calculated for the nanofiltration study NF1 was 4.7 bar. This osmotic pressure difference represents a significant driving force $(\Delta P - \Delta \pi)$ decrease, for which the contribution of salts rejection (4.4 bar) is much higher than that of low molecular weight phenols (0.3 bar). This calculation (4.7 bar) agrees with the value estimated using the concentration of total dissolved solids in the feed and permeate sides (4.6 bar), as described by EPA [49]. This decrease in driving force explains in large extent the flux decline (31% decrease) observed in **Figure 4.2** since a hydrostatic pressure difference (ΔP) of 10 bar was applied during nanofiltration, this decline is largely related to the increase of osmotic pressure difference between the retentate and the permeate streams. The important contribution of osmotic pressure difference, mainly due to the partial retention of salts, explains also the successful and easy recovery of membrane flux (for filtration volumes up to 200 L/m^2) by simply carrying out the rinsing of the membrane with tap water during 5 minutes. This feature is advantageous for the wastewater treatment since carrying out a rinsing instead of a chemical cleaning to restore membrane flux is much less time consuming and cheaper.

4.4.2 Rejection performance

Rejection and adsorption values determined for total suspended solids, total solids, total organic carbon, chemical oxygen demand, oil and grease, and total phenols in the assays NF1 to NF4 are depicted in **Figure 4.3**.

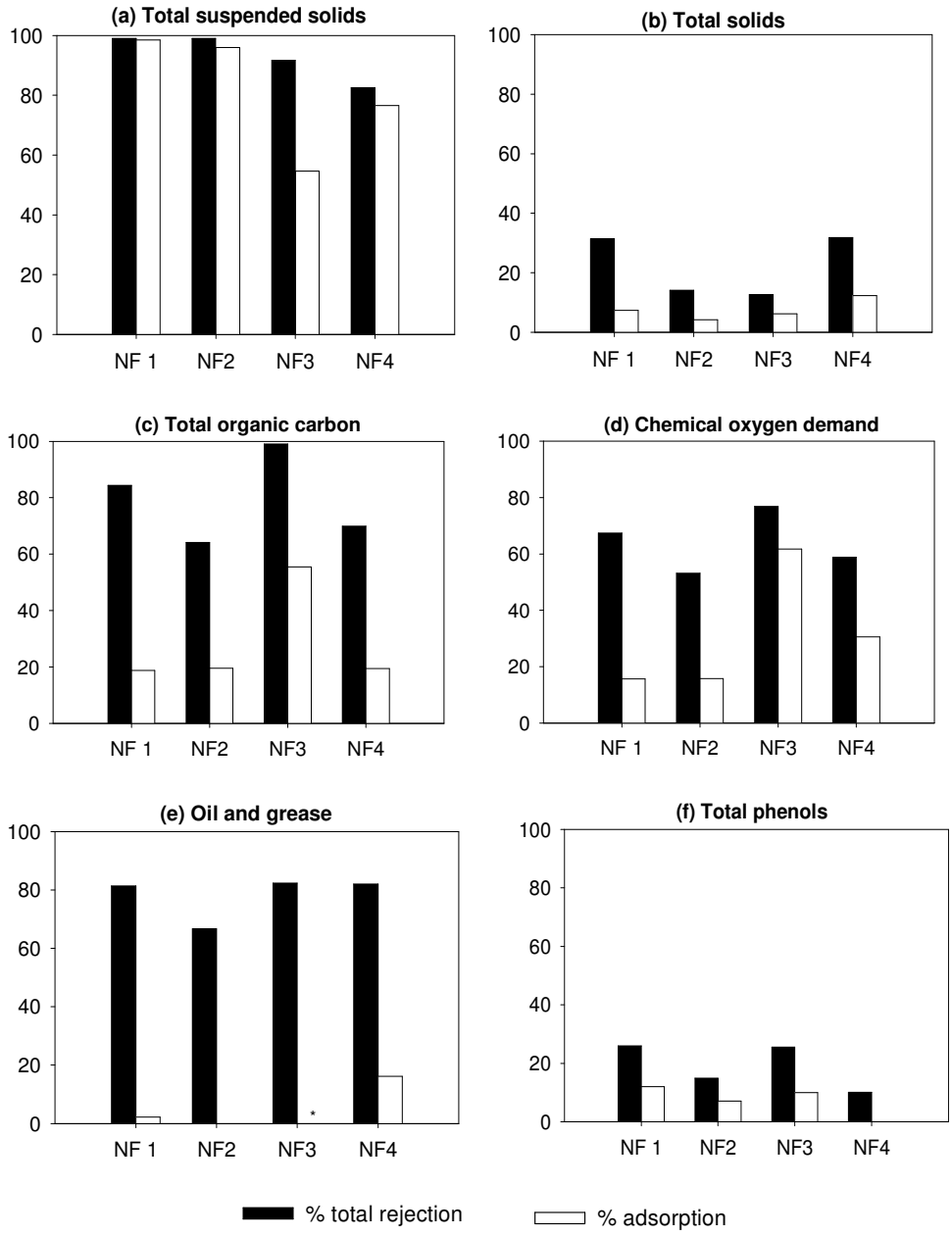

Figure 4.3 *Total rejection and adsorption percentages determined in NF1 (VRF-29), NF2 (VRF-45), NF3 (VRF-58), and NF4 (VRF-81) assays for total suspended solids (a), total solids (b), total organic carbon (c), chemical oxygen demand (d), oil and grease (e), and total phenols (f), taking into account the concentration of feed wastewater and total permeate*

Generally, very high rejections were attained for total suspended solids (83 to >99%), total organic carbon (64 to 99%), chemical oxygen demand (53 to 77%), and oil and grease (67 to >82%) while lower rejections were observed for total solids (13 to 32%) and total phenols (10 to 26%). The differences observed in the parameters might be explained by temperature fluctuations between studies and even during the same study as previously reported (e.g. [165]. Furthermore, possible interactions between different solutes in the real feed wastewaters used, namely solutes that were not addressed, may also play a role. COD values determined in the present study are concurrent with previous studies using different NF membranes to treat olive mill wastewaters: 59-79%, using NP010, NP030, and NF270 membranes at 10 bar [157]; 54-93%, using NF-90, NF-270, and a NF-(self-made) membranes at 5 bar [150]; 42.7-58.9%, depending on pressure (5-9 bar), using a DK membrane [146]. Depending on the membrane, total phenols' rejections reported by other authors vary significantly. Although rejection of total phenols between 80 and 99% were attained, depending on the membrane (NF-90, NF-270, and a NF-(self-made)) and pressure (5-20 bar) by Zirehpour et al. [138], much lower rejections (1-21%) were reported using a N30F membrane in another study [27]. Phenolic compounds detected in olive mill wastewaters present molecular weights in the range of 137-685 Da and several have molecular weights below 300 Da [164]. For instance, tyrosol and hydroxytyrosol, two of the most relevant phenolic compounds in this type of wastewater, have molecular weights of 137 and 153 Da, respectively. Since the molecular weight cut-off of the membrane is 150-300 Da, compounds with such molecular weights may permeate. Despite the significant difference in the concentration of target components in the nanofiltration feeds reported here and in literature, the concurrency of rejections attained demonstrates that nanofiltration is able to cope with feed wastewaters with variable compositions, validating its applicability at industrial scale, where fluctuations on feed composition are frequent.

Figure 4.3 evidences that adsorption on the membrane plays a relevant role in the rejection of total suspended solids and also has significant impact on the rejection of all the other components, except oil and grease. During the NF4 study, several permeate samples were taken as VRF factor increased to assess the variation of membrane efficiency towards the components addressed (**Figure 4.4**).

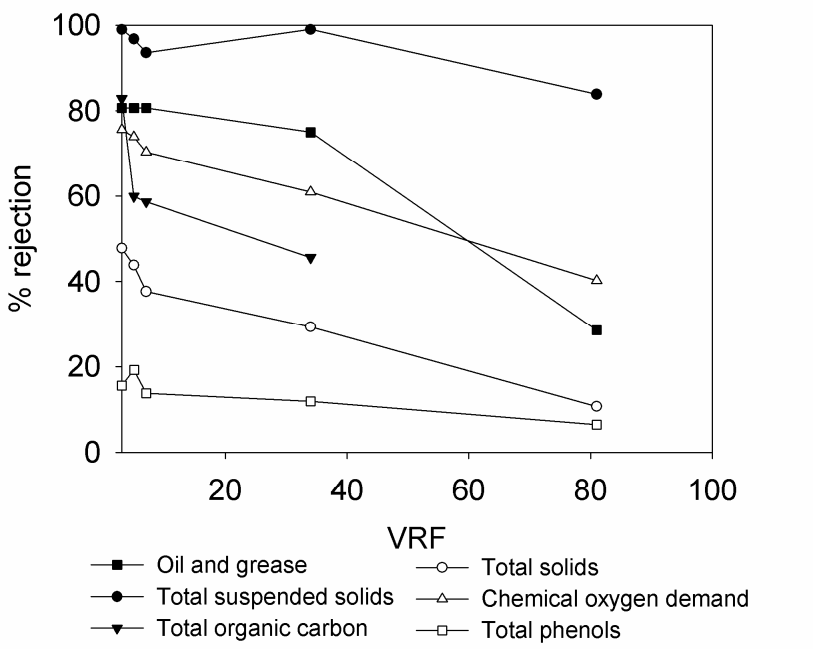

Figure 4.4 *Variation of the rejection of total suspended solids, total solids, total organic carbon, oxygen demand, oil and grease, and total phenols with the volume reduction factor (VRF) throughout the longest assay (NF4; VRF-81)*

Overall, noteworthy differences in the rejection of the components addressed were not observed up to VRF-34. However, between VRF-34 and VRF-81, a pronounced decrease in the membrane performance was observed. Assuming that the goal of an olive mill producer is to treat 1000 m^3, working with VRFs of 34 and 81 would result in the production of 29 and 12 m^3 of retentate, respectively, which in terms of the final treated water (971 and 988 m^3, respectively) are not very different. Therefore, treating olive mill wastewater at a VRF of 34 would be more interesting. Furthermore, filtration up to VRF of 34 is remarkable for the treatment of this type of effluent.

The rejection of solutes is considerably impacted by the increase of local concentration of solutes at the membrane surface, leading to lower rejection factors. The concentration of solutes at the membrane surface leads to a solute concentration gradient, enhancing the transport of solutes through the membrane [166]. The decrease of solutes rejection throughout nanofiltration has been widely reported in other studies [31, 75, 167, 168].

The concentration of the different components in the permeate, in the nanofiltration assays carried out, are shown in **Table 4.2**, where European legal limits for discharge into water bodies [169] are also presented. Total suspended solids (<0.2 to 2 mg/L) as well as oil and grease (<2.7 to 5.3 mg/L) concentrations are well below the legal limits (36-60 mg/L and 15 mg/L of total suspended solids and oils and grease, respectively). The permeate COD levels detected (288-506 mg O_2/L) might be correlated with the presence of total phenols (114-153 mg/L), which were poorly removed by the membrane (**Figure 4.3**) and are, thus, present at concentrations considerably

above the legal limits (0.5 mg/L). Low molecular weight phenols were expected to break through the membrane at some extent given their low molecular weight comparatively with the membrane molecular weight cut-off (150-300 Da) as previously observed by Garcia-Castello et al. [27]. In that study, almost all phenols were recovered in the NF permeate and further concentrated by osmotic distillation for application in food, cosmetic or pharmaceutical industries.

Other compounds, namely volatile compounds, could also contribute for COD values (**Table 4.4**). In this study, feed and permeate samples from the NF4 assay were analyzed by GC-MS and the mass spectra obtained for the different chromatogram peaks detected in each sample were compared with a mass spectra library, presenting similarities of 86-98%.

Table 4.4 *Volatile compounds identified in permeate and feed samples of the longest assay (NF4; VRF-81) by GC-MS, respective identifications similarities with the database as well as their molecular weight (MW)*

Tentative identification	Molecular structure*	Similarity (%)	MW (Da)	log K_{ow}
Cyclohexanol	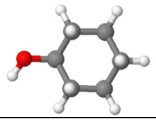	91	100.2	1.64**
2-Heptanone	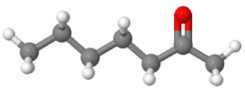	90	114.2	1.73**
2,4,4-Trimethyl- 1-pentanol	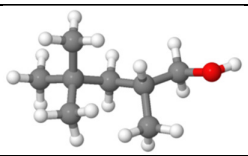	97	130.2	-
2-ethyl-Hexanal	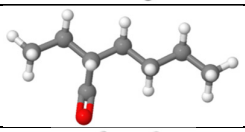	86	128.2	2.71**
Phenol	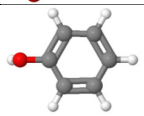	95	94.1	1.51**
2-ethyl-1-Hexanol,	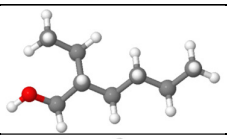	98	130.2	2.73**
m-cresol	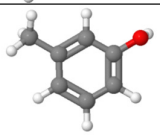	96	108.1	1.94***

The colors of the atoms in the molecular structures have the following meaning: gray represents carbon, white represents hydrogen, and red represents oxygen; a Jmol; b EPI Suite; c ChemSpider

All peaks were detected in the feed and global permeate samples and noteworthy differences in the peaks intensity in these samples were not detected, suggesting that they break through the

membrane. This feature is supported by the lower molecular weight of the molecules (94.1-130.2 Da) comparatively to the molecular weight cut-off of the membrane used (150-300Da) as well as their relatively low hydrophobicity, given by the logarithm of the octanol-water partition coefficient, log K_{ow} (**Table 4.4**). Size exclusion and hydrophobic interactions were, thus, not expected to be significantly relevant in the rejection of these molecules. One exception is the peak identified as 2-ethyl-1-hexanol, which is considerably more intense in the feed sample. This compound has one of the highest log K_{ow} values, which might lead to adsorption on the membrane at some extent, increasing its rejection. Even though the compound identified as 2-ethyl-hexanal presents similar molecular weight and log K_{ow}, its molecular structure is likely to allow a better orientation of the molecule, facilitating its partition into the membrane structure (**Table 4.4**). The following compounds identified have been previously reported in olive oil: 2-heptanone [170, 171], phenol [172, 173], and 2-ethyl-1-hexanol [173].

The combination of olive mill wastewater with the recovery of added value by-products was evaluated in this study as a potential economical and sustainable strategy for the treatment of these effluents. The low rejection of total phenols by the NF membrane addressed (**Figure 4.3**f) suggested that the recovery of valuable phenolic compounds could be economically interesting. To further assess this feature, a chromatographic analysis was conducted to quantify the phenolic compounds hydroxytyrosol, tyrosol, and oleuropein. However, these compounds were not present at concentrations above the detection limits of the analytical method (30-60 mg/L), suggesting that their recovery would not be economically viable. Therefore, for further improvement of the treated water quality towards legislation fulfillment, a lower molecular weight cut-off membrane could be used or a polishing step comprising advanced oxidation could be carried out for further removal of phenolic compounds and reduction of COD levels. Previous studies from the authors [136] proved that Fenton's process would probably allow compliance with European legislation given that chemical oxygen demand and total phenols were reduced up to 90 and 92%, respectively [136, 174]. COD and total phenol removals (>80%) by Fenton and Fenton-like [145] as well as by H_2O_2/UV and O_3/UV (99%) [168] were also previously reported. Among them, Fenton's process could be the most economically viable since it may be conducted at ambient temperature and pressure conditions, besides the simplicity of the equipment required and operation [175].

4.4.3 Economic study evaluation

The economic feasibility of treating 1000 m^3 of pre-treated olive mill wastewater by nanofiltration was evaluated. The olive mill wastewater assessed in the present study was provided by an olive oil industry where production takes place during 7 days/week and 24 h/day, from November to March. Presently, the annual treatment of 1000 m^3 of wastewater consists in a screening, coagulation/flocculation, and catalytic oxidation (Fenton process). This treatment is carried out after the 5 month production period since a 1000 m^3 capacity lagoon is available for wastewater

accumulation on the wastewater treatment plant onsite. However, a lagoon with such capacity is not available on many olive oil production sites due to footprint constraints. In these cases, wastewater must be readily treated. Having this into consideration, an economical evaluation study was conducted for the two scenarios. In case wastewater is treated during the 5 months production period, the treatment takes place 7 days/week (plant required capacity of 7 m^3/day, based on the wastewater volume to be treated and the respective treatment period). In the other scenario, treatment could be carried out in a shorter period of time when olive oil production is finished. In this scenario, the treatment of 30 m^3/day was set, resulting in a working plan schedule of 33 days/year, 5 days/week. In both cases, the NF plant was assumed to operate 22 h/day and the remaining 2 h used to CIP, filling, and start-up. The economical evaluation is presented for the volume reduction factors of 34 and 81 (**Table 4.5**). The VRF-34 was selected based on **Figure 4.4**, where a deterioration of treated water quality was observed beyond this value while VRF-81 corresponds to the longest NF study presented.

For a plant capacity of 7 m^3/d, two spiral-wound Desal DK elements would be needed with total membrane areas of 12 m^2 (6 m^2 each) or 18.2 m^2 (9.1 m^2 each), depending on the VRF value. For the plant capacity of 30 m^3/d, two spiral-wound Desal DK elements would be needed with total membrane areas of 50.2 m^2 (25.1 m^2 each) or 59.4 m^2 (29.7 m^2 each). The membrane area required for each case was determined by calculating an average flux, considering the integral of the permeate flux over time in the NF studies presented. Implemented areas (**Table 4.5**) are overestimated and were set based on the filtration area of Desal DK membranes available in the market, providing some flexibility for the treatment of larger wastewater volumes, if required.

Capital costs involved in the implementation of the NF plant were determined based on the current prices available for membranes and equipment, which include a feed pump, pressure transmitter, pressure regulators, valves, membrane housings, pipelines, and a metallic microfilter cartridge for the pre-filtration step. Safety and control mechanisms were also considered: control of minimum inlet pressure and control of maximum operating pressure; safety valve for maximum operating pressure; external emergency stop button; pressure and recirculation regulators; flowmeters for permeate, retentate, and recirculation; electric switchboard with an electronic circuit with inlet and outlet conductivity reader and adjustable set points, alarm for minimum inlet pressure and maximum operating pressure, control of maximum tank level and electronic hour counter. Metal parts in the plant contacting with liquids are considered to be made of AISI316 stainless steel. Tanks for nanofiltration and CIP operations were not included given the existence of several tanks in the current existing treatment plant that could be used for these purposes. Costs with equipment (4800-7280 € and 20080-23760 € for plant capacities of 7 m^3/d and 30 m^3/d, respectively) were determined, assuming that all the nanofiltration equipment costs 400 € per each m^2 of membrane implemented area (reference value provided by a manufacturer of nanofiltration equipment).

Total operation costs were determined considering costs with energy, manpower, membrane replacement, CIP (chemicals and water), retentate disposal, as well as repair and maintenance. Energy demand was determined based on the selection of adequate pumps to deliver the feed flow rates required. Energy costs were calculated considering the EU28 average industry electricity prices applied in 2014 (0.120 €/kWh) [176]. Considering the time needed for the cleaning of the NF plant (approximately 1 h/d), expedition of the retentate for disposal (10 h/year), and monitorization of permeate quality (50 or 100 h/year, depending on plant capacity), total manpower hours of 96 or 208 h were determined. Manpower costs were determined taking into account the daily payment of workers in the olive oil industry in 2015/2016 (53.90 €/day) [177] and the number of manpower hours. Given the annual short operation period (1-5 months), membrane replacement costs were determined based on a membrane element life-time of 5 years and current membrane prices. Costs related with cleaning in place chemicals (P3-Ultrasil 11®) were determined based on the cleaning protocol described in the Materials and Methods section, which was demonstrated to provide an adequate recovery of the membrane performance in terms of permeability and solutes rejection. Water costs were also accounted for and were estimated based on the volume of water required for CIP as well as the current costs of water for Spanish industries (1.81 €/m^3). It was assumed that retentate disposal would cost 32 €/m^3 [178]. Repair and maintenance costs were determined as 2% of capital costs.

Total operation costs were, then, determined as 2.56-3.07 €/m^3 (plant capacity of 7 m^3/day) and 2.62-3.08 €/m^3 (plant capacity of 30 m^3/day). Very similar operation costs were obtained for the different plant capacities. However, wastewater treatment during the 5 months production would be economically advantageous in terms of capital costs (**Table 4.5**) and plant footprint (the implementation of a lagoon would not be required).

Table 4.5 *Economic feasibility study for the nanofiltration treatment of olive mill wastewater, considering different plant capacities, defined according*

		Treatment plant schedule for 5 months/year; 7 days/week (November-March)		Treatment plant schedule for 33 days/year; 5 days/week (after March)	
		VRF-34	**VRF-81**	**VRF-34**	**VRF-81**
Nanofiltration	**Assumptions**				
	Capacity of the NF treatment plant (m^3/day)	7	7	30	30
	Implemented membrane area (m^2)	12.0	18.2	50.2	59.4
	Desal DK membrane	DK4040C1025	DK4040C1024	DK8040C-50P	DK8040F1071
	Investment costs				
	Equipment cost of the NF plant (400 €/m^2) (€)	4800	7280	20080	23760
	Operation costs				
	Energy (0.12 €/kWh) (€)	88	88	62	62
	Manpower (€)	1499	1499	645	645
	Membrane replacement (lifetime of 5 years) (€)	384	400	1000	1040
	Cleaning chemicals (€)	34.5	34.5	7.6	7.6
	Cleaning tap water (€)	6.9	6.9	1.6	1.6
	Retentate disposal (€)	965	386	965	386
	Repair and maintenance (2% of capital costs) (€)	96	146	402	475
	Total operation costs/year (€/year)	3074	2561	3083	2618
	Total operation costs/m^3 (€/m^3)	3.07	2.56	3.08	2.62

For each plant capacity, the economic study is presented for VRF-34 and VRF-81

Table 4.5 *Economic feasibility study for the nanofiltration treatment of olive mill wastewater, considering different plant capacities, defined according (continuation)*

Screening	**Investment costs (€)**	11 500			
DAF	**Investment costs (€)**	21 000			
	Operation costs (€/m^3)	1.25			
Fenton	**Investment costs (€)**	75 900			
	Operation costs (€/m^3)	0.36			
	TOTAL OPERATION COSTS (€/m^3)	4.68	4.17	4.69	4.23

A sensitivity analysis was conducted for the 5 month treatment at VRF-34 by determining the impact of varying the cost of water, retentate disposal, energy, and membrane replacement on total operation cost (**Figure 4.5**). Retentate disposal significantly impacts total operation cost, followed by membrane replacement. Fluctuations associated with water and energy costs have minor influence.

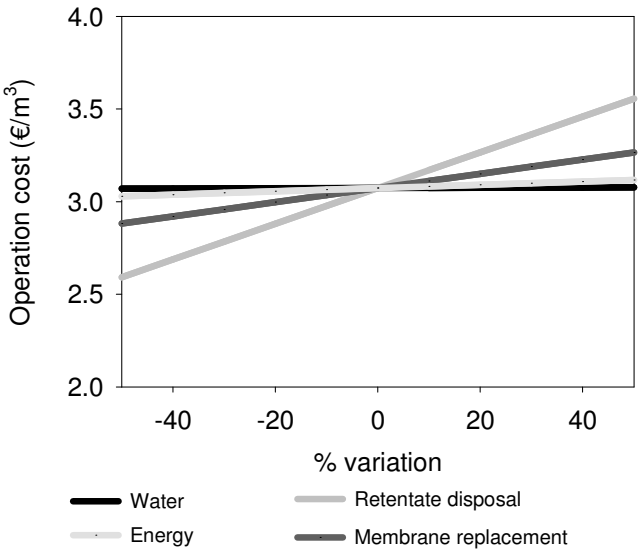

Figure 4.5 *Sensitivity analysis: impact of the cost of water, retentate disposal, energy, and membrane replacement on total operation cost for the 5 month treatment at VRF-34*

Besides nanofiltration, other processes would be needed to be integrated to ensure adequate treatment of olive mill wastewater: screening, DAF (pre-treatment), and Fenton process (post-treatment for further removal of chemical oxygen demand and phenols). The screening unit is already in place in the existing plant and has an investment cost of 11 500 €. Regarding the DAF pre-treatment, an operating cost of 1.25 €/m^3 was estimated accounting for the amount of coagulant, flocculant, and hydrogen peroxide consumed. Investment costs that include the DAF unit, an electric switchboard, a system for chemicals dosage, and a pump were estimated at 21 000 € (according with manufacturers). According with a recent study carried out by the authors, Fenton process would have an operation cost of 1.09 € per kg of chemical oxygen demand removed, which included iron and hydrogen peroxide as well as pH adjustment reagents such as sodium hydroxide and sulfuric acid. Using this value, the operation cost associated to the Fenton process was estimated at 0.36 €/m^3 (**Table 4.5**). In this calculation, it was considered that a decrease of COD from 455 mg O_2/L (concentration in the NF permeate for the longest experiment, NF4) to 125 mg O_2/L (maximum legal value for discharge within European legislation) would be required. This process is already implemented in the wastewater treatment plant currently available and involved an investment cost of 75 900 €.

Taking into account the operation costs associated with DAF, NF, and Fenton process, total operation costs between 4.17-4.69 €/m^3 were estimated (**Table 4.5**). The current treatment strategy adopted by the olive oil producer comprising screening, coagulation/flocculation and Fenton oxidation has an operation cost of 7.76 €/m^3. This operation cost is much higher than the value estimated for the treatment proposed in present study and would render savings of 3.07-3.59 €/m^3, demonstrating that the implementation of nanofiltration is a viable economical alternative to the current treatment. The savings related to the shift from the current treatment to NF would almost covers NF plant investment costs for a plant operating during the 5 month period at a VRF-34 (the most likely scenario for producers with limited treatment plant area). Regarding the investment costs, the current treatment applied by the olive oil production facility (screening, coagulation/flocculation and Fenton oxidation) required a higher investment (143 450 €) comparatively with the treatment proposed in the present study (screening, dissolved air flotation, nanofiltration, and Fenton oxidation) (113 200-132 160 €). For the specific case of this olive oil producer, a much lower investment would be needed (25 800 – 44 760 €) to swap the treatment strategy since the screening and Fenton oxidation units already exist. This swap would also allow the reduction of the treatment plant footprint from 196 to 52 m^2.

4.5 CONCLUSIONS

Overall, data attained in this study demonstrates that nanofiltration can be operated at considerably high VRF values and still be effective towards the removal of the components addressed. Considerably high rejections of total suspended solids, total organic carbon, chemical oxygen demand as well as oil and grease were attained. Only the concentration of total phenols and chemical oxygen demand in permeate could not comply with the European legislation for discharge into water bodies. The concentration of total phenols determined in the permeate as well as the presence of volatile compounds probably contributed to chemical oxygen demand above legal limits. Since the recovery of phenolic compounds was found not economically relevant, the use of AOPs as a polishing step to further remove chemical oxygen demand would allow compliance with legislation regarding these components.

The economic study demonstrated that nanofiltration is not only technical but also economically feasible. Operation costs were determined for different treatment plan schedules and VRF: 2.56-3.07 €/m^3 (7m^3/d) or 2.62-3.08 €/m^3 (30 m^3/d). NF treatment, combined with DAF and Fenton process, is an economically viable alternative since the total operation costs obtained (4.17-4.69 €/m^3) only represent approximately 54-60% of the total operation costs associated to the treatment currently applied.

4.6 ACKNOWLEDGEMENTS

Financial support from the EU FP7/SME theme [SME-2013-1] through the project O-WaR (grant agreement no: 605641) as well as from Fundação para a Ciência e a Tecnologia through the post-doc fellowship SFRH/BPD/94303/2013, is gratefully acknowledged. iNOVA4Health - UID/Multi/04462/2013, a program financially supported by Fundação para a Ciência e Tecnologia/Ministério da Educação e Ciência, through national funds and co-funded by FEDER under the PT2020 Partnership Agreement is also acknowledged. This work was also supported by the Associate Laboratory for Green Chemistry LAQV which is financed by national funds from FCT/MEC (UID/QUI/50006/2013) and co-financed by the ERDF under the PT2020 Partnership Agreement (POCI-01-0145-FEDER - 007265). The authors would also like to acknowledge Renata Tomczak-Wandzel and Charles Otis for providing the pre-treated wastewaters as well as Ana Almeida for analytical support.

5 SOL-GEL MEMBRANE MODIFICATION FOR ENHANCED PHOTOCATALYTIC ACTIVITY

Published as: R.M. Huertas, M.C. Fraga, J.G. Crespo, V.J. Pereira, Sol-gel membrane modification for enhanced photocatalytic activity, Separation and Purification Technology 180 (2017) 69-81.
The author M.C. Fraga was directly involved in planning and executing the filtration experiments, on their sample and data analysis.

5.1 SUMMARY

Novel materials comprising titanium dioxide (TiO_2), silicon dioxide (SiO_2) and silicon carbide (SiC) semiconductors, were deposited over silicon-carbide substrates to develop photocatalytic membranes. The synergistic effect between TiO_2 obtained by sol–gel process, Degussa P25 and silicon carbide nanoparticles were tested in terms of photocatalytic degradation of methylene blue and their influence over porosity. The surface of the photocatalyst layers developed were characterized by scanning electron microscopy (SEM) showing that the immobilization was carried out successfully whereas the contact angle measurements revealed improved hydrophilic properties. Different surface properties were obtained depending on the different coating compositions applied.

Several photocatalytic experiments were conducted and reproducibility was tested using the most promising membranes in terms of photodegradation potential that reached up to 72% degradation of methylene blue. Comparison of UV degradation efficiency between unmodified and modified substrates revealed a synergistic effect when TiO_2 and silicon carbide were combined. The most promising membrane in terms of photocatalytic effectiveness and reusability was modified with SiO_2 obtained by sol-gel combined with Degussa TiO_2 nanoparticles. This membrane was used in a dead-end filtration system combined with UV light. Results confirmed the photocatalytic activity of the membrane combined with filtration, showing that the modified membranes have a high potential to degrade organic contaminants.

5.2 INTRODUCTION

Several contaminants such as oil, pesticides, pharmaceuticals and personal care products, have been detected in water sources all over the world at ng L^{-1} to low µg L^{-1} levels, causing a particular concern due to their threat to the aquatic environment and potential toxicity [3, 179-181].

Advanced oxidation processes (AOPs) employing heterogeneous photocatalysis proved to be one of the most effective treatments for wastewaters that are difficult to treat biologically [65]. Among the heterogeneous catalyst widely tested, TiO_2 nanoparticles revealed to be promising materials to promote a good level of efficient degradation, being reported as chemically stable and biologically benign [65, 182]. Silicon carbide membranes display good chemical, thermal and mechanical properties, useful for harsh environmental applications [183]. In addition, due to their porous structure, these supports provide a high-surface area structure over which TiO_2 nanoparticles may be homogeneously immobilized. Moreover, silicon carbide can be used in ultrafiltration processes at industrial scale, given their advantages in terms of high throughput, reduced cost and footprint needed by sustainable processes. However, their effectiveness may be hindered by fouling caused by organic compounds present in wastewaters that severely decrease the water flux and the membrane lifetime [184]. The use of silicon carbide membranes to treat aqueous streams is rather limited [38, 185, 186]. Recent studies state that the development of a defect free top layer on silicon carbide membranes represents a challenge [38, 187].

Coupling stable photoactive TiO_2 layers with water filtration technology can thus be beneficial to produce defect free top layers, decrease fouling components and improve the water quality of effluents [85, 182, 188-191]. However, coupling of photoactive layers in ceramic substrates was not explored widely [192]. Moreover, the control of membrane porous size in water filtration is extremely important to adjust the molecular weight cut-off of the membranes and thus improve the retention of pollutants.

The well studied sol-gel route, is highly recommended to synthetize TiO_2-based photocatalysts with high oxidation efficiency as well as for TiO_2 immobilization in a large number of supports to control their porosity [85, 86, 190-192], and eliminate substrate defects of the photoactive top layer [188, 189].

The addition of SiO_2 to TiO_2 was reported to lead to a higher hydrophilicity and photocatalytic activity [193, 194], which enhanced the self-cleaning ability of glass surfaces [195].

This work focuses on the modification of silicon carbide ceramic membranes, aiming to maintain or improve their permeability to aqueous media while providing them with photocatalytic activity, allowing for degradation of fouling agents during operation and improving the water quality of effluents.

5.3 MATERIAL AND METHODS

5.3.1 Materials and reagents

Commercial flat sheet silicon carbide membranes with *a* porosity gradient were provided by LiqTech International and used as substrates.

Silicon carbide (SiC) nanoparticles provided by *LiqTech* International (with 360 nm of nominal diameter measured by dynamic light scattering using a Zetasizer Nano ZS90 equipment) were used in a polyvinyl alcohol (PVA) **(**Sigma Aldrich**)** solution (1% w/v).

Titanium*(IV)* isopropoxide (TTIP) (Sigma Aldrich, ≥97%) and tetraethyl orthosilicate (TEOS) (Sigma Aldrich, 98%), were used as precursor reagents in the sol-gel procedure. Isopropyl alcohol supplied by Across Organic (99,6%) and polyethylene glycol sorbitan monooleate (Tween 80;1,310 Da) supplied by Merck were used as received**.** Commercially available Degussa P25 *titanium dioxide nanoparticles* (30-90 nm of nominal diameter), were also employed in this study. All solvents employed were of reagent-grade quality and used without further purification. Distilled water and rapeseed oil (Sigma Aldrich) were used to characterize the contact angle of the unmodified and modified surfaces. Methylene blue (Merck) was employed as a tester dye to characterize the photocatalytic activity of the membranes.

5.3.2 Preparation of modified membranes

Commercially available silicon carbide flat membranes were cut (thickness of 0.3 cm and area of 11.4 cm^2) and thoroughly cleaned with acetone, methanol and water followed by heating at 80ºC overnight. The top layer of unmodified substrate, with the lowest nominal pore size was modified using the drop-casting deposition method.

5.3.2.1 Deposition process of sol-titanium dioxide

Silicon carbide membranes were coated with three layers (L_3) of titanium dioxide obtained by the sol-gel procedure [196, 197], to ensure a good mechanical stability without sacrificing the photocatalytic activity. During the sol-gel process, different concentrations of precursor were tested (**Table 5.1**). In this procedure, a molar ratio previously optimized of the other reagents Tween 80, isopropyl alcohol and acetic acid (1:45:6) were used with different precursor concentrations.

The following procedure was used: in an amber bottle, Tween 80 was dissolved vigorously in isopropyl alcohol for 10 min with a magnetic stirrer. Acetic acid was then incorporated for esterification, during 20 min. Then, the different amounts of TTIP precursor detailed in **Table 5.1**

were added and the reactants thoroughly mixed during 2h to prepare the different modified membranes.

This preparation process was used to obtain all titanium solutions hereinafter described.

The sol solutions prepared were easily deposited (0.750mL) onto the silicon carbide surfaces by *drop-casting*. The modified membranes (denoted as SGTi) were subsequently dried for 1 h at room temperature and calcined in a multi-segment programmable furnace using a ramp rate of 3 ºC/min up to 500 ºC, maintained for 15 min to remove the organic reagents, stabilize the pore structure and induce crystallization of titanium dioxide. Finally, the membranes were cooled down naturally to room temperature, to avoid cracks and obtain a densified structure. This protocol was repeated three times to add three modified layers to the membranes (**Figure 5.1**).

For the most promising photocatalytic membranes (measured in terms of their methylene blue degradation potential), with the same molar ratio of the sol solution, thermal protocol and number of layers determined were also employed over an intermediate layer of silicon carbide (**SiC**/**SGTi**) **(Figure 5.1**). The incorporation of specific nanoparticles as an intermediate layer could help to improve the mechanical stability of the membrane by producing defect-free surfaces and improve the adhesion of the top layer [198]. Moreover, the presence of SiC nanoparticles could also increase the UV photocatalytic activity due to its activity as semiconductor with wide bang gap [199]. This intermediate layer was prepared from a SiC slurry (1% w/v) using a solution of 1% w/v of polyvinyl alcohol as binder. The sonicated solution of SiC nanoparticles (1 mL) described before was finally dropped over the SiC substrates and heated in air at 400ºC during 5 h to achieve a complete removal of the binder.

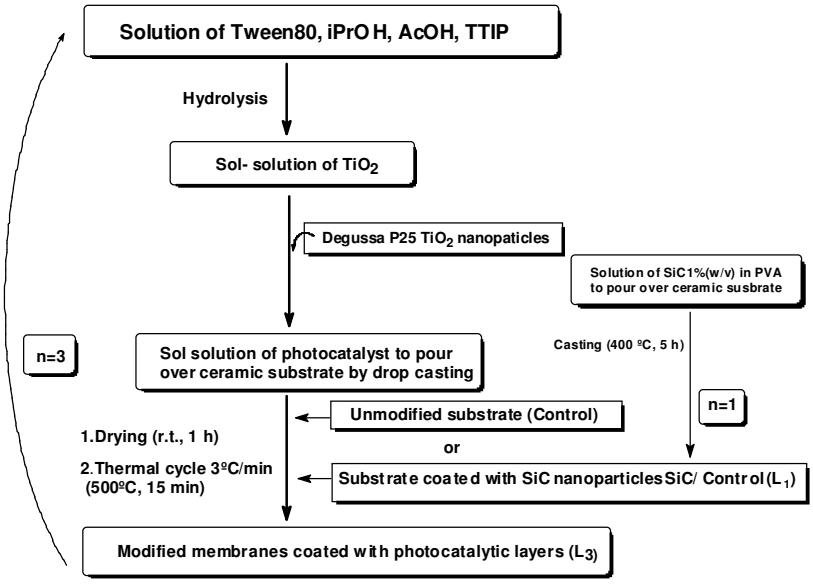

Figure 5.1 *Flow chart depicting the basic experimental procedures followed for sol deposition process with titania.*

5.3.2.2 Deposition process of sol-titanium dioxide with Degussa P25 TiO_2 nanoparticles

Ceramic substrates were also modified by mixing the TiO_2 obtained by sol-gel with commercial Degussa P25 TiO_2 nanoparticles **(Figure 5.1**). The synthesis of sol-gel TiO_2 was carried out using the previously described procedure with addition of the suitable amount of Degussa P25 nanoparticles after titania hydrolysis, to obtain different modified membranes in terms of the molar ratios of sol titania:Degussa (**SGTi-D**) of 1:1, 2:1, 1:2 and 1:3 (**Table 5.1**). After sonication, the set amounts of Degussa mixed with sol-gel TiO_2 were poured over substrates, dried for 1 h at room temperature and calcined using the thermal protocol described before (**Figure 5.1)**. This procedure was repeated three times for each membrane (L_3).

The SiC slurry prepared (1% w/v in polyvinyl alcohol), was deposited (1 mL) to prepare also the SiC intermediate layer in these membranes, before coating with the TiO_2 photocatalyst (**Figure 5.1)**.

Table 5.1 *Molar ratio compositions followed for the preparation of different membranes with photocatalytic properties.*

MEMBRANE MODIFICATION	MEMBRANES	TTIP (SGTi) Molar	P25 (D) Molar	TEOS (SGSi) Molar
SOL-GEL(SG)	**SGTi 0.5(L_3)** (*)	0.5	-	-
	SGTi 1 (L_3) (*) (**)	1.0	-	-
	SGTi 1.5 (L_3) (*) (**)	1.5	-	-
	SGTi 2 (L_3) (*)	2.0	-	-
	SGTi 3 (L_3) (*)	3.0	-	-
COMBINATION OF SOL GEL(SG) AND DEGUSSA(D)	**SGTi 0.5-D0.5 (L_3)** (*) (**)	0.5	0.5	-
	SGTi 1-D0.5 (L_3) (*) (**)	1.0	0.5	-
	SGTi 0.5-D1 (L_3) (*) (**)	0.5	1.0	-
	SiC/SGTi 0.5-D1.5 (L_3) (*)	0.5	1.5	-
	SGSi/SGSi-D (L_1) (***)	-	1.0	1.5
	SGSi/SGSi-D (L_2) (***)	-	1.0	9.3
	SGSi-D (L_3) (***)	-	1.0	0.9

(*) Molar ratio respect to surfactant Tween 80.

(**) Also tested with intermediate layer of silicon carbide

(***) Molar ratio between total SiO_2 and Degussa TiO_2 nanoparticles present in the sample.

5.3.2.3 Deposition process of sol-silica with Degussa P25 TiO2 nanoparticles

Three different substrates were modified with SiO_2/TiO_2 as reported by Fateh *et al*. [194]. The presence of SiO_2 as intermediate layer was proposed as a coupling agent, due to compatibility with the substrate. Different silica sol solutions were attained using TEOS as silicon dioxide precursor and commercial Degussa P25 TiO_2 nanoparticles (**Table 5.1** and **Figure 5.2**).

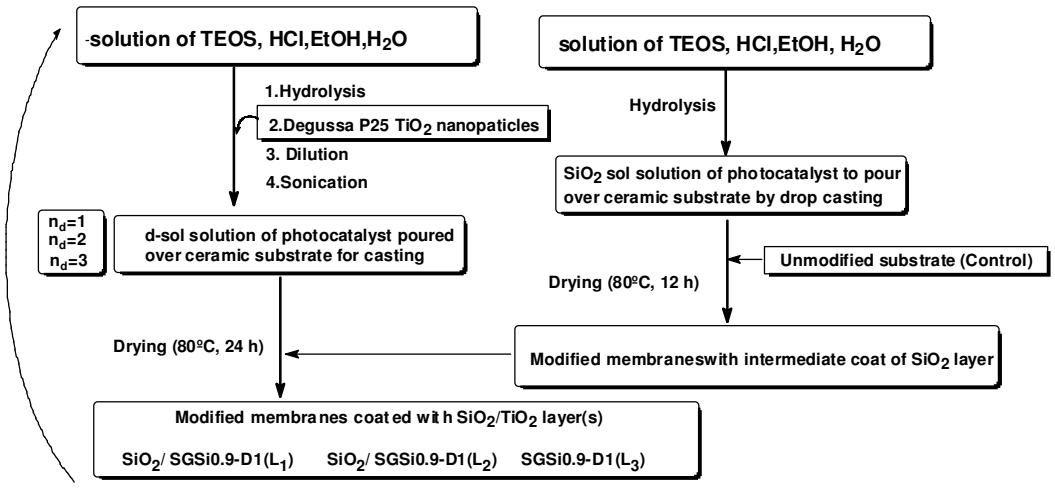

Figure 5.2 *Flow chart depicting the basic experimental procedures followed for sol deposition process and designation of membranes with silicon dioxide and titanium dioxide.*

5.3.3 Material characterization

5.3.3.1 Evaluation of photocatalytic activity

The photocatalytic properties of the unmodified and modified membranes were evaluated based on their ability to degrade methylene blue. UV experiments were conducted in a bench-scale UV collimated beam set-up with an UVH 1019 Q-6 lamp (UV-Technik, UK), that emits polychromatic light, housed in a shuttered box with PN310 quartz (UV-Technik, UK) that eliminates the wavelengths below 310nm. A maximum irradiance value (power per square centimetre of lamp) of 6mW/cm^2 was measured using a calibrated radiometer (IL393, International Light, Newburyport, MA), placed at the same height of the solution level in the Petri dish.

The photocatalytic experiments were conducted in a specially designed double-walled glass Petri dish (refrigerated within walls) placed beneath the UV source. The temperature through the double-wall glass petri dish inside the reactor was maintained at 23±2 ºC by the circulation of cold water. 30 mL of a constantly stirred aqueous solution of 30µM of methylene blue, was subject to

UV direct (without membrane) and indirect photolysis. Indirect photolysis was achieved when the modified membranes pieces were placed in the middle of the reactor.

Dark reactions were performed under the same conditions to test the adsorption capacity of the unmodified and modified membranes. Before each experiment, the absorbance of several standard solutions was measured at 664 nm to prepare a calibration curve using a UV-Vis spectrophotometer (Ultrospec 2100 pro UV-VIS). This curve was used to determine the concentration of methylene blue in the different samples taken at different experimental times (0, 20, 40 and 60 minutes). The concentration of methylene blue in each sample was determined by six absorbance measurements. The percent of photocatalytic degradation of the methylene blue solution obtained by each membrane after 60 minutes was calculated using Equation 5.1:

$$\% \text{ Degradation of methylene blue} = \frac{C0-C60}{C0} x100 \qquad \text{(Equation 5.1)}$$

where C_0 is the initial average concentration and C_{60} the average concentration of the methylene blue measured after 60 minutes.

For the most promising membrane, in terms of photocatalytic activity and reusability potential, a long term assay was also performed to determine the time needed to achieve total degradation of methylene blue.

5.3.3.2 Membrane characterization

The top layer and cross section morphology of the unmodified and the most promising modified membranes (in terms of sol-gel composition, photocatalytic properties and reusability potential) were characterized by scanning electron microscopy (SEM). The membranes were prepared by carefully cutting the membrane surface that were sputter coated with an Au/Pd thin film using a South Bay E5100 apparatus. They were then analysed by scanning electron microscopy in a JEOL FEG-SEM model JSM-7001 microscope.

Analysis of the porous features of the SEM images was made using the ImageJ software (an image processing program*)* to compare the different top layers produced [200, 201] (**Figures A.1-A.13** from the Section A1).

The contact angle of a sessile drop was determined on three different places randomly chosen of each membrane, to measure their hydrophilicity and oleophilicity using distilled water and rapeseed oil, respectively. A KSV CAM2008 equipment, a fully computer controlled instrument

based on video capture of images and automatic image analysis was used for this purpose. The determination of the contact angle was carried out by letting water or oil drop (10-12µL) fall on the surface of the material, for which the contact angle was determined. A camera captured the drop over time (consecutive frames), and the software coupled to the equipment retrieved the left contact angle, the right contact angle, and the mean of these values. Several measurements were carried out in three different zones of the membranes. Twenty frames were attained for each measurement, with a frame interval of 100 ms.

In order to ensure that Si or Ti were not released from the membrane surfaces, several modified membranes were subject to the same photocatalytic conditions using distilled water instead of the methylene blue solution as matrix. Si and Ti elements were analysed by inductively coupled plasma–atomic emission spectroscopy (Horiba Jobin-Yvon, France).

5.3.3.3 Membrane filtration performance

A dead-end filtration system (**Figure 5.3)** inserted within a collimated beam reactor and coupled to a vacuum pump (model: DOA-P504A-BN, GAST Manufacturing) was used to compare the performance of the unmodified and the most promising modified membrane in terms of photocatalytic activity, reusability, controlled porosity, homogeneity and hydrophilicity (**SGSi-D(L_3)**). Circular membranes with 4.7 cm diameter (3 cm of filtration diameter that correspond to 7 cm^2 filtration area) were used for this purpose. Tests were conducted in the presence and absence of UV light in order to study the effect of the modification on the membrane performance and the photocatalytic activity.

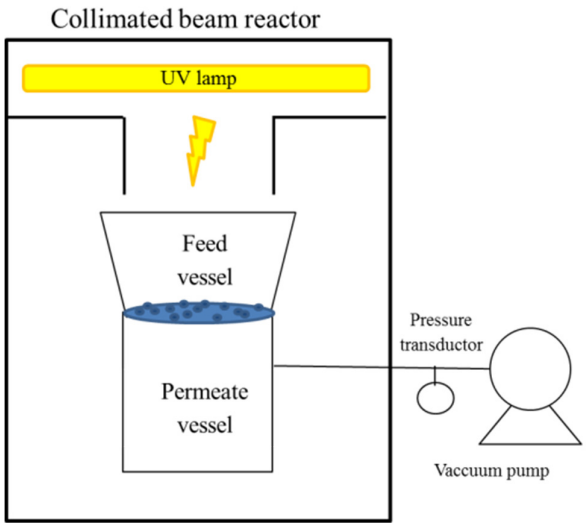

Figure 5.3 *Setup used to test the membrane filtration performance.*

The membrane filtration performance of the unmodified and modified membranes was compared by filtering 250 mL of a 30 µM methylene blue solution. The applied transmembrane pressure was 0.2 bar. The percent removal of methylene blue was calculated using Equation 5.2:

$$\% \text{ removal of methylene blue} = \frac{Cfeed - Cpermeate}{Cfeed} x100 \qquad \text{(Equation 5.2)}$$

5.4 RESULTS AND DISCUSSION

5.4.1 Evaluation of photocatalytic activity

The different membranes were compared in terms of the average photocatalytic degradation and adsorption of methylene blue obtained after 60 min exposure to UV light (**Figure 5.4, Table 5.2**).

The photocatalytic activity of the unmodified membranes used was measured using membrane substrates from different batches. The error bars in **Figure 5.4** present the variability in the degradation results obtained with different unmodified membrane batches and the degradation of methylene blue obtained after modification of a single membrane batch (each sample result corresponds to the average of six absorbance measurements). In the absence of the photocatalyst (without membranes), the degradation of methylene blue under the same experimental conditions, was found to be negligible.

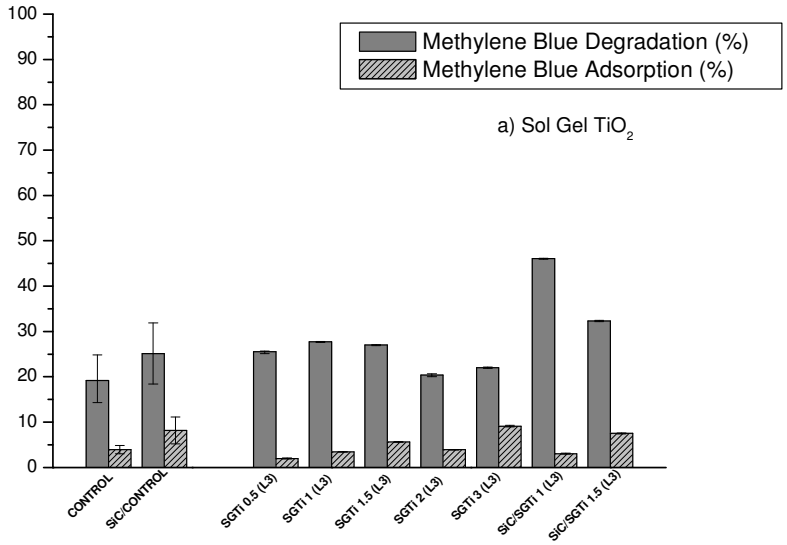

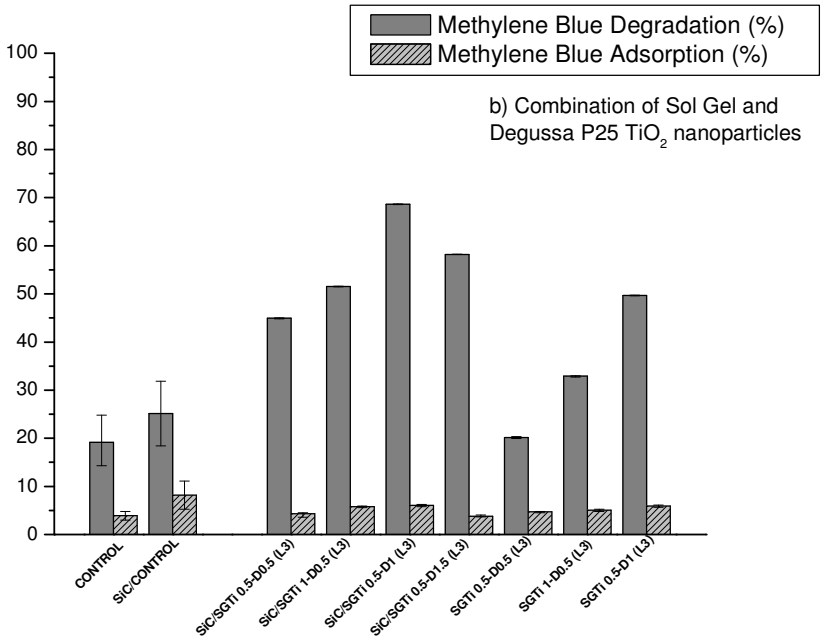

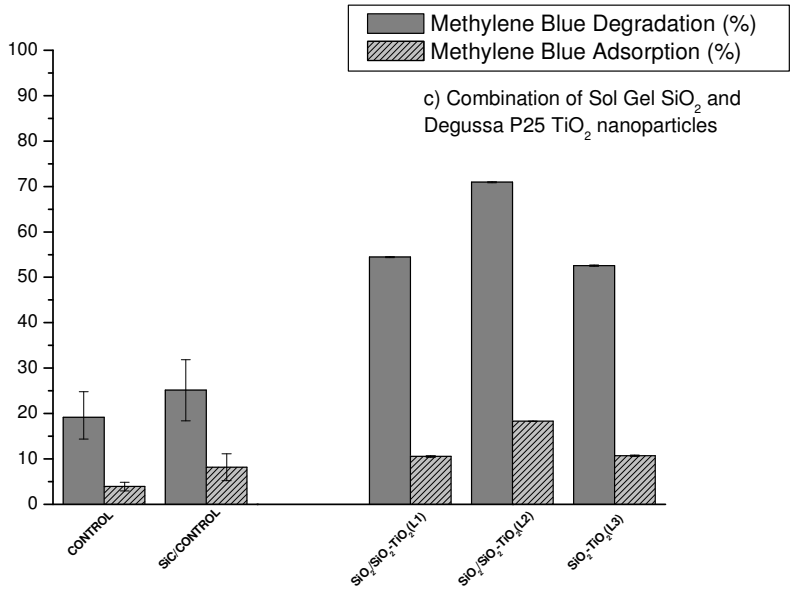

Figure 5.4 *Degradation and adsorption of methylene blue using the unmodified substrates and: (a) membranes modified with sol-gel TiO_2, (b) a combination of sol-gel and Degussa P25 TiO_2 nanoparticles and (c) a combination of sol-gel SiO_2 and Degussa P25 TiO_2 nanoparticles*

Table 5.2 *Methylene blue degradation, methylene blue adsorption and first constant angle values obtained for the different membranes.*

MEMBRANES	Methylene Blue Degradation (%)	Methylene Blue Adsorption (%)	Contact angle in water (Degree)	Contact angle in rapeseed oil (Degree)
CONTROL	19	4	44±1.7	59±19.9
SiC/CONTROL	25	8	13±7.8	49±4.2
SGTi 0.5(L_3)	25	2	13±0.8	43±9.2
SGTi 1(L_3)	28	3	19±9.0	55±12.1
SGTi 1.5(L_3)	27	6	30±1.0	34±8.3
SGTi 2(L_3)	20	4	30±5.4	52±7.3
SGTi 3(L_3)	22	9	19±3.1	56±17.7
SiC/SGTi 1 (L_3)	46	3	13±4.7	51±2.2
SiC/SGTi 1.5 (L_3)	32	8	7±1.4	60±10.7
SiC/SGTi 0.5-D0.5 (L_3)	45	4	15±4.1	59±10.9
SiC/SGTi 1-D0.5 (L_3)	51	6	6±2.9	54±5.8
SiC/SGTi 0.5-D1 (L_3)	69	6	8±0.7	36±14.0
SiC/SGTi 0.5-D1.5 (L_3)	58	4	13± 0.1	56±4.4
SGTi 0.5-D0.5 (L_3)	20	5	8±0.1	60±15.8
SGTi 1-D0.5 (L_3)	33	5	4±0.5	58±5.4
SGTi 0.5-D1 (L_3)	50	6	5±1.2	47±15.2
SGSi/SGSi-D (L_1)	54	11	10±0.8	63±6.3
SGSi/SGSi-D (L_2)	71	18	14±1.8	52±8.8
SGSi-D (L_3)	53	11	18±2.8	61±6.3

The average of total degradation obtained for the unmodified membrane (**Control**) suggested an important self-photoactivity with a percentage of degradation of 19%.

Consistent results were obtained for the **SiC/Control** that proved to be 1.3 times more photocatalytically active than the control as expected taking into account the photocatalytic activity reported for SiC material [202]. This behavior can be attributed to additional amount of SiC photocatalyst particles included in the intermediate layer, which could increase the membrane surface area and therefore increase the photodegradation of methylene blue.

As shown in **Figure 5.4**a), when comparing the membranes prepared by the deposition of TiO_2 prepared by the sol-gel method, we observed that the membranes **SGTi 1(L_3)** and **SGTi 1.5 (L_3)** (prepared with a Tween 80: TTIP molar ratio of 1:1 and 1:1.5, respectively) showed the best degradation behaviour. A low increase in the degradation (8%) was observed for these membranes compared to the control membrane.

Based on the sol-gel results obtained, the conditions employed to produce the **SGTi** membranes with the best methylene blue degradation behaviour, were used to deposit the coating over an intermediate layer of SiC. The prepared **SiC/SGTi1(L_3)** and **SiC/SGTi1.5(L_3)** membranes showed an important improvement in the photocatalytic activity being 1.7 and 1.2 times more photoactive respectively, compared to membranes without the additional SiC layer. The total degradation obtained was 46 and 32 percent, respectively. This synergistic effect of SiC and TiO_2 was previously reported [203].

To further increase the photocatalytic activity of the modified membranes, Degussa P25 TiO_2 nanoparticles were used as additives. Andronic *et al.* [204] reported that a highly hydrophilic and photocatalytic surface could be obtained combining titanium dioxide sol-gel and Degussa P25 powder.

The most promising membranes with 1 and 1.5 molar sol-gel TiO_2 content were therefore tested after preparing different mixtures of TiO_2 obtained by sol-gel and Degussa nanoparticles with and without the SiC intermediate layer.

The results obtained (**Figure 5.4**b) show a strong improvement in the total degradation of methylene blue for the membranes prepared with titanium dioxide Degussa particles embedded (especially in the presence of the SiC intermediate layer), with an optimal titanium dioxide ratio composition sol-gel:Degussa of 1:2. Thus, the membrane **SiC/SGTi 0.5-D1 (L_3)**, with a total molar ratio of 1.5:1 of TiO_2:Tween 80, exhibited the highest total degradation of 69% being 3.6 times and 2.7 times more efficient than the control and SiC/Control membranes, respectively (**Table 5.2** and **Figure 5.4**b).

The results obtained show that a further increase in the concentration of TiO_2 nanoparticles will lead to a decrease in the photocatalytic activity efficiency. This behaviour is in accordance with other authors, who noted that an increase of the catalyst concentration beyond a certain limit may hinder the efficiency of degradation [65]. However, the membrane with the highest content in Degussa titania (**SiC/SGTi 0.5-D1.5 (L_3)**) shown in **Figure 5.4**b, still showed a total methylene blue degradation of 58%, 3 times more effective compared to the control.

The total degradation behaviour of the membranes without the SiC intermediate layer (**SGTi 0.5-D0.5 (L_3), SGTi 1-D0.5 (L_3)** and **SGTi 0.5-D1(L_3)**), showed the same trend compared to the SiC coated membranes with the intermediate layer (**SiC/SGTi 0.5-D0.5 (L_3)**, **SiC/SGTi 1-D0.5 (L_3)** and **SiC/SGTi 0.5-D1(L_3))** but with lower degradation efficiencies of 20, 33 and 50 % respectively, being 2.2, 1.5 and 1.4 times lower than the SiC coated membranes with same TiO_2 composition. These results confirm that having an intermediate layer of SiC increases the photocatalytic activity.

When modified membranes were coated with TiO_2 doped with silicon dioxide, an important increase in the total degradation percentage of methylene blue was observed (**Figure 5.4c**) compared to the control membranes. However, similar photocatalytic performances were obtained compared to the membranes prepared with a combination of TiO_2 prepared by sol-gel and Degussa nanoparticles (**Figure 5.4b**).The **SGSi/SGSi-D (L_2)** membrane showed the highest photocatalytic efficiency (71% with 3.7 times higher degradation levels than the control membrane), whereas the remaining two membranes **SGSi/SGSi-D(L_1)** and **SGSi-D(L_3)** also showed an important increment in the degradation of methylene blue, around 2.8 times better than the control membrane. This behaviour may be attributed to the highest content of Si–OH groups and consequent higher photocatalytic activity for TiO_2 reported by other authors [205].

The increase in the silica molar ratio compared to Degussa P25 (**Table 5.1**), highly increased the photocatalytic degradation of methylene blue by SiO_2-based membranes (**Figure 5.4c**). Besides the higher degradation of methylene blue (71%), the **SGSi/SGSi-D(L_2)** membrane coated with a higher silica proportion, also showed the highest adsorption value (18%) compared to the remaining membranes modified with silicon dioxide **(SGSi/SGSi-D(L_1)** and **SGSi-D(L_3)** (**Table 5.2**). Percent adsorption values lower than 11% were reported for all the other modified membranes (**Figure 5.4** and **Table 5.2**).

The photocatalytic degradation of methylene blue followed a pseudo-first-order decay kinetics. The corresponding half-lives and time based degradation rate constant (k_t) were calculated by plotting the $ln(C_t/C_0)$ versus time (Equation 5.3), where C_0 and C_t correspond to the initial concentration of the dye and the concentration after a certain irradiation time (t, min).

$$Ln\left(\frac{C_t}{C_0}\right) = -k.t \qquad \text{(Equation 5.3)}$$

The time based degradation rate constants and $t_{1/2}$ values are shown in **Table 5.3** and **Figure A.14** (Section A1).

Table 5.3 *Pseudo-first-order kinetic parameters for the methylene blue degradation.*

MEMBRANES	K (min^{-1})	Half-life time $t_{1/2}$ (min)	R^2
CONTROL	0.0035	198	0.9817
SiC/CONTROL	0.0044	158	0.9116
SGTi 0.5(L_3)	0.0048	144	0.9766
SGTi 1(L_3)	0.0054	128	0.9988
SGTi 1.5(L_3)	0.0052	133	0.9997
SGTi 2(L_3)	0.0038	182	0.9952
SGTi 3(L_3)	0.0042	165	0.9812
SiC/SGTi 1 (L_3)	0.0093	74	0.8728
SiC/SGTi 1.5 (L_3)	0.0065	107	0,9996
SiC/SGTi 0.5-D0.5 (L_3)	0.0098	71	0.9939
SiC/SGTi 1-D0.5 (L_3)	0.0120	58	0,9979
SiC/SGTi 0.5-D1 (L_3)	0.0194	36	0.9971
SiC/SGTi 0.5-D1.5 (L_3)	0.0139	50	0.9833
SGTi 0.5-D0.5 (L_3)	0.0037	187	0.9964
SGTi 1-D0.5 (L_3)	0.0066	105	0,9822
SGTi 0.5-D1(L_3)	0.0114	61	0.9998
SGSi/SGSi-D (L_1)	0.0131	53	0.9764
SGSi/SGSi-D (L_2)	0.0207	34	0.9967
SGSi-D (L_3)	0.0125	56	0.9840

The overall most promising membranes in terms of methylene blue degradation (**SiC/SGTi 0.5-D1 (L_3)** and **SGSi/SGSi-D (L_2)**) achieved degradation rate constants of 0.0194 min^{-1} ($t_{½}$= 36 min) and 0.0207 min^{-1} ($t_{½}$= 34 min), respectively. With these membranes, 50% of methylene blue is expected to be degraded in 36 and 34 min.

5.4.2 Reuse efficiency of the photocatalytic layer

In order to investigate the development of efficient photocatalytic *membranes* for different industrial applications, one of the pre-requisites is the long term stability of the photocatalyst. Thus, it is desirable to investigate the reusability of materials, after each methylene blue photodegradation assay. The most promising membranes in terms of photocatalytic behaviour, **SiC/SGTi 1(L_3)**, **SiC/SGTi 0.5-D1 (L_3), SGTi 0.5-D1(L_3)** and **SGSi/SGSi-D (L_2)** were therefore evaluated after two or three photocatalytic degradation experiments under the same experimental conditions (**Figure 5.5**).

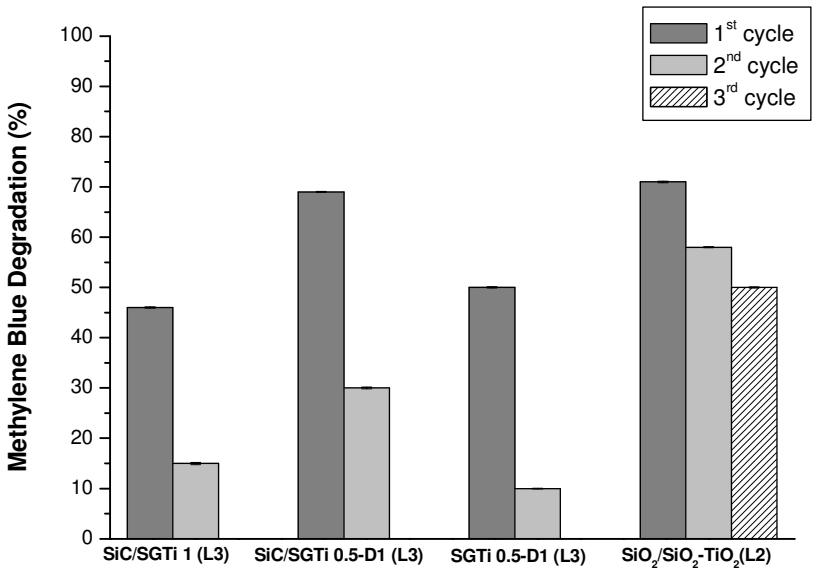

Figure 5.5 *Removal efficiency of the most promising membranes after different photocatalytic assays.*

The membranes **SiC/SGTi 1 (L_3)**, **SiC/SGTi 0.5-D1 (L_3)** and **SGTi 0.5-D1(L_3)** exhibited an abrupt decrease in photocatalytic efficiency in the second assay: 3, 2.3 and 5 times lower than the photocatalytic degradation obtained in first assay, respectively. Moreover, in the case of the **SiC/SGTi 1 (L_3)** and **SGTi 0.5-D1 (L_3)** membranes, the total degradation levels obtained in the second assay (15% and 10%, respectively) were even lower than the degradation values obtained in the first assay by the control membrane (19%). In case of the **SGSi/SGSi-D (L_2)** membrane, the activity of the catalyst did not deteriorate so strongly after repeated cycles.

Loss of reusability for these membranes could be due to loss of SiC, TiO_2 or SiO_2. However, elemental analysis by inductively coupled plasma showed that the contents of titanium and silicon in the solution after the degradation experiments were below the limit of detection (40µg/L).

Since the activity of the membrane with SiO_2 (**SGSi/SGSi-D (L_2)**) exhibited the best removal efficiency after 3 cycles (**Figure 5.5**) the membrane of SiO_2 with 3 layers (**SGSi-D(L_3)**) was also tested in terms of reusability (**Figure 5.6**). The removal efficiency for the **SGSi-D(L_3)** membrane was still constant after five successive cycles (Membrane I), with an average total degradation of 57% (**Figure 5.6**).

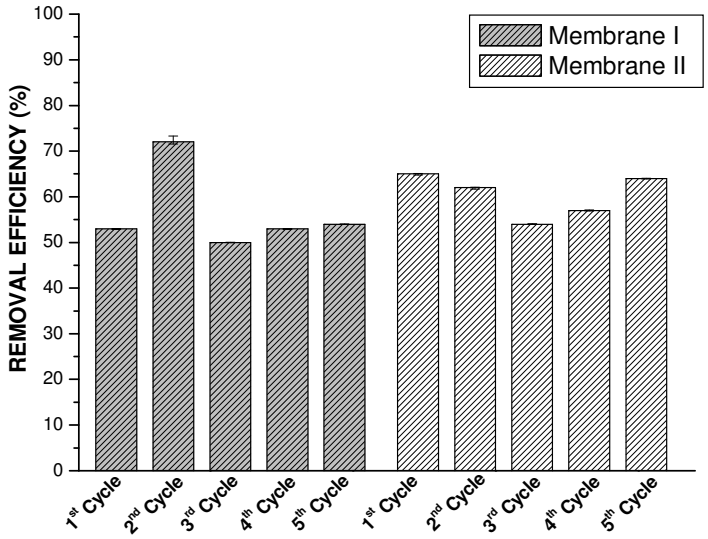

Figure 5.6 *Reproducibility of methylene blue degradation after different assays using two different commercial membrane batches (Membrane I and Membrane II) modified with a combination of SiO_2 and TiO_2.*

To further check the reproducibility of the proposed modification, another silicon carbide membrane substrate from a different commercial batch (Membrane II), was modified using the same procedure to obtain a structure with the same composition of membrane I. The average of total degradation obtained after five cycles was 60 %, similar to the photocatalytic behaviour of membrane I (**Figure 5.6**). The observed reproducibility turns this membrane into an extremely promising material in terms of photocatalytic activity and reusability potential. This membrane was also tested in a long term assay to determine the time needed to achieve total degradation of methylene blue. The results obtained show that total degradation of methylene blue is achieved after 160 min of UV exposure (**Figure 5.7**).

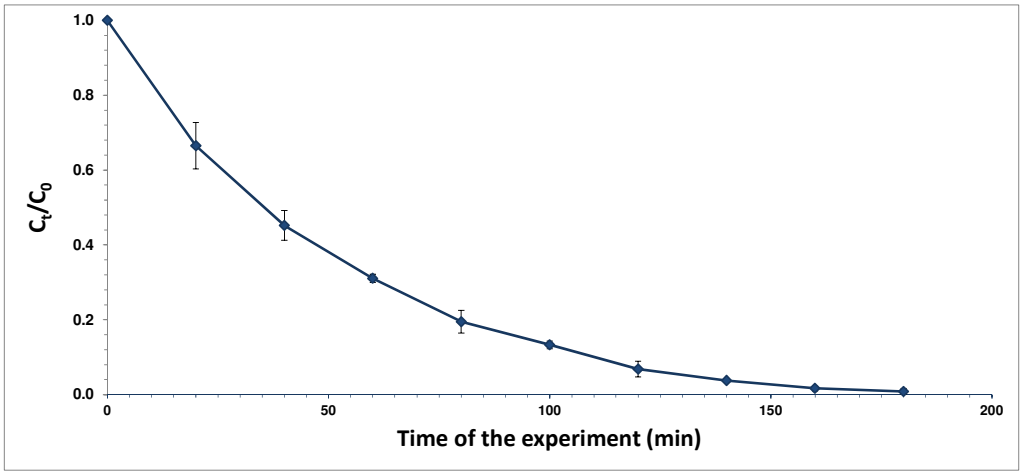

Figure 5.7 *Photocatalytic degradation of methylene blue during a long term assay with the membrane SiO_2-TiO_2 (L3). Error bars correspond to duplicate experiments.*

5.4.3 Membrane characterization

5.4.3.1 Scanning electron microscopy and image analysis

The top layer of the most promising membranes in terms of photocatalytic activity containing Degussa (SiC/SGTi 0.5-D1 (L3), SGTi 0.5-D1(L3) and SGSi-D(L3)) were compared with the membrane coated with three layers of titanium dioxide obtained by the sol-gel procedure (SGTi 1.5 (L3)) and the unmodified membranes using SEM (**Figure 5.8**), in order to investigate differences in morphology and homogeneity, which affects the photocatalytic capability, retentive properties and permeability.

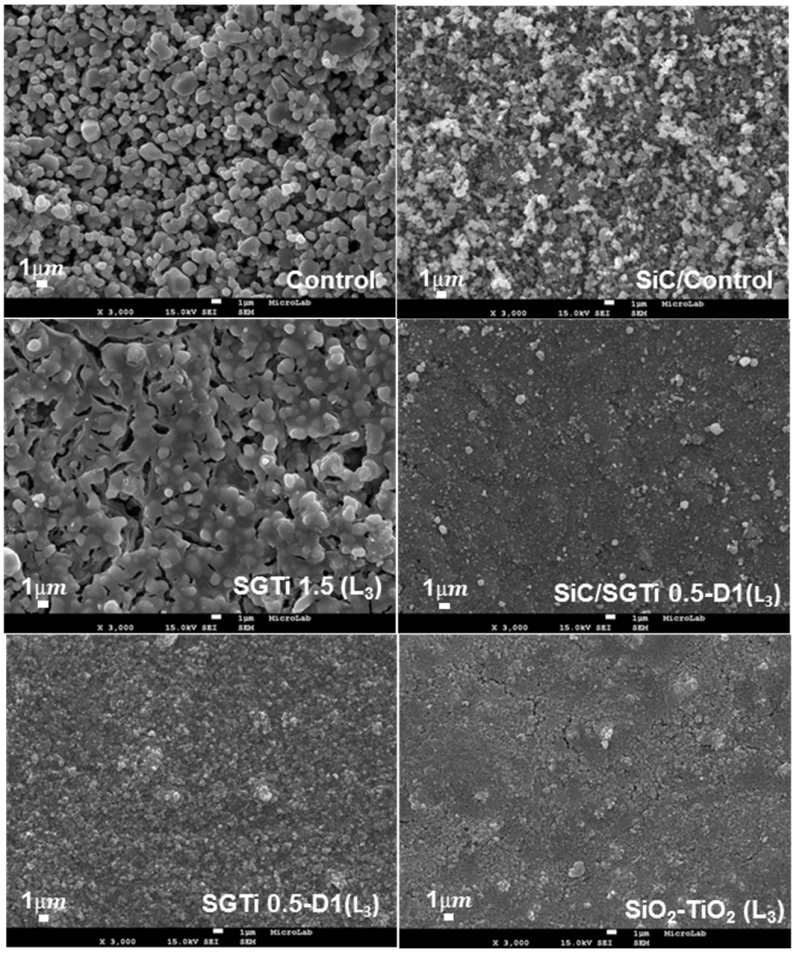

Figure 5.8 *Top view of SEM images of control membranes and most promising modified membranes (magnification 3000).*

Membranes **SiC/SGTi 0.5-D1 (L_3)**, **SGTi 0.5-D1 (L_3)** and **SGSi-D(L_3)** containing commercial Degussa P25 TiO_2 nanoparticles exhibit a high nanoporous structure. The membrane surfaces showed a rougher appearance, due to the grains of titanium dioxide compared to the compact material surface obtained by the membrane modified using the TiO_2 precursor **SGTi 1.5 (L_3)**. In the latter, this feature could be attributed to growing of TiO_2 during crystallization, closing the gaps between the nanoparticles and thus obtaining a smoother surface [206].

The membrane obtained by sol-gel (**SGTi 1.5 (L_3)**) presented microcracks that have been previously described in ceramic deposits produced by sol-gel with non-optimal thickness [189] or rapid heating rates [207]. Thermal treatment and crystallization affect the adherence of the layer to the substrate, may also lead to stress in the coating plane inducing crack formation [207].

The pre-coated membranes with SiC nanoparticles and the presence of titanium dioxide P25 nanoparticles were found to be crack-free with an increased film thickness. The presence of

preformed nanoparticles in the colloidal solution was described as beneficial for repairing defects preventing the appearance of cracks in the final layers [208].

The cross section images of the substrates (**Figure 5.9**) presented different layered structures depending on the modifications performed.

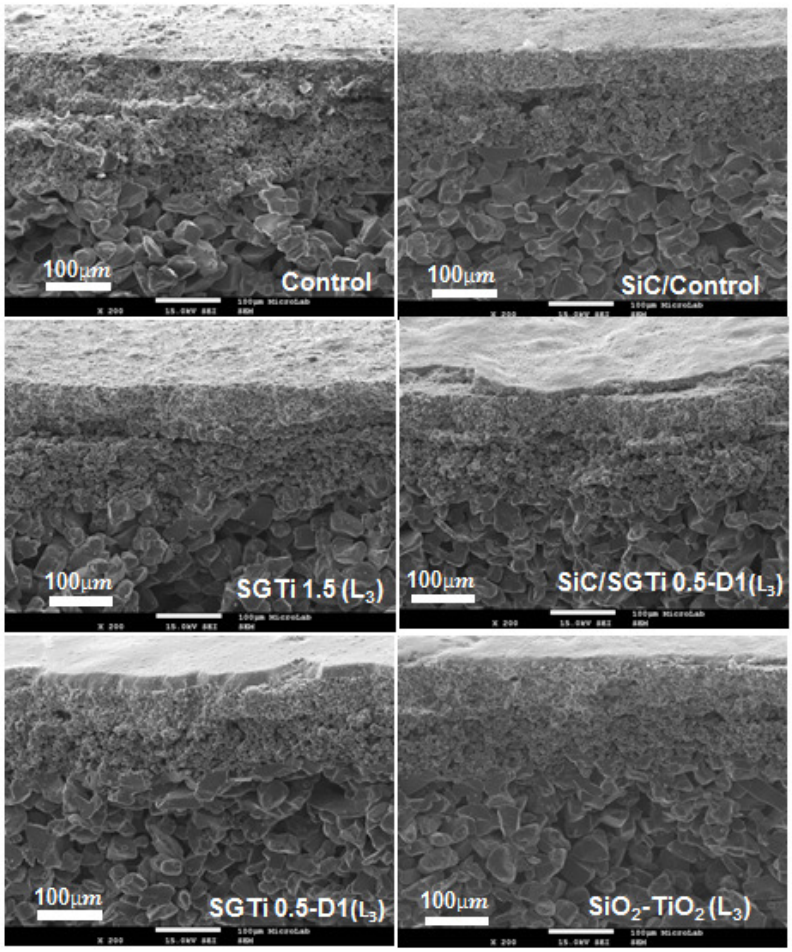

Figure 5.9 *Cross-section of SEM images of control membranes and most promising modified membranes (magnification 200).*

Figure 5.9 shows that the top layer of the unmodified membrane presented an irregular surface and sometimes delaminated with variable thickness. However, the upper layers containing embedded TiO_2 nanoparticles showed a regular thickness, appreciably wider compared to the layer prepared by TiO_2 sol-gel.

5.4.3.2 Porosity of membranes

Membrane porosity affects the mechanical properties and the performance of the membranes in terms of the permeability and selective behaviour. The most promising modified membranes (**SGTi 1.5 (L_3), SiC/SGTi 0.5-D1(L_3)**, **SGTi 0.5-D1(L_3)** and **SGSi-D(L_3)**) and controls (**Control**, **SiC**/ **Control**), were characterized in two different membrane zones using the image analysis software ImageJ. The estimated parameters are summarized in **Table 5.4** and graphically illustrated in **Figure 5.10.**

Table 5.4 *Image J analysis of two SEM images from different membrane zones Z1 and Z2 (threshold value: 35; magnification: 3000; membrane area: 1365 µm^2).*

MEMBRANES	Control Z1	Control Z2	SiC/Control Z1	SiC/Control Z2	SGTi 1.5 (L_3) Z1	SGTi 1.5 (L_3) Z2	SiC/SGTi 0.5-D1 (L_3) Z1	SiC/SGTi 0.5-D1 (L_3) Z2	SGTi 0.5-D1 (L_3) Z1	SGTi 0.5-D1 (L_3) Z2	SGSi-D (L_3) Z1	SGSi-D (L_3) Z2
Number of pores	985	956	2117	3838	788	727	1078	2598	1982	4677	3073	3674
Pore density (µm^{-2})	0.7	0.7	1.6	2.8	0.6	0.5	0.8	1.9	1.5	3.4	2.3	2.7
Mean Pore Area (µm^2)	0.140±0.345	0.157±0.435	0.015±0.030	0.033±0.093	0.084±0.222	0.122±0.285	0.011±0.037	0.004±0.009	0.002±0.002	0.004±0.006	0.004±0.010	0.003±0.005
Minimum Pore Area (µm^2)	0.001	0.001	0.001	0.001	0.001	0.001	0.001	0.001	0.001	0.001	0.001	0.001
Maximum Pore Area (µm^2)	3.554	6.903	0.368	2.049	2.043	3.240	0.800	0.173	0.024	0.156	0.360	0.081
Total Pore Area (µm^2)	138	150	32	128	66	89	12	10	4	17	13	12
Porosity (%)	10.1	11.0	2.4	9.4	4.8	6.5	0.9	0.7	0.3	1.2	0.9	0.9
Average Circularity	0.673±0.300	0.663±0.289	0.813±0.224	0.744±0.270	0.702±0.286	0.644±0.288	0.855±0.223	0.923±0.162	0.960±0.107	0.911±0.169	0.921±0.157	0.924±0.156
Average Feret diameter (µm)	0.508±0.737	0.541±0.737	0.180±0.166	0.257±0.298	0.397±0.535	0.533±0.657	0.142±0.163	0.089±0.076	0.069±0.037	0.089±0.067	0.097±0.084	0.085±0.068
Maximum Feret's diameter (µm)	5.500	6.786	1.418	3.512	3.375	4.649	1.908	0.989	0.340	0.910	0.267	0.787
Minimum Feret's diameter (µm)	0.044	0.047	0.047	0.047	0.047	0.047	0.047	0.047	0.046	0.044	0.048	0.044

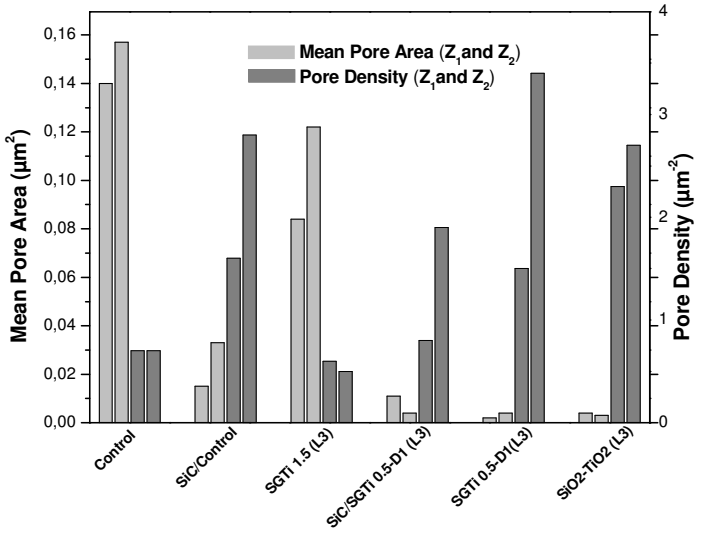

Figure 5.10 *Representation of mean pore size area and pore density estimated with the software ImageJ in two different membrane zones (denoted Z1 and Z2) for the most promising membranes.*

Compared with the unmodified membrane (**Control**), the membrane with the intermediate layer of silicon carbide (**SiC/Control**) shows a much higher number of pores and consequent pore density, a lower pore area and consequent porosity, a lower feret's diameter and a higher circularity (**Table 5.4**).

After modification with the sol-gel process, a reduction in porosity was achieved for all membranes with higher homogeneity (lower differences between the parameters estimated in two different membranes zones compared to the **SiC/Control** membrane). The percent porosity was around 2 times lower for the **SGTi 1.5** membrane compared to the **Control** membrane, whereas a strong reduction was achieved for membranes bearing the Degussa P25 TiO_2 nanoparticles. The modified membrane **SGSi-D(L_3)** with silicon dioxide and titanium dioxide nanoparticles exhibited the lowest porosity values and higher homogeneity with a 0.9 % porosity estimated in the two different zones observed (Z_1 and Z_2).

The differences in porosity are explained by changes in the total *pore area.* **Figure 5.10***shows that* the lower mean pore area values were obtained for the membranes modified with **SiO_2-TiO_2** and **SGTi 0.5-D1** with a mean pore size area between 0.004 and 0.002 µm^2, being around 35-78 times lower compared to the unmodified membrane (**Table 5.4**).

The decrease in pore area leads to a lower molecular weight cut off and a higher pollutant rejection.

The circularity values may range from 0 (infinitely elongated polygon) to 1 (perfect circles). Comparing the average circularity values between membranes, it was observed an important improvement in the symmetry and homogeneity (given by the error measurements) of the pore circularity for the **SiO_2-TiO_2** and **SGTi 0.5-D1** membranes. The high pore circularity for the **SGSi-D(L_3)** membrane, as well as its low mean pore area and the higher pore density compared to the other modified membranes (**Table 5.4**) may contribute to the higher adsorption percentages reported for the membranes modified with silicon dioxide **(Table 5.2).**

The image analysis also revealed an important decrease in the maximum Feret´s diameter (longest distance between two points along the selection boundary) with values from 5.5 to 6.8µm for the unmodified membrane and 0.3 to 0.9 µm for the **SGTi 0.5-D1(L_3)** membrane that exhibited the lowest value. Therefore, the molecular weight cut-off of the modified membranes is expected to decrease compared to the unmodified membrane.

From this analysis, the best membranes in terms of structural porosity parameters are the **SGSi-D (L3)** and **SGTi 0.5-D1(L_3)** membranes.

5.4.3.3 Contact angle

The hydrophilicity and oleophilicity of the surfaces were evaluated by contact angle measurements using distilled water and rapeseed oil (**Table 5.2**).

The water and oil molecules in contact with the unmodified and modified surfaces got into the pores very quickly (**Figures A.15 and A.16** from the section A1). It was thus impossible to measure a static contact angle value. All the membranes were thus found to be extremely hydrophilic and oleophilic. The first contact angle (average values) obtained at three different places randomly chosen for each membrane was measured at 100ms (first frame of 20 recorded) ranged between 4 and 44 degrees for water and 34 and 63 degrees for oil.

Vladuta et. al. correlated the measurements of initial contact angle with the morphology of hydrophilic dense and porous substrates [209].

The first contact angle measured using distilled water showed variable values depending on the different coating compositions. Higher hydrophilicity (13 degrees) was obtained when SiC intermediate layer was incorporated, compared to unmodified membrane (44 degrees).

All the modified membranes showed lower water first contact angle measurements compared to the unmodified membrane, probably due to the increase in OH groups.

5.4.3.4 Membrane filtration performance

Table 5.5 shows the hydraulic permeability values for the unmodified membrane and the most promising modified membrane (**SGSi-D(L_3)**) measured in a dead-end filtration system (**Figure 5.3**) in the absence and presence of UV radiation. The permeability values obtained for the unmodified membrane were the same with and without UV radiation.

Table 5.5 *Hydraulic permeability and percent (%) rejection of methylene blue during membrane filtration (MF) conducted in the absence and presence of ultraviolet (UV) radiation obtained with the unmodified membrane and the modified membrane SGSi-D (L3).*

	Unmodified membrane		**SGSi- D(L_3)**	
	MF	**MF + UV**	**MF**	**MF + UV**
Hydraulic permeability ($Lh^{-1}m^{-2}bar^{-1}$)	38680	38680	2127	3581
Time of filtration (min)	2.5	2.5	50	42.5
% Removal	8	8	23	50

A significant decrease of hydraulic permeability was observed in the modified membrane that may be explained due to the lower pore size of this membrane (detailed in **Table 5.4**).

An increase of the hydraulic permeability was observed for the modified membrane in presence of UV light. The increase in flux due to a higher wettability of photocatalytic membranes when exposed to UV radiation was previously observed by other authors [192].

Figure 5.11 depicts the concentration of methylene blue measured in the permeate of the different filtration experiments as a function of the filtration volume per unit membrane area (allowing for comparison with the results reported by other authors).

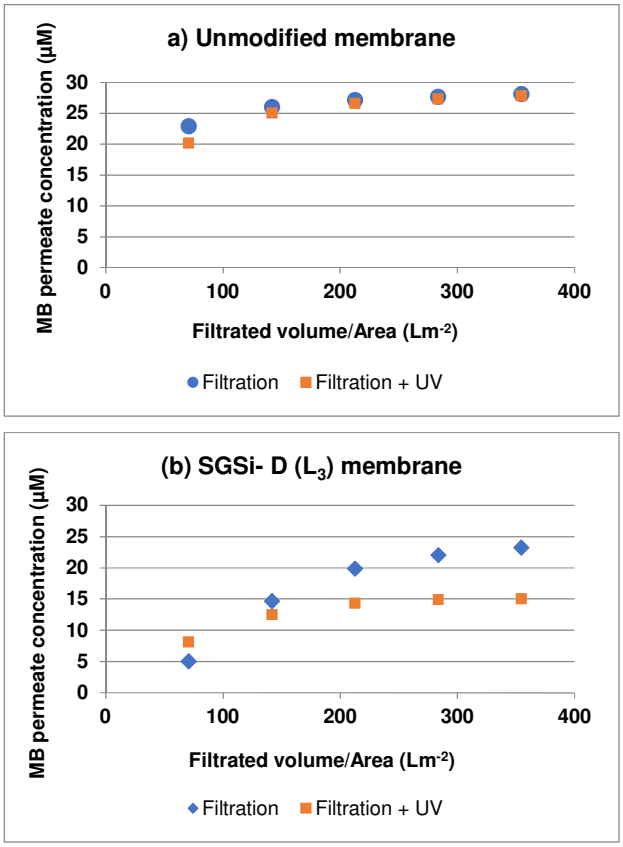

Figure 5.11 *Concentration of methylene blue (MB) in the permeate during membrane filtration conducted in the absence (filtration) and presence of ultraviolet (UV) radiation (filtration+UV) obtained with the (a) unmodified membrane and the (b) modified membrane SGSi*

The results obtained show that the unmodified membrane does not retain methylene blue since the concentration in the permeate tends to the feed concentration, 30 µM, while, for the modified membrane, an initial high quality of the permeate produced by membrane filtration (in the absence of radiation) deteriorates as a function of the filtration volume. This result indicates that the rejection of methylene blue is mainly due to its adsorption to the membrane surface and thus that the modification performed increased the adsorption capacity of the membrane. In the presence of UV radiation, the concentration of methylene blue in the permeate obtained by the modified membrane achieved a plateau at 15µM. This result confirms the photocatalytic results already presented and shows that the modified membrane has catalytic activity in presence of UV light.

Table 5.5 summarizes the significant improvement in the removal of methylene blue for the modified membrane in both tests (50% with UV radiation and 23% without) compared to the unmodified membrane (8%). The increase in the removal of methylene blue for the modified membrane in the test without UV radiation (23%) is due to adsorption while the increase in the removal of methylene blue for the modified membrane in the test with UV radiation (50%) is due to a combined effect of adsorption with photocatalytic activity. Taking into account that the feed

vessel was completely stirred and the permeate flux constant, the average exposure time of methylene blue was 21 min. These results concur with the results presented in **Figure 5.7**, where it can be seen that 27% degradation of methylene blue was achieved given the same exposure time. To attain 90% degradation, a hybrid reactor could be assembled with an hydraulic retention time that would ensure an UV exposure time of 100min.

The combination of both processes is therefore proven to be beneficial and can be further optimized to achieve high quality permeates for different industrial applications.

5.5 CONCLUSIONS

Extremely promising photocatalytic membranes were developed combining titanium dioxide, silicon carbide and silicon dioxide. The sol-gel method employed guaranteed the fixation of the photocatalyst and increased the effectiveness of photodegradation.

Analysis of top surface showed that all the modified membranes are expected to have a lower molecular weight cut-off as well as higher hydrophilicity and oleophilicity compared to the unmodified commercial membranes. The most promising membranes in terms of photocatalytic effectiveness and reusability were modified with SiO_2 obtained by sol-gel combined with Degussa TiO_2 nanoparticles. These membranes have a high potential to degrade recalcitrant and toxic pollutants and could thus be used in hybrid processes that combine UV advanced oxidation processes with membrane filtration in different industry applications.

5.6 ACKNOWLEDGEMENTS

The authors thank Liqtech for supplying the silicon carbide membranes used in this study, in the frame of the EC project O-WaR. Financial support from the European Commission through the projects O-WaR (FP7-SME) and D-Factory (FP7-KBBE) is gratefully acknowledged.

iNOVA4Health - UID/Multi/04462/2013, a program financially supported by Fundação para a Ciência e Tecnologia/Ministério da Educação e Ciência, through national funds and co-funded by FEDER under the PT2020 Partnership Agreement is gratefully acknowledged. The Associate Laboratory for Green Chemistry LAQV which is financed by national funds from FCT/MEC (UID/QUI/50006/2013) and co-financed by the ERDF under the PT2020 Partnership Agreement (POCI-01-0145-FEDER - 007265) is also gratefully acknowledged.

6 TREATMENT OF OLIVE MILL WASTEWATERS USING A SUBMERGED PHOTOCATALYTIC MEMBRANE REACTOR

Subitted to Separation and Purification Technology as: ***Fraga, M.C****, Huertas, R, Crespo, J.G, Pereira, J.V, Treatment of olive mill wastewaters using a submerged photocatalytic membrane reactor*
The author M. C. Fraga was involved in developing the reactor, planning all the filtration experiments, on the sample and data analysis, discussion and interpretation and manuscript elaboration.

6.1 SUMMARY

A hybrid photocatalytic membrane reactor that can easily be scaled-up was assembled and used to test photocatalytic membranes developed using the sol-gel technique. Extremely high removals of total suspended solids, chemical oxygen demand, total organic carbon, phenolic and volatile compounds were obtained when the hybrid photocatalytic membrane reactor was used to treat olive mill wastewaters. These membranes have a high potential to degrade recalcitrant and toxic pollutants and can thus be used in hybrid processes that combine UV advanced oxidation processes with membrane filtration to treat olive mill wastewaters.

6.2 INTRODUCTION

The treatment of wastewaters generated by the olive oil industry is a challenge, mainly in Mediterranean Countries. Their high content in solids, organic matter and phenolic compounds, make these wastewaters difficult to be treated by traditional methods. New processes such as membrane filtration [112] and TiO_2 photocatalysis [210] are alternatives that are being studied to treat these effluents.

High quality permeates can be obtained when membrane processes are used to treat olive mill wastewaters [129, 211]. However, the treatment of a highly concentrated retentate produced during membrane filtration and the development of fouling on the membrane surface are problems that still need to be addressed [3].

Several approaches can be employed to minimize the occurrence of fouling, such as an adequate pretreatment of the wastewater to be treated [212], optimization of chemical cleaning [213], the employment of backpulses or backwashes [211] and modification of the membrane surface in order to give superhydrophilic properties to the membrane [214]. Nanoparticles are widely used for this purpose, being titanium dioxide (TiO_2) the most studied due to its particular advantages [52]. The antifouling properties of TiO_2 are based on its strongly hydrophilic character [58] and

ability to catalyse the degradation of organic substances [215], both enhanced in the presence of UV radiation.

In what concerns to the degradation of organic compounds, TiO_2 photocatalysis can be performed in photocatalytic reactors with the photocatalyst suspended or immobilized on a carrier. Several schemes of photocatalytic membrane reactors are described and extensively reviewed elsewhere [69, 70]. Regarding the membrane location, it can be placed outside in an external loop [71, 72] or inside [73] the photocatalytic reactor. In the latter case, the system is defined as a submerged photocatalytic membrane reactor. In the literature, most of the work published regarding the removal of organic compounds from water using submerged photocatalytic membrane reactors was performed with the photocatalyst in suspension [73, 74, 216].

When TiO_2 is in suspension, loss of TiO_2 due to adsorption to the system is expected [75]. Moreover, a further step is required in order to separate it from the treated water [69]. Furthermore, TiO_2 in suspension was reported to contribute to the development of fouling on the membrane surface [76-78]. In this context, the immobilization of TiO_2 on the membrane surface is the best solution for combining the two processes: photocatalysis and membrane separation. The immobilization of TiO_2 on the membrane surface showed to be useful in the mitigation of fouling [79-83] and is expected to contribute to the degradation of compounds retained in the concentrated retentate produced.

The sol-gel process consists of a chemical process (hydrolysis-condensation) of a metal alkoxide (or semi metal) precursor with itself creating a three-dimensional continuous solid linkage, through a basic or acid catalysis process [84]. This process has been proposed to synthetize TiO_2-based photocatalysts with high oxidation efficiency, as well as for TiO_2 immobilization in a large number of supports to control their porosity [85, 86].

In a previous work, an extremely promising and reproducible photocatalytic activity was reported when silicon carbide surfaces were modified with TiO_2 obtained by sol–gel process, using Degussa P25 and silicon carbide nanoparticles [217].

This work aims to prove that these membranes can be used to treat real olive mill wastewaters to attain the degradation of dissolved compounds. The commercial silicon carbide membranes, used in this work as control membranes, were previously tested using the same matrix and proved to be extremely efficient in total suspended solids and oil and grease removal [211], ensuring compliance with the limits defined in the European legislation [87] for these two parameters. However, a higher removal of the dissolved fraction of chemical oxygen demand, total organic carbon and phenolic compounds is required to ensure that these parameters comply with current and future more stringent legislation. The modified photocatalytic membrane was tested in a new submerged photocatalytic membrane reactor conceived and assembled for this purpose, which can be easily scaled up. The pore size control, hydrophilicity and the photocatalytic activity of the

membrane were studied and the efficiency of the individual and combined treatment processes assessed.

6.3 MATERIAL AND METHODS

6.3.1 Submerged photocatalytic membrane reactor

In this work, a new submerged photocatalytic membrane reactor (**Figure 6.1**) was developed and tested. The reactor is made of polyethylene. The basis is a square with 19 cm diameter and the height of the reactor is 34 cm. The membrane is placed in the centre of the reactor. Two diaphragm pumps (12V 3.0A, 5.5bar; SZY-4155, Shui Zhi Yuan) ensure the pressure difference needed to achieve the intended permeate flux. A pressure sensor and controller (Aplisens, PCE 28) was used in order to measure and guarantee a constant pressure difference. The permeate flux was monitored using a pluviometer which indicates when 5ml of permeate are collected. The data was continuously acquired by the software TeraTerm. The mixing of the system was done by an aeration of 0.33 vvm. The activation of the photocatalytic layer of the membrane is done through two low pressure UV lamps (Duran Normax).

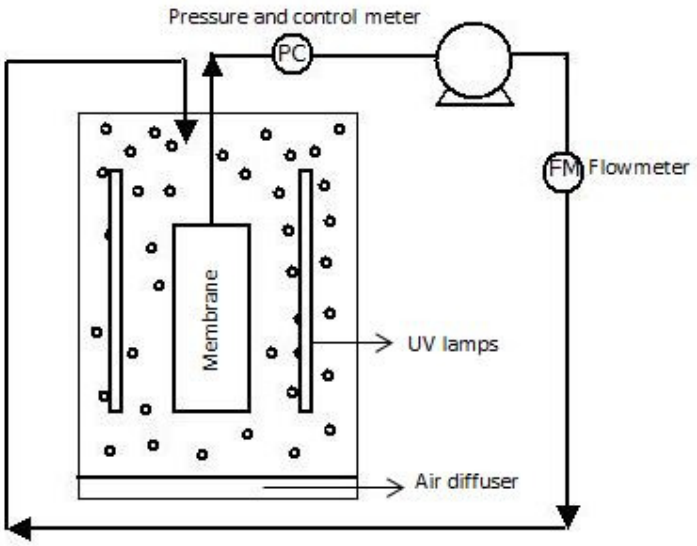

Figure 6.1 *Submerged membrane photocatalytic reactor, developed and tested to treat olive mill wastewaters*

6.3.2 Wastewater matrix and analytical methods

This work was conducted using a real olive mill wastewater matrix, collected after the sedimentation process at an olive oil industry.

The samples were characterized in terms of several parameters commonly used to evaluate the water quality [100]: - total solids (Standard Method 2540B), total suspended solids (Standard Method 2540D), chemical oxygen demand (COD) (Standard Method 5220) and total organic carbon (TOC) (Standard Method 5310B). Total dissolved solids were quantified subtracting the value obtained for total suspended solids from the value of total solids. Phenolic compounds were also quantified by the Folin-Ciocalteu method [218]. The results of a characterization of the wastewater matrix are shown in **Figure 6.2**.

The presence of volatile compounds was determined in different samples by solid phase microextraction (SPME) followed by gas chromatography mass spectrometry (GC/MS). The SPME procedure was conducted with a divinylbenzene/carboxen/polydimethylsiloxane fiber; (d=50/30 µm; needle size: 23Ga) from Supleco. The extraction temperature was set to 40ºC, the agitation speed to 250 rpm, the extraction time to 40 min and the desorption time to 3 min. A Shimadzu QP 2010 GC/MS with a Sapiens – Wax MS (TeknoKroma), 60 m, 0.25 mm (d.i.), 0.25 µm analytical column was used to detect the volatile compounds after splitless injection. The column temperature was held at 40ºC for 5min, increased to 170ºC at a 5ºC/min rate, then to 230ºC at a 30ºC/min rate held for 4 minutes and finally to 270ºC at a 30ºC/min rate held for 5 minutes. The ion source and interface temperatures were set at 245˚C. The volatile compounds detected on the chromatograms were identified using the mass spectra libraries NIST 21, 27, 107, 147 and Wiley 229.

6.3.3 Preparation of the photocatalytic membrane

Commercial flat silicon carbide membranes (17cmx10cmx0.5cm) were provided by LiqTech International and used as substrates. Tetraethyl orthosilicate (TEOS, Sigma-Aldrich, 98%) was used as precursor reagent in sol-gel preparation. Commercially available Degussa P25 titanium dioxide nanoparticles with 30-90 nm of nominal diameter were also employed in this study. All solvents employed were of reagent-grade quality and used without further purification. The modification protocol followed (labelled as SGSi-D (L_3)) was previously optimized and detailed by Huertas et al [217]. The only difference in this work was the deposition method since both sides of an entire membrane were modified in this study. Dip-coating was therefore used instead of drop casting.

After the inner membrane channels were sealed with silicone, the membranes were dipped in the sol-gel suspension for 30 s at a speed of 150 mm s^{-1}, and taken out at a the same speed followed

by drying at room temperature during 30 min and heating at 80°C overnight. The procedure was repeated three times.

6.3.4 Determination of the hydraulic permeability and the optimal transmembrane pressure conditions

To define the best operating pressure difference, that minimizes fouling, for further application in the filtration assays, a preliminary study was carried out using the real wastewater matrix and the modified membrane, by assessing flux variations under different pressures during five-minute intervals. The selected pressure to conduct the experiments was the last respecting the linearity observed between the transmembrane pressure and the permeate flux.

6.3.5 Wastewater treatment in the photocatalytic membrane reactor

Six filtration tests of 10L of wastewater were performed during 4 hours in the photocatalytic membrane reactor, using the unmodified membrane (control) and the modified photocatalytic membrane (**Table 6.1**). For each membrane, a test with the membrane in the presence of UV radiation was performed in order to evaluate the effect of direct photolysis and the photocatalytic activity of the membrane material; another test of membrane filtration in the absence of UV light was conducted in order to evaluate the rejection of compounds due to size exclusion and adsorption. This control was performed since the modification of the membrane leads to a pore size reduction and the different material of the top layer may affect the membrane adsorption.

Finally, a test combining filtration and UV radiation with the two membranes was carried out to evaluate the maximum potential of the hybrid combination. The four filtration tests were conducted with total recirculation and at constant pressure (0.2 bar) which was chosen based on the results obtained in the preliminary experiments detailed in section 6.3.4. For all the tests, samples were taken each 20 minutes in the first hour and then each hour until the end of the test (4 hours of assay). The hydraulic permeability of the control and modified membranes were measured before the experiments. After the filtration experiments, the membranes were cleaned with water at 60±5◦C until at least 90% of their hydraulic permeability was restored. All the tests with the control and the photocatalytic membranes were performed with the same membrane to allow a reliable comparison between the different assays performed.

Table 6.1 *Description of the six tests performed in the submerged photocatalytic membrane reactor*

Test ID	Membrane type	UV light	Filtration	Objective
C.UV	Control	Yes	No	Evaluate direct photolysis using low pressure UV lamps
C.F		No	Yes	Evaluate the filtration performance of the control membrane
C.UVF		Yes	Yes	Evaluate the combined effect of the control membrane
M.UV	Modified	Yes	No	Evaluate the photocatalytic properties of the modified membrane surface
M.F		No	Yes	Evaluate the filtration performance of the modified membrane
M.UVF		Yes	Yes	Evaluate the combined effect of the modified membrane

6.4 RESULTS AND DISCUSSION

6.4.1 Characterization of the wastewater matrix

The composition of the olive mill wastewaters is dependent of several factors such as type of extraction, type and degree of maturation of the olives, region and climacteric conditions [18].

Before each experiment, the pre-treated olive mill wastewater was characterized and **Figure 6.2** depicts the range and average values obtained for each parameter assessed.

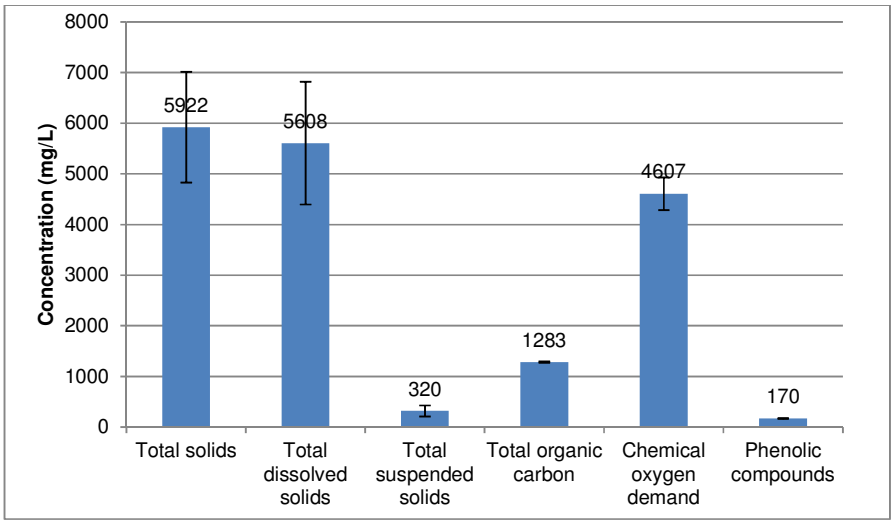

Figure 6.2 *Characterization of the olive mill wastewater in terms of total solids, total dissolved solids, total suspended solids, total organic carbon, chemical oxygen demand and phenolic compounds*

The volatile compounds detailed in Table 6.2 were identified in the wastewater matrix by comparing the mass spectra obtained for the different chromatogram peaks detected in each sample with mass spectra libraries (NIST 21, 27, 107, 147 and Wiley 229).

Table 6.2 *Volatile compounds detected in the feed samples*

Compound	% similarity*
n-buthyl-eter	97
2-Hexanone	95
2-octanone	87
2-heptanone	95
trans-3,4-Epoxyoctane	83
Acetic acid	93
2-nonanone	94
2-buthoxyethanol	96
Propionic acid	94
Butyric Acid	87
Pentanoic acid	93
Hexanoic Acid	96
Heptanoic Acid	94
Cyclohexanecarboxylic acid	89

* % similarity between the spectra and the libraries (NIST 21, 27, 107, 147 and Wiley 229); the values presented correspond to the lower values detected in the samples analysed

The peaks reported present the highest similarity (between 84 and 98% similarity) between the library compounds and the mass spectra obtained. More compounds were identified in the chromatograms, but only the ones with percent area higher than 1% were considered.

Most of the compounds identified in this study have been previously reported in olives and olive oil by several authors [219, 220], being responsible for the characteristic aroma and flavor of olive fruits and olive oil.

Determination of the hydraulic permeability and the optimal transmembrane pressure conditions

The hydraulic permeability was determined for the unmodified (control) membrane (550 ± 50 $Lh^{-1}m^{-2}bar^{-1}$) and the modified membrane (254 ± 55 $Lh^{-1}m^{-2}bar^{-1}$). Thus, the pore size reduction that the modified membrane presents was translated in a decrease of the hydraulic permeability. The intrinsic resistances of the membranes were calculated through the Equation 6.1:

$$R_m = \frac{1}{Lp \times \mu} \qquad \text{(Equation 6.1)}$$

where R_m refers to the intrinsic resistance of the membrane, L_p to the hydraulic permeability of the membrane and μ to the viscosity of water at the temperature of filtration. Values of resistance of $6x10^8$ m^{-1} to the control membrane and $1.2x10^9$ m^{-1} to the modified membrane were obtained.

In order to determine the optimum transmembrane pressure to use in the filtration assays, different controlled transmembrane pressures were set for 5 minutes and the corresponding permeate flux values obtained with the real wastewater matrix recorded. **Figure 6.3** shows the flux increase with the transmembrane pressure variation.

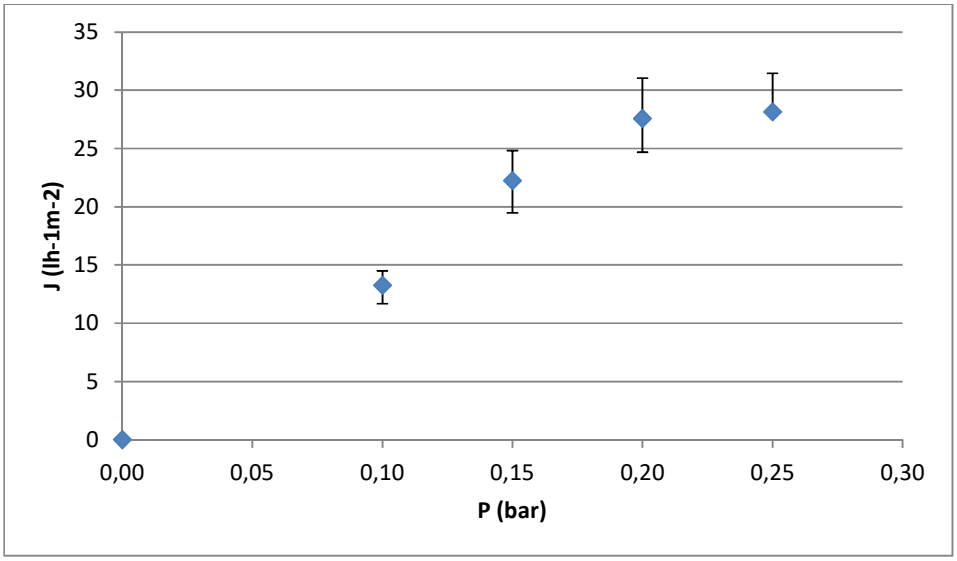

Figure 6.3 *Determination of the optimal transmembrane pressure*

A value of transmembrane pressure of 0.2 bar was chosen since it was the last value maintaining the linearity between the transmembrane pressure and the permeate flux.

6.4.2 Wastewater treatment in the photocatalytic membrane reactor

An improvement of the membrane permeability during the filtration tests was observed when the modified membrane was used in the presence of UV light, mainly after 2h of experiment (**Figure 6.4**). This difference can be explained by the photo-induced antifouling or superhydrophilic properties of TiO_2 [56-58], which is translated in a lower decrease of the membrane permeability.

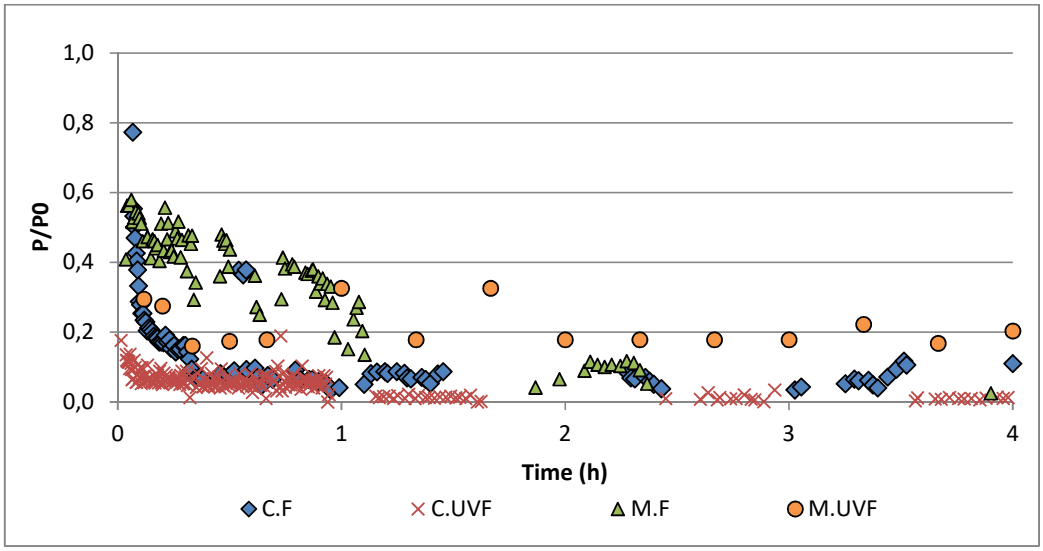

Figure 6.4 *Variation of the permeability of the membranes in the four filtration tests*

The total membrane resistances obtained in the end of the different assays, after 4h of operation, were calculated using Equation 6.2:

$$R_t = R_m + R_f = \frac{TMP}{\mu_t \times J} \qquad \text{(Equation 6.2)}$$

Where total membrane resistance (R_t), corresponds to the sum of the intrinsic membrane resistance (R_m) and the resistance due to fouling (R_f), TMP refers to the transmembrane pressure, J to the flux and μ_t to the fluid viscosity at working temperature (20˚C).

An analysis of the resistances due to fouling was performed in order to do a direct comparison between the two different membranes (control and modified membranes), taking into account their different intrinsic resistances (R_m =6x10^8 m^{-1} for the control membrane; R_m =1.2x10^9 m^{-1} for the modified membrane). Results obtained show a decrease in the resistance due to fouling when the modified membrane (R_f=5.8x10^9) was used in the presence of UV radiation (test M.UVF) when compared with the control membrane (R_f=1.33x10^{10}) in absence of UV radiation (test C.F), revealing that the hybrid system has an effective effect in the mitigation of fouling.

Six experiments were conducted to study the direct photolysis and photocatalytic properties, the filtration performance and the combined effect of the control and modified membranes (**Table 6.1**). Different parameters typically used to assess the water quality (total solids, total suspended solids, chemical oxygen demand, total organic carbon and phenolic compounds) were quantified.

No effect of direct photolysis and the photocatalytic activity of the modified membrane surface were detected in terms of degradation of the target parameters (tests C.UV and M.UV, detailed in **Table 6.1**).

Total solids, total suspended solids and total dissolved solids were quantified only at the end of the assay (after 4h of filtration) due to volume constraints of the samples. **Table 6.3** shows the results obtained of the removals of these parameters.

Table 6.3 *Removals of total solids, total suspended solids and total dissolved solids after 4h of filtration*

Test	**% removals after 4h of filtration test**		
	Total solids	Total suspended solids	Total dissolved solids
C.F	14	93	8
C.UVF	14	92	10
M.F	17	89	13
M.UVF	20	98	18

The increase in the rejections obtained for the combined system using the modified membrane compared with the combined system using the unmodified membrane is probably due to the pore size reduction in the modified membrane and its photocatalytic activity.

The results of the removals obtained over time for chemical oxygen demand, total organic carbon and phenolic compounds in each filtration test (C.F, C.UVF, M.F, M.UVF) are depicted in **Figure 6.5**.

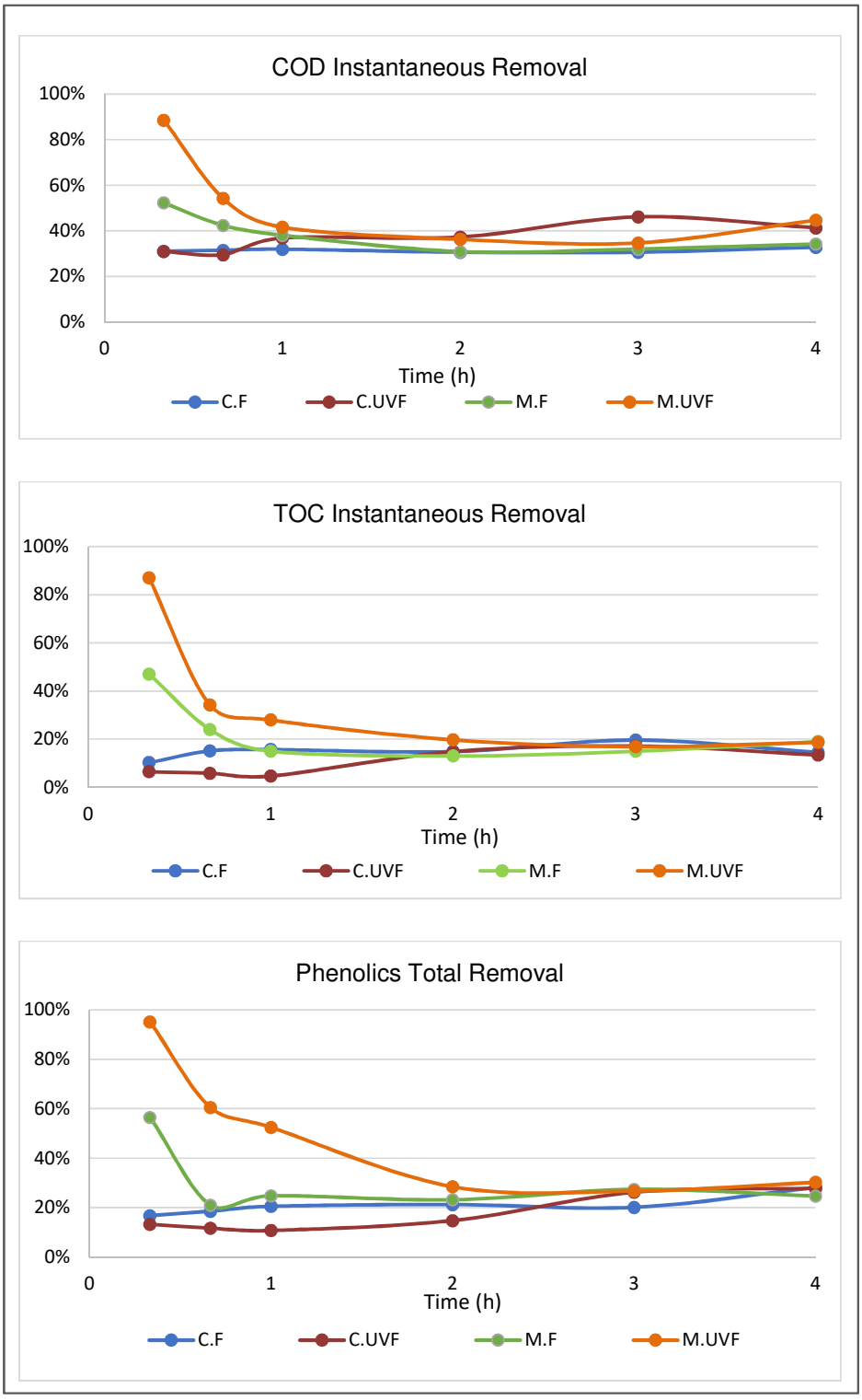

Figure 6.5 *Percent removals of chemical oxygen demand, total organic carbon and phenolic compounds in the tests C.F, C.UVF, M.F and M.UVF*

When the control membrane was used in the absence of UV radiation (test C.F), removals with a constant trend were obtained, between 10% and 20% of total organic carbon, 31% and 37% of chemical oxygen demand and between 20% and 25% of total phenolic compounds. On the other hand, when the control membrane was used in the presence of UV radiation (test C.UVF), removals between 6% and 13% of total organic carbon, 31% and 46% of chemical oxygen demand were obtained and between 13% and 29% of total phenolic compounds.

Results obtained in the test M.F showed that a reduction of the pore size of the membrane was achieved due to the surface modification. Removals of total organic carbon (47%), chemical oxygen demand (42%) and phenolic compounds (56%) were achieved in the first sampling time of the experiment, correspondent to 20 minutes of filtration, being considerable higher than the removals obtained in the same filtration time in the tests C.F and C.UVF (**Figure 6.5**). Nevertheless, a gradual decrease of the percent removals over time was observed until 1h, being maintained constant after this time, probably due to the accumulation of dissolved compounds on the membrane surface leading to their breakthrough through the membrane.

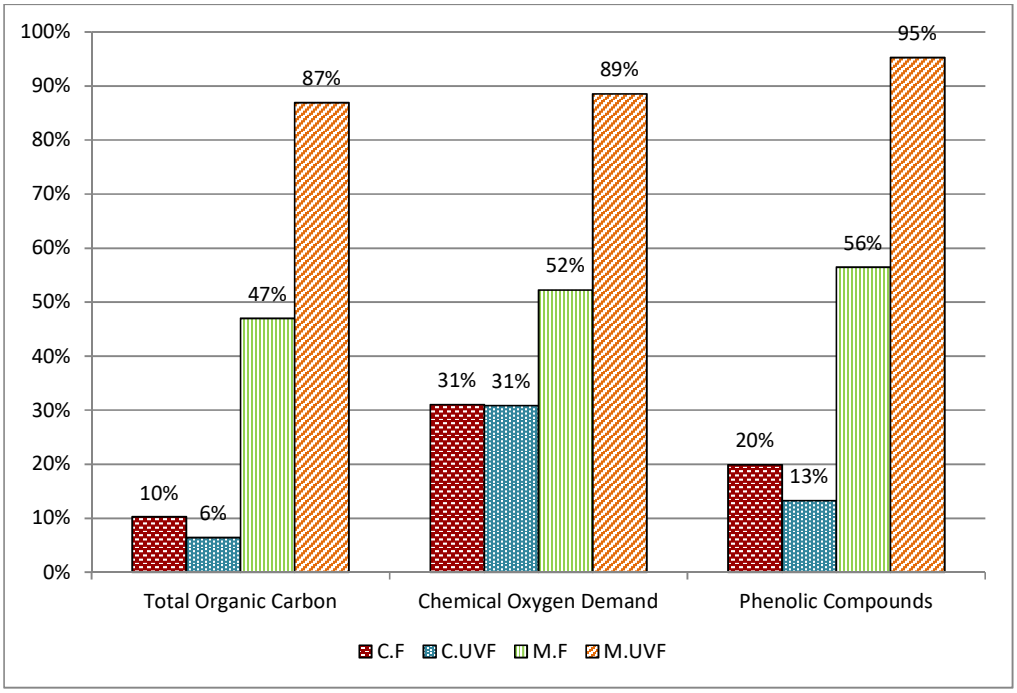

Figure 6.6 *Percent removals of the analysed compounds after 20 min of experiment*

The filtration tests with the modified membrane conducted in the presence of UV radiation (test M.UVF) proved that the membrane has photocatalytic activity since extremely high removals of total organic carbon (87%), chemical oxygen demand (89%) and phenolic compounds (95%)

were achieved in the first sampling time of the experiment, correspondent to 20 minutes of reaction and filtration (**Figure 6.6**). In this case, the wastewater was forced to be in contact with the photocatalytic membrane surface due to the transmembrane pressure. Thus, the degradation of dissolved compounds was obtained due to the formation of free radicals, consequence of the activation of the TiO_2 by the UV radiation. Therefore, a significant decrease of the analysed compounds in the permeate was observed.

These high removals gradually decreased until 2h of experiment, being maintained constant after this time. This fact could be explained by the building of a fouling layer and eventually a cake on the membrane surface, due to the high concentration of particulates in this specific effluent, which prevented the light to activate the photocatalytic layer. A consequent reduction of the photocatalytic activity of the membrane was observed, with a reduction of the degradation of these compounds, which was clear during the initial phase of these experiments. This problem could be overcome in a system built with an effective pre-filtration step or/and backpulse and /or backwash devices. These systems consist in very short pulses of air in the reverse direction to the permeation in the case of the backpulses, and pumping a given volume of permeate in the case of backwashes. These systems were already tested in a previous work conducted in a pilot scale unit using unmodified honeycomb silicon carbide membranes to treat the same matrix and proved to be efficient in fouling mitigation [211], being thus a promising solution to overcome this problem.

The volatile compounds detailed in **Table 6.4** were identified in the different assays by comparing a mass spectra library with the mass spectra obtained for the different chromatogram peaks detected in each initial feed and permeate collected after 20 minutes of filtration. The peaks reported present the highest similarity (between 84 and 98% similarity) between the library compounds and the mass spectra obtained.

Table 6.4 *Percent of similarity and removal of the organic volatile compounds detected in the feed and permeate samples*

Compound	C.F		C.UVF		M.F		M.UVF	
	Similarity (%)	Removal (%)	Similarity (%)	Removal (%)	Similarity (%)	Removal (%)	Similarity (%)	Removal (%)
n-buthyl-eter	97	100%	97	100%	96	100%	97	100%
2-Hexanone	96-98	35%	95-98	62%	98	68%	98	92%
2-octanone	87-91	37%	87-95	100%	98	98%	87	100%
2-heptanone	95	100%	91-96	-104%	98	79%	97-98	44%
trans-3,4-Epoxyoctane	94	100%	83	100%	83	100%	84	100%
Acetic acid	93-98	-25%	98	-25%	95-98	-72%	94-98	86%
2-nonanone	94	100%	97	100%	98	100%	98	100%
2-buthoxyethanol	96-98	-27%	96-97	-46%	95-98	67	98	100%
Propionic acid	94-95	-11%	95-98	-6%	94-96	18%	94-98	79%
Butiric Acid	89-94	100%	94	100%	87-95	30%	90-97	88%
Pentanoic acid	93-96	-8%	94	-2%	na	na	96-98	91%
Hexanoic Acid	94-96	6%	96	-22%	96-98	85%	96	94%
Heptanoic Acid	98	-57%	94-96	-123%	96	61%	94	100%
Cyclohexanecarboxylic acid	84-89	2%	83-84	-3%	89-90	42%	89-90	89%

A comparison between the obtained peak areas of the feed samples and permeate at 20 minutes of test was done in order to calculate the removals of each compound in the different tests. In the case of negative removals values, it can be considered that these compounds were formed during the tests as consequence of reactions non-monitored in this work, probably as a consequence of the aeration and direct photolysis. Since the objective of this research is to obtain treated water, removals as higher as possible are desirable. Results show that n-buthyl-ether, trans-3,4-Epoxyoctane and 2-nonanone were totally removed in all the tests, due to adsorption/rejection by both membranes, since their molecular weight is lower than the molecular weight cut off of the membranes.

An effect of degradation due to UV light was observed in the case of the 2-hexanone and 2-octanone since the removals increased in the presence of radiation with the control membrane.

The effect of the pore size reduction also lead to an increase in the removals of these two compounds, observed when the modified membrane was used in the absence of radiation.

In the case of 2-hexanone, the effect of the photocatalytic membrane was observed, increasing the removals from 68% to 92%. A production of 2-heptatone in the presence of UV radiation was perceived. 86% of acetic acid was removed when the photocatalytic membrane was tested with UV radiation while in the other tests a production of this compound was observed. Regarding the hexanoic acid, heptanoic acid, cyclohexanecarboxylic acid and 2-buthoxyethanol, the use of the modified membrane enabled removals while production was observed with the control, being even higher in the presence of UV light.

In general, the modified membrane in the presence of UV radiation allowed achieving much higher removals of the identified volatile compounds (higher than 79% in all the cases, except 2-heptanone) with no production of any volatile compound. In fact, the degradation of organic volatile compounds by means of TiO_2 photocatalysis is widely studied and reported [221, 222].

6.5 CONCLUSIONS

In this research work, a novel photocatalytic membrane reactor was developed and tested to treat real olive mill wastewater and enhance the degradation of organic compounds. Results proved the photocatalytic activity of the membrane. Extremely high removals of chemical oxygen demand, total organic carbon and phenolic compounds were achieved with this system at 20 min of operation. Subsequent cake formation on the membrane surface, due to high concentration of particulates in this specific effluent, prevents the light from reaching the photocatalytic layer of the membrane with a consequent expected reduction of the permeate quality produced. It was concluded that this problem could be easily solved in a pilot scale system through the effective application of a pre-filtration step and/or strategies to minimize fouling, such as backwashes and backpulses. These strategies were already proven effective and optimized when unmodified silicon carbide membranes were tested at pilot scale for the treatment of these wastewaters [211].

The proposed reactor can be easily scaled up and, with proper flux maintenance strategies to minimize cake build up, is expected to be an extremely efficient olive mill wastewater treatment process.

6.6 ACKNOWLEDGEMENTS

The authors thank Adventech for supplying the wastewater matrices.

iNOVA4Health - UID/Multi/04462/2013, a program financially supported by Fundação para a Ciência e Tecnologia/Ministério da Educação e Ciência, through national funds and co-funded by FEDER under the PT2020 Partnership Agreement is gratefully acknowledged. Associate Laboratory for Green Chemistry LAQV which is also financed by national funds from FCT/MEC (UID/QUI/50006/2013) and co-financed by the ERDF under the PT2020 Partnership Agreement (POCI-01-0145-FEDER - 007265) is gratefully acknowledged.

7 CONCLUSIONS AND FUTURE WORK

7.1 CONCLUSIONS

In the first study presented in this thesis, a new silicon carbide membrane with a single top layer fabricated by only one firing step (2nd generation membrane) was developed, characterized and compared with a commercial membrane developed with two layers and firing steps (1st generation membrane). This new 2nd generation membrane showed similar structural, chemical and removal efficiency characteristics, but higher permeability than the commercially available silicon carbide membrane previously developed with two layers and firing processes. Consequently, the results obtained proved the advantage in the replacement of the 1st generation membrane manufacture procedure in terms of economics and time savings, without affecting separation performance. Taking into account the higher permeability of the 2nd generation membrane, its application is expected to increase the production of treated water. Furthermore, given the extremely high removals determined for total suspended solids as well as oil and grease at laboratory scale, this membrane proved to be a promising solution for the treatment of oily wastewaters.

This new generation of silicon carbide membranes was therefore used at pilot scale to treat real olive mill wastewaters, ensuring extremely high removals of total suspended solids and oil and grease and moderate removals of chemical oxygen demand (COD) and total organic carbon (TOC). Removal of oil and grease was largely due to adsorption/deposition of the compounds on the surface of the membrane and harder to remove using the flux maintenance strategies compared with other fouling agents. The employment of strategies to reduce the appearance of fouling and maintain the permeate flux were optimized, being observed that backpulses every 10 min is an effective strategy to achieve a reduction of fouling formation at the surface of the membrane since it enables a release of the adsorbed compounds. When the backpulses are combined with backwashes, the percent of adsorption/deposition of the analyzed compounds is further reduced. The combination of backpulses every 10 min and backwash every 1 h was found to minimize fouling, maintain flux and avoid high transmembrane pressure increase. A high reduction of adsorption/deposition of oil and grease in the membrane surface was observed. This result can explain the decrease of the resistance due to the fouling observed when working under the pre-determined optimum constant permeate flux (67 $L \cdot m^{-2} \cdot h^{-1}$) together with backpulses every 10 min and backwashes every hour, indicating that oil and grease are an important component of fouling. A strategy to clean the membrane and recover the permeability was also optimized. The simplest and most effective strategy is to rinse and alternate a basic and an acid cleaning solution. All these steps must be performed under controlled temperature, between 60 and 65 ºC. Rinsing at 60–65 ºC seems to be the step that most contributes to the removal of oil and grease and total suspended solids, followed by the basic cleaning with 4% NaOH.

Results demonstrated that membrane filtration using this new generation of silicon carbide membranes is extremely effective to remove total suspended solids and oil and grease from different real olive mill effluents. However, due to the high organic content of these wastewaters, chemical oxygen demand and total organic carbon in the permeate were still present at high concentrations. To overcome this problem, two different strategies were used: further membrane processing using a nanofiltration Desal 5DK membrane and a modification of the silicon carbide membrane, which was done in order to obtain a photocatalytic membrane able to degrade organic compounds that constitute potential foulants.

Nanofiltration was conducted at pilot scale using a Desal 5DK to treat an effluent with similar characteristics to the previous permeate. Results show that this process can be operated at considerably high volume reduction factor (VRF) values and still be effective towards the removal of the target contaminants. Considerably high rejections of total suspended solids, total organic carbon, chemical oxygen demand, as well as oil and grease were achieved. Only the concentration of total phenols and chemical oxygen demand in the permeate could not comply with the European legislation for discharge into water bodies. The concentration of total phenols determined in the permeate, as well as the presence of volatile compounds, probably contributed to the chemical oxygen demand above legal limits. Since the recovery of phenolic compounds was not found to be economically relevant, the use of advanced oxidation processes as a polishing step to further remove chemical oxygen demand would allow compliance with legislation regarding these components. The economic study performed in this work demonstrated that nanofiltration is not only technically but also economically feasible. Operation costs were determined for different treatment plan schedules and volume reduction factors: 2.56–3.07 €/m^3 (7 m^3/day) or 2.62–3.08 €/m^3 (30 m^3/day). Nanofiltration treatment, combined with dissolved air flotation and Fenton process, is an economically viable alternative since the total operation costs obtained (4.17–4.69 €/m^3) represent approximately only 54– 60% of the total operation costs associated to the treatment currently applied.

As an alternative treatment approach, photocatalytic membranes were developed to achieve degradation of dissolved organic compounds in wastewaters. Extremely promising photocatalytic membranes were developed combining titanium dioxide, silicon carbide and silicon dioxide. The sol-gel method employed guaranteed the fixation of the photocatalyst and increased the effectiveness of photodegradation. Analysis of the top surface showed that all the modified membranes are expected to have a lower molecular weight cut-off as well as higher hydrophilicity, compared to the unmodified commercial membranes. The most promising membranes in terms of photocatalytic effectiveness and reusability were modified with SiO_2 obtained by sol-gel combined with Degussa TiO_2 nanoparticles. These membranes have a high potential to degrade recalcitrant and toxic pollutants and were tested in hybrid processes that combine UV advanced oxidation processes with membrane filtration in different industry applications.

A novel photocatalytic membrane reactor was therefore developed and tested to treat real olive mill wastewater and enhance the degradation of organic compounds using the developed photocatalytic membrane. Results proved the photocatalytic activity of the membrane. Extremely high removals of chemical oxygen demand, total organic carbon and phenolic compounds were achieved with this system after 20 min of operation. Subsequent cake formation on the membrane surface, due to high concentration of particulates in this specific effluent, prevents the light from reaching the photocatalytic layer of the membrane with a consequent expected reduction of the permeate quality produced. It was concluded that this problem could be easily solved in a pilot scale system through the effective application of a pre-filtration step and/or strategies to minimize fouling, such as backwashes and backpulses, since these strategies were already proven effective and optimized when unmodified silicon carbide membranes were tested at pilot scale for the treatment of these wastewaters.

7.2 CURRENT AND FUTURE WORK

The use of a hybrid reactor proved to be a promising approach in the treatment of olive mill wastewaters. Some improvements regarding the photocatalytic membrane and the reactor are currently being planned and executed.

The production of the photocatalytic membranes is being improved to propose a sustainable modification process [223]. Extremely low cost and promising photocatalytic membranes are being developed combining SiO_2 with Degussa TiO_2 nanoparticles using a solvent free sol-gel process (water is used as solvent). The method employed guarantees the fixation of the titanium dioxide photocatalyst and increases the effectiveness of photodegradation when compared with the membranes used in the work developed in this thesis. The analysis of the top surface showed that all the solvent free modified membranes are expected to have a lower molecular weight cut-off as well as higher hydrophilicity compared to the unmodified silicon carbide substrate. The most promising membrane in terms of photocatalytic effectiveness in long term assays, permeability, reusability and homogeneous porous properties was obtained for SiO_2 and Degussa TiO_2 nanoparticles without the need to apply high temperatures in the thermal treatment. The modification process proposed is low cost and environmentally friendly (without the use of toxic solvents and with a low temperature thermal treatment). These membranes have a high potential to degrade target recalcitrant and toxic pollutants and should therefore be further tested for different industrial applications in a pilot scale hybrid reactor.

In what concerns to the hybrid reactor, improvements must be implemented to avoid the formation of the cake layer and the consequent loss of the photocatalytic activity of the membrane. A pilot scale system with effective application of strategies to minimize fouling such as backwashes and backpulses should be assembled, since these strategies were already proved effective and optimized when unmodified silicon carbide membranes were tested at pilot scale for the treatment

of these wastewaters. Alternatively, the high load in particulates that these wastewaters exhibit should be reduced using effective pre-treatment processes, such as pre-filtration. This reactor proved to be extremely promising for the treatment of wastewaters and may also replace the traditional final disinfection in drinking water treatment plants to achieve effective disinfection and removal of emerging contaminants.

REFERENCES

[1] M.N. Vissers, P.L. Zock, A.J.C. Roodenburg, R. Leenen, M.B. Katan, Olive Oil Phenols Are Absorbed in Humans, Human Nutrition and Metabolism 132 (2001) 409-417.

[2] A. Cassano, C. Conidi, L. Giorno, E. Drioli, Fractionation of olive mill wastewaters by membrane separation techniques, Journal of Hazardous Materials 248–249 (2013) 185-193.

[3] J.M.O. Pulido, A review on the use of membrane technology and fouling control for olive mill wastewater treatment, Science of The Total Environment 563–564 (2016) 664-675.

[4] J.M. Ochando-Pulido, M.D. Víctor-Ortega, A. Martínez-Ferez, Membrane fouling insight during reverse osmosis purification of pretreated olive mill wastewater, Separation and Purification Technology 168 (2016) 177-187.

[5] A.Y. Gebreyohannes, R. Mazzei, L. Giorno, Trends and current practices of olive mill wastewater treatment: Application of integrated membrane process and its future perspective, Separation and Purification Technology 162 (2016) 45-60.

[6] M. Belaqziz, A. El-Abbassi, E.K. Lakhal, E. Agrafioti, C.M. Galanakis, Agronomic application of olive mill wastewater: Effects on maize production and soil properties, Journal of Environmental Management 171 (2016) 158-165.

[7] A.G. Vlyssides, M. Loizides, P.K. Karlis, Integrated strategic approach for reusing olive oil extraction by-products, Journal of Cleaner Production 12(6) (2004) 603-611.

[8] S. Filidei, G. Masciandaro, B. Ceccanti, Anaerobic digestion of olive oil mill effluents: Evaluation of wastewater organic load and phytotoxicity reduction, Water Air and Soil Pollution 145(1) (2003) 79-94.

[9] A.G. Vlyssides, D.L. Bouranis, M. Loizidou, G. Karvouni, Study of a demonstration plant for the co-composting of olive-oil-processing wastewater and solid residue, Bioresource Technology 56(2-3) (1996) 187-193.

[10] R. Sarika, N. Kalogerakis, D. Mantzavinos, Treatment of olive mill effluents Part II. Complete removal of solids by direct flocculation with poly-electrolytes, Environment International 31(2) (2005) 297-304.

[11] C. Paredes, J. Cegarra, A. Roig, M.A. Sanchez-Monedero, M.P. Bernal, Characterization of olive mill wastewater (alpechin) and its sludge for agricultural purposes, Bioresource Technology 67(2) (1999) 111-115.

[12] E.S. Aktas, S. Imre, L. Ersoy, Characterization and lime treatment of olive mill wastewater, Water Research 35(9) (2001) 2336-2340.

[13] C.I. Piperidou, C.I. Chaidou, C.D. Stalikas, K. Soulti, G.A. Pilidis, C. Balis, Bioremediation of olive oil mill wastewater: Chemical alterations induced by Azotobacter vinelandii, Journal of Agricultural and Food Chemistry 48(5) (2000) 1941-1948.

[14] C.J. McNamara, C.C. Anastasiou, V. O'Flaherty, R. Mitchell, Bioremediation of olive mill wastewater, International Biodeterioration & Biodegradation 61(2) (2008) 127-134.

[15] M. Hamdi, Toxicity and biodegradability of olive mill wastewaters in batch anaerobic digestion, Applied Biochemistry and Biotechnology 37(2) (1992) 155-163.

[16] D. Mantzavinos, N. Kalogerakis, Treatment of olive mill effluents: Part I. Organic matter degradation by chemical and biological processes—an overview, Environment International 31(2) (2005) 289-295.

[17] R. Capasso, A. Evidente, L. Schivo, G. Orru, M.A. Marcialis, G. Cristinzio, Antibacterial polyphenols from olive oil mill waste waters, Journal of Applied Bacteriology 79(4) (1995) 393-398.

[18] P. Paraskeva, E. Diamadopoulos, Technologies for olive mill wastewater (OMW) treatment: a review, Journal of Chemical Technology and Biotechnology 81(9) (2006) 1475-1485.

[19] I. Saadi, Y. Laor, M. Raviv, S. Medina, Land spreading of olive mill wastewater: Effects on soil microbial activity and potential phytotoxicity, Chemosphere 66(1) (2007) 75-83.

[20] M.J. Paredes, E. Moreno, A. Ramos-Cormenzana, J. Martinez, Characteristics of soil after pollution with waste waters from olive oil extraction plants, Chemosphere 16(7) (1987) 1557-1564.

[21] R. Jarboui, F. Sellami, C. Azri, N. Gharsallah, E. Ammar, Olive mill wastewater evaporation management using PCA method: Case study of natural degradation in stabilization ponds (Sfax, Tunisia), Journal of Hazardous Materials 176(1) (2010) 992-1005.

[22] A. Roig, M.L. Cayuela, M.A. Sanchez-Monedero, An overview on olive mill wastes and their valorisation methods, Waste Management 26(9) (2006) 960-969.

[23] B. Van der Bruggen, M. Mänttäri, M. Nyström, Drawbacks of applying nanofiltration and how to avoid them: A review, Separation and Purification Technology 63(2) (2008) 251-263.

[24] M.J. Ochando-Pulido, A. Martinez-Ferez, On the Recent Use of Membrane Technology for Olive Mill Wastewater Purification, Membranes 5(4) (2015) 513-531.

[25] S. Mondal, S.R. Wickramasinghe, Produced water treatment by nanofiltration and reverse osmosis membranes, Journal of Membrane Science 322(1) (2008) 162-170.

[26] F.L. Hua, Y.F. Tsang, Y.J. Wang, S.Y. Chan, H. Chua, S.N. Sin, Performance study of ceramic microfiltration membrane for oily wastewater treatment, Chemical Engineering Journal 128(2–3) (2007) 169-175.

[27] E. Garcia-Castello, A. Cassano, A. Criscuoli, C. Conidi, E. Drioli, Recovery and concentration of polyphenols from olive mill wastewaters by integrated membrane system, Water Research 44(13) (2010) 3883-3892.

[28] A. Zirehpour, A. Rahimpour, M. Jahanshahi, M. Peyravi, Mixed matrix membrane application for olive oil wastewater treatment: Process optimization based on Taguchi design method, Journal of Environmental Management 132 (2014) 113-120.

[29] A. Cassano, C. Conidi, E. Drioli, Comparison of the performance of UF membranes in olive mill wastewaters treatment, Water Research 45(10) (2011) 3197-3204.

[30] C.A. Paraskeva, V.G. Papadakis, E. Tsarouchi, D.G. Kanellopoulou, P.G. Koutsoukos, Membrane processing for olive mill wastewater fractionation, Desalination 213(1) (2007) 218-229.

[31] A. Zirehpour, M. Jahanshahi, A. Rahimpour, Unique membrane process integration for olive oil mill wastewater purification, Separation and Purification Technology 96 (2012) 124-131.

[32] T. Coskun, E. Debik, N.M. Demir, Treatment of olive mill wastewaters by nanofiltration and reverse osmosis membranes, Desalination 259(1–3) (2010) 65-70.

[33] M. Servili, S. Esposto, G. Veneziani, S. Urbani, A. Taticchi, I. Di Maio, R. Selvaggini, B. Sordini, G. Montedoro, Improvement of bioactive phenol content in virgin olive oil with an olive-vegetation water concentrate produced by membrane treatment, Food Chemistry 124(4) (2011) 1308-1315.

[34] S.M. Samaei, S. Gato-Trinidad, A. Altaee, The application of pressure-driven ceramic membrane technology for the treatment of industrial wastewaters – A review, Separation and Purification Technology 200 (2018) 198-220.

[35] B. Xiong, A.L. Zydney, M. Kumar, Fouling of microfiltration membranes by flowback and produced waters from the Marcellus shale gas play, Water Research 99 (2016) 162-170.

[36] C. Moulin, M.M. Bourbigot, A. Tazi-Pain, F. Bourdon, Design and performance of membrane filtration installations: Capacity and product quality for drinking water applications, Environmental Technology 12 (2008) 841 - 858.

[37] W. Deng, X. Yu, M. Sahimi, T.T. Tsotsis, Highly permeable porous silicon carbide support tubes for the preparation of nanoporous inorganic membranes, Journal of Membrane Science 451 (2014) 192-204.

[38] K. König, V. Boffa, B. Buchbjerg, A. Farsi, M.L. Christensen, G. Magnacca, Y. Yue, One-step deposition of ultrafiltration SiC membranes on macroporous SiC supports, Journal of Membrane Science 472 (2014) 232-240.

[39] B. Hofs, J. Ogier, D. Vries, E.F. Beerendonk, E.R. Cornelissen, Comparison of ceramic and polymeric membrane permeability and fouling using surface water, Separation and Purification Technology 79(3) (2011) 365-374.

[40] F. Bazzarelli, E. Piacentini, T. Poerio, R. Mazzei, A. Cassano, L. Giorno, Advances in membrane operations for water purification and biophenols recovery/valorization from OMWWs, Journal of Membrane Science 497 (2016) 402-409.

[41] J. Cui, X. Zhang, H. Liu, S. Liu, K.L. Yeung, Preparation and application of zeolite/ceramic microfiltration membranes for treatment of oil contaminated water, Journal of Membrane Science 325(1) (2008) 420-426.

[42] S.R.H. Abadi, M.R. Sebzari, M. Hemati, F. Rekabdar, T. Mohammadi, Ceramic membrane performance in microfiltration of oily wastewater, Desalination 265(1–3) (2011) 222-228.

[43] H. Peng, A.Y. Tremblay, Membrane regeneration and filtration modeling in treating oily wastewaters, Journal of Membrane Science 324(1) (2008) 59-66.

[44] R.W. Field, D. Wu, J.A. Howell, B.B. Gupta, Critical flux concept for microfiltration fouling, Journal of Membrane Science 100(3) (1995) 259-272.

[45] S.E. Weschenfelder, C.P. Borges, J.C. Campos, Oilfield produced water treatment by ceramic membranes: Bench and pilot scale evaluation, Journal of Membrane Science 495 (2015) 242-251.

[46] J.A. Ramirez, R.H. Davis, Application of cross-flow microfiltration with rapid backpulsing to wastewater treatment, Journal of Hazardous Materials 63(2–3) (1998) 179-197.

[47] Liqtech, Flux Maintenance on Ceramic, Liqtech International A/S, Ballerup, Denmark, 2014.

[48] P. Malmrose, Committee Report: Residuals Management for Low-pressure Membranes, Journal - American Water Works Association 95(6) (2003) 68-82.

[49] U.S.E.P.A.-. EPA, Membrane filtration guidance manual, 2005.

[50] D.J. Miller, S. Kasemset, D.R. Paul, B.D. Freeman, Comparison of membrane fouling at constant flux and constant transmembrane pressure conditions, Journal of Membrane Science 454 (2014) 505-515.

[51] J. Kim, B. Van der Bruggen, The use of nanoparticles in polymeric and ceramic membrane structures: Review of manufacturing procedures and performance improvement for water treatment, Environmental Pollution 158(7) (2010) 2335-2349.

[52] A. Fujishima, T.N. Rao, D.A. Tryk, Titanium dioxide photocatalysis, Journal of Photochemistry and Photobiology C: Photochemistry Reviews 1(1) (2000) 1-21.

[53] I. Kovács, G. Veréb, S. Kertész, C. Hodúr, Z. László, Fouling mitigation and cleanability of TiO2 photocatalyst-modified PVDF membranes during ultrafiltration of model oily wastewater with different salt contents, Environmental Science and Pollution Research (2017) 1-10.

[54] M. Li, T. Deng, S. Liu, F. Zhang, G. Zhang, Superhydrophilic surface modification of fabric via coating with nano-TiO2 by UV and alkaline treatment, Applied Surface Science 297 (2014) 147-152.

[55] H. Shi, Y. He, Y. Pan, H. Di, G. Zeng, L. Zhang, C. Zhang, A modified mussel-inspired method to fabricate TiO2 decorated superhydrophilic PVDF membrane for oil/water separation, Journal of Membrane Science 506 (2016) 60-70.

[56] S.S. Madaeni, N. Ghaemi, A. Alizadeh, M. Joshaghani, Influence of photo-induced superhydrophilicity of titanium dioxide nanoparticles on the anti-fouling performance of ultrafiltration membranes, Applied Surface Science 257(14) (2011) 6175-6180.

[57] Z. Song, M. Fathizadeh, Y. Huang, K.H. Chu, Y. Yoon, L. Wang, W.L. Xu, M. Yu, TiO2 nanofiltration membranes prepared by molecular layer deposition for water purification, Journal of Membrane Science 510 (2016) 72-78.

[58] R. Wang, K. Hashimoto, A. Fujishima, M. Chikuni, E. Kojima, A. Kitamura, M. Shimohigoshi, T. Watanabe, Light-induced amphiphilic surfaces, Nature 388 (1997) 431.

[59] K. Ikeda, H. Sakai, R. Baba, K. Hashimoto, A. Fujishima, Photocatalytic Reactions Involving Radical Chain Reactions Using Microelectrodes, The Journal of Physical Chemistry B 101(14) (1997) 2617-2620.

[60] G. Balasubramanian, D.D. Dionysiou, M.T. Suidan, I. Baudin, J.-M. Laîné, Evaluating the activities of immobilized TiO2 powder films for the photocatalytic degradation of organic contaminants in water, Applied Catalysis B: Environmental 47(2) (2004) 73-84.

[61] K. Nakata, A. Fujishima, TiO2 photocatalysis: Design and applications, Journal of Photochemistry and Photobiology C: Photochemistry Reviews 13(3) (2012) 169-189.

[62] M.I. Badawy, F.E. Gohary, M.Y. Ghaly, M.E.M. Ali, Enhancement of olive mill wastewater biodegradation by homogeneous and heterogeneous photocatalytic oxidation, Journal of Hazardous Materials 169(1–3) (2009) 673-679.

[63] A.M.T. Silva, E. Nouli, N.P. Xekoukoulotakis, D. Mantzavinos, Effect of key operating parameters on phenols degradation during H2O2-assisted TiO2 photocatalytic treatment of simulated and actual olive mill wastewaters, Applied Catalysis B: Environmental 73(1) (2007) 11-22.

[64] H. El Hajjouji, F. Barje, E. Pinelli, J.R. Bailly, C. Richard, P. Winterton, J.C. Revel, M. Hafidi, Photochemical UV/TiO2 treatment of olive mill wastewater (OMW), Bioresource Technology 99(15) (2008) 7264-7269.

[65] M.N. Chong, B. Jin, C.W.K. Chow, C. Saint, Recent developments in photocatalytic water treatment technology: A review, Water Research 44(10) (2010) 2997-3027.

[66] R. Molinari, C. Lavorato, P. Argurio, Recent progress of photocatalytic membrane reactors in water treatment and in synthesis of organic compounds. A review, Catalysis Today 281, Part 1 (2017) 144-164.

[67] V. Augugliaro, M. Litter, L. Palmisano, J. Soria, The combination of heterogeneous photocatalysis with chemical and physical operations: A tool for improving the photoprocess performance, Journal of Photochemistry and Photobiology C: Photochemistry Reviews 7(4) (2006) 127-144.

[68] S.S. Chin, T.M. Lim, K. Chiang, A.G. Fane, Hybrid low-pressure submerged membrane photoreactor for the removal of bisphenol A, Desalination 202(1) (2007) 253-261.

[69] S. Mozia, Photocatalytic membrane reactors (PMRs) in water and wastewater treatment. A review, Separation and Purification Technology 73(2) (2010) 71-91.

[70] O. Iglesias, M.J. Rivero, A.M. Urtiaga, I. Ortiz, Membrane-based photocatalytic systems for process intensification, Chemical Engineering Journal 305 (2016) 136-148.

[71] P. Le-Clech, E.-K. Lee, V. Chen, Hybrid photocatalysis/membrane treatment for surface waters containing low concentrations of natural organic matters, Water Research 40(2) (2006) 323-330.

[72] K.V. Plakas, V.C. Sarasidis, S.I. Patsios, D.A. Lambropoulou, A.J. Karabelas, Novel pilot scale continuous photocatalytic membrane reactor for removal of organic micropollutants from water, Chemical Engineering Journal 304 (2016) 335-343.

[73] S.I. Patsios, V.C. Sarasidis, A.J. Karabelas, A hybrid photocatalysis–ultrafiltration continuous process for humic acids degradation, Separation and Purification Technology 104 (2013) 333-341.

[74] C.S. Ong, W.J. Lau, P.S. Goh, B.C. Ng, A.F. Ismail, Investigation of submerged membrane photocatalytic reactor (sMPR) operating parameters during oily wastewater treatment process, Desalination 353 (2014) 48-56.

[75] S. Sanches, A. Penetra, A. Rodrigues, V.V. Cardoso, E. Ferreira, M.J. Benoliel, M.T. Barreto Crespo, J.G. Crespo, V.J. Pereira, Removal of pesticides from water combining low pressure UV photolysis with nanofiltration, Separation and Purification Technology 115 (2013) 73-82.

[76] L. Erdei, N. Arecrachakul, S. Vigneswaran, A combined photocatalytic slurry reactor–immersed membrane module system for advanced wastewater treatment, Separation and Purification Technology 62(2) (2008) 382-388.

[77] W. Zhang, L. Ding, J. Luo, M.Y. Jaffrin, B. Tang, Membrane fouling in photocatalytic membrane reactors (PMRs) for water and wastewater treatment: A critical review, Chemical Engineering Journal 302 (2016) 446-458.

[78] S.S. Chin, T.M. Lim, K. Chiang, A.G. Fane, Factors affecting the performance of a low-pressure submerged membrane photocatalytic reactor, Chemical Engineering Journal 130(1) (2007) 53-63.

[79] T.-H. Bae, T.-M. Tak, Effect of TiO2 nanoparticles on fouling mitigation of ultrafiltration membranes for activated sludge filtration, Journal of Membrane Science 249(1–2) (2005) 1-8.

[80] G. Mustafa, K. Wyns, P. Vandezande, A. Buekenhoudt, V. Meynen, Novel grafting method efficiently decreases irreversible fouling of ceramic nanofiltration membranes, Journal of Membrane Science 470 (2014) 369-377.

[81] H. Younas, H. Bai, J. Shao, Q. Han, Y. Ling, Y. He, Super-hydrophilic and fouling resistant PVDF ultrafiltration membranes based on a facile prefabricated surface, Journal of Membrane Science 541 (2017) 529-540.

[82] G. Mustafa, K. Wyns, S. Janssens, A. Buekenhoudt, V. Meynen, Evaluation of the fouling resistance of methyl grafted ceramic membranes for inorganic foulants and co-effects of organic foulants, Separation and Purification Technology 193 (2018) 29-37.

[83] J.-K. Pi, H.-C. Yang, L.-S. Wan, J. Wu, Z.-K. Xu, Polypropylene microfiltration membranes modified with TiO2 nanoparticles for surface wettability and antifouling property, Journal of Membrane Science 500 (2016) 8-15.

[84] G.R. Lee, J.A. Crayston, Sol-gel processing of transition-metal alkoxides for electronics, Advanced Materials 5(6) (1993) 434-442.

[85] R. Goei, T.-T. Lim, Asymmetric TiO2 hybrid photocatalytic ceramic membrane with porosity gradient: Effect of structure directing agent on the resulting membranes architecture and performances, Ceramics International 40(5) (2014) 6747-6757.

[86] R. Goei, Z. Dong, T.-T. Lim, High-permeability pluronic-based TiO2 hybrid photocatalytic membrane with hierarchical porosity: Fabrication, characterizations and performances, Chemical Engineering Journal 228 (2013) 1030-1039.

[87] 91/271/EEC, Council Directive of 21 May 1991 concerning urban waste water treatment.

[88] M. Decloux, M.-L. Lameloise, A. Brocard, E. Bisson, M. Parmentier, A. Spiraers, Treatment of acidic wastewater arising from the refining of vegetable oil by crossflow microfiltration at very low transmembrane pressure, Process Biochemistry 42(4) (2007) 693-699.

[89] R.A. Pandey, P.B. Sanyal, N. Chattopadhyay, S.N. Kaul, Treatment and reuse of wastes of a vegetable oil refinery, Resources Conservation and Recycling 37(2) (2003) 101-117.

[90] Y. Saatci, E.I. Arslan, V. Konar, Removal of total lipids and fatty acids from sunflower oil factory effluent by UASB reactor, Bioresource Technology 87(3) (2003) 269-272.

[91] M. Cheryan, N. Rajagopalan, Membrane processing of oily streams. Wastewater treatment and waste reduction, Journal of Membrane Science 151(1) (1998) 13-28.

[92] I.H. Huisman, G. Trägårdh, C. Trägårdh, A. Pihlajamäki, Determining the zeta-potential of ceramic microfiltration membranes using the electroviscous effect, Journal of Membrane Science 147(2) (1998) 187-194.

[93] C.d.M. Coutinho, M.C. Chiu, R.C. Basso, A.P. Badan Ribeiro, L.A. Guaraldo Goncalves, L.A. Viotto, State of art of the application of membrane technology to vegetable oils: A review, Food Research International 42(5-6) (2009) 536-550.

[94] T. Tsuru, Inorganic porous membranes for liquid phase separation, Separation and Purification Methods 30 (2001) 191 - 220.

[95] B. Van der Bruggen, C. Vandecasteele, T. Van Gestel, D. Wim, R. Leysen, A review of pressure-driven membrane processes in wastewater treatment and drinking water production, Environmental progress 22 (2003) 46 - 56.

[96] J.P. Chen, S.L. Kim, Y.P. Ting, Optimization of membrane physical and chemical cleaning by a statistically designed approach, Journal of Membrane Science 219(1–2) (2003) 27-45.

[97] U. Haok, Stobbe, P., Porous ceramic body and method for production theref 2006. Patent US7699903B2

[98] J.H. Johansen, Kjaer J.H., Ceramic dead-end filter, a filter system, a method of filtering and a method of producing a ceramic dead-end filter, 2011. Patent EP2274066A1

[99] M.V. Martínez de Yuso, Neves, L.A. , Coelhoso, I.M. , Crespo, J.G. , Benavente, J. , Rodríguez-Castellón, E., A Study of Chemical Modifications of a Nafion Membrane by Incorporation of Different Room Temperature Ionic Liquids, Fuel cells 12 (2012) 606-613.

[100] A.D. Eaton, L.S.C. Clesceri, A.E. Greenberg, Standard Methods for the Examination of Water and Wastewater, American Public Health Association, American Water Works Association, Water Environment Federation 1995.

[101] W.H. Walton, Feret‘s Statistical Diameter as a Measure of Particle Size, Nature 162 (1948) 329-330.

[102] S.W.F. Moulder J.F. , Sobol P.E. , Bomben K.D., Handbook of X-Ray Photoelectron Spectroscopy, Perkin-Elmer Corporation, Minneapolis (USA), 1992.

[103] D. Brigg, Seah M.P., Practical Surface Analysis: Auger and X-Ray Photoelecton Spectroscopy, 1995.

[104] M. Brenes, A. García, P. García, J.J. Rios, A. Garrido, Phenolic Compounds in Spanish Olive Oils, Journal of Agricultural and Food Chemistry 47(9) (1999) 3535-3540.

[105] I.E. Kapellakis, K.P. Tsagarakis, C. Avramaki, A.N. Angelakis, Olive mill wastewater management in river basins: A case study in Greece, Agricultural Water Management 82(3) (2006) 354-370.

[106] A. Cicci, M. Stoller, M. Bravi, Microalgal biomass production by using ultra- and nanofiltration membrane fractions of olive mill wastewater, Water Research 47(13) (2013) 4710-4718.

[107] S. Mseddi, L. Chaari, C. Belaid, I. Chakchouk, M. Kallel, Valorization of treated olive mill wastewater in fertigation practice, Environmental Science and Pollution Research 23(16) (2016) 15792-15800.

[108] L. Ioannou-Ttofa, I. Michael-Kordatou, S.C. Fattas, A. Eusebio, B. Ribeiro, M. Rusan, A.R.B. Amer, S. Zuraiqi, M. Waismand, C. Linder, Z. Wiesman, J. Gilron, D. Fatta-Kassinos, Treatment efficiency and economic feasibility of biological oxidation, membrane filtration and separation processes, and advanced oxidation for the purification and valorization of olive mill wastewater, Water Research 114 (2017) 1-13.

[109] M.J. Rusan, A.A. Albalasmeh, S. Zuraiqi, M. Bashabsheh, Evaluation of phytotoxicity effect of olive mill wastewater treated by different technologies on seed germination of barley (Hordeum vulgare L.), Environ Sci Pollut Res Int 22(12) (2015) 9127-35.

[110] C. Justino, A.G. Marques, K.R. Duarte, A.C. Duarte, R. Pereira, T. Rocha-Santos, A.C. Freitas, Degradation of phenols in olive oil mill wastewater by biological, enzymatic, and photo-Fenton oxidation, Environ Sci Pollut Res Int 17(3) (2010) 650-6.

[111] M.J. Ochando-Pulido, G. Hodaifa, D.M. Victor-Ortega, A. Martinez-Ferez, Performance Modeling and Cost Analysis of a Pilot-Scale Reverse Osmosis Process for the Final Purification of Olive Mill Wastewater, Membranes 3(4) (2013) 285-297.

[112] M.J. Ochando-Pulido, A. Martinez-Ferez, On the Recent Use of Membrane Technology for Olive Mill Wastewater Purification, Membranes 5(4) (2015) 513-581.

[113] G. Han, J.S. de Wit, T.S. Chung, Water reclamation from emulsified oily wastewater via effective forward osmosis hollow fiber membranes under the PRO mode, Water Res 81 (2015) 54-63.

[114] M. Padaki, R. Surya Murali, M.S. Abdullah, N. Misdan, A. Moslehyani, M.A. Kassim, N. Hilal, A.F. Ismail, Membrane technology enhancement in oil–water separation. A review, Desalination 357 (2015) 197-207.

[115] M.-J. Um, S.-H. Yoon, C.-H. Lee, K.-Y. Chung, J.-J. Kim, Flux enhancement with gas injection in crossflow ultrafiltration of oily wastewater, Water Research 35(17) (2001) 4095-4101.

[116] R.W. Baker, Technology and Applications, John Wiley & Sons, Ltd, Chichester, UK, 2004.

[117] D.J. Miller, D.R. Paul, B.D. Freeman, A crossflow filtration system for constant permeate flux membrane fouling characterization, Rev Sci Instrum 84(3) (2013) 3-11.

[118] P. Bacchin, P. Aimar, R.W. Field, Critical and sustainable fluxes: Theory, experiments and applications, Journal of Membrane Science 281(1–2) (2006) 42-69.

[119] R.W. Field, G.K. Pearce, Critical, sustainable and threshold fluxes for membrane filtration with water industry applications, Advances in Colloid and Interface Science 164(1–2) (2011) 38-44.

[120] S. Luque, D. Gómez, J.R. Álvarez, Industrial Applications of Porous Ceramic Membranes (Pressure-Driven Processes), Membrane Science and Technology, Elsevier2008, pp. 177-216.

[121] R. Vinoth Kumar, A. Kumar Ghoshal, G. Pugazhenthi, Elaboration of novel tubular ceramic membrane from inexpensive raw materials by extrusion method and its performance in microfiltration of synthetic oily wastewater treatment, Journal of Membrane Science 490 (2015) 92-102.

[122] C. Moulin, M.M. Bourbigot, A. Tazi-Pain, F. Bourdon, Design and performance of membrane filtration installations: Capacity and product quality for drinking water applications, Environmental Technology 12(10) (1991) 841-858.

[123] J. Zhong, X. Sun, C. Wang, Treatment of oily wastewater produced from refinery processes using flocculation and ceramic membrane filtration, Separation and Purification Technology 32(1–3) (2003) 93-98.

[124] M.C. Fraga, S. Sanches, V.J. Pereira, J.G. Crespo, L. Yuan, J. Marcher, M.V.M. de Yuso, E. Rodríguez-Castellón, J. Benavente, Morphological, chemical surface and filtration characterization of a new silicon carbide membrane, Journal of the European Ceramic Society 37(3) (2017) 899-905.

[125] C. Yang, G. Zhang, N. Xu, J. Shi, Preparation and application in oil–water separation of ZrO2/α-Al2O3 MF membrane, Journal of Membrane Science 142(2) (1998) 235-243.

[126] R. Muppalla, S.K. Jewrajka, A.V.R. Reddy, Fouling resistant nanofiltration membranes for the separation of oil–water emulsion and micropollutants from water, Separation and Purification Technology 143 (2015) 125-134.

[127] T. Rajasekhar, M. Trinadh, P. Veera Babu, A.V.S. Sainath, A.V.R. Reddy, Oil–water emulsion separation using ultrafiltration membranes based on novel blends of poly(vinylidene fluoride) and amphiphilic tri-block copolymer containing carboxylic acid functional group, Journal of Membrane Science 481 (2015) 82-93.

[128] J.M. Ochando-Pulido, M. Stoller, L. Di Palma, A. Martínez-Ferez, On the optimization of a flocculation process as fouling inhibiting pretreatment on an ultrafiltration membrane during olive mill effluents treatment, Desalination 393 (2016) 151-158.

[129] S. Sanches, M.C. Fraga, N.A. Silva, P. Nunes, J.G. Crespo, V.J. Pereira, Pilot scale nanofiltration treatment of olive mill wastewater: a technical and economical evaluation, Environmental Science and Pollution Research 24(4) (2017) 3506-3518.

[130] R.C. Martins, A.M. Ferreira, L.M. Gando-Ferreira, R.M. Quinta-Ferreira, Ozonation and ultrafiltration for the treatment of olive mill wastewaters: effect of key operating conditions and integration schemes, Environmental Science and Pollution Research 22(20) (2015) 15587-15597.

[131] H. Huang, T. A. Young, J. G. Jacangelo, Unified membrane fouling index for low pressure membrane filtration of natural waters: principles and methodology, Environmental Science & Technology 42 (2008) 714-720.

[132] J. Hermia, Constant pressure blocking filtration laws-Application to power-law non-Newtonian fluids, Transactions of Institution of Chemical Engineers 60 (1982) 183-187.

[133] A. Salahi, M. Abbasi, T. Mohammadi, Permeate flux decline during UF of oily wastewater: Experimental and modeling, Desalination 251(1–3) (2010) 153-160.

[134] J. Zhou, D. Wandera, S.M. Husson, Mechanisms and control of fouling during ultrafiltration of high strength wastewater without pretreatment, Journal of Membrane Science 488 (2015) 103-110.

[135] D. Vasanth, G. Pugazhenthi, R. Uppaluri, Cross-flow microfiltration of oil-in-water emulsions using low cost ceramic membranes, Desalination 320 (2013) 86-95.

[136] N. Amaral-Silva, R.C. Martins, S. Castro-Silva, R.M. QuintaFerreira, Integration of traditional systems and advanced oxidation process technologies for the industrial treatment of olive mill wastewaters, Environmental Technology 37 (2016) 2524-2535.

[137] I.O.O. Council, 2014. Last accessed: December 2015.

[138] A. Zirehpour, A. Rahimpour, M. Jahanshahi, The filtration performance and efficiency of olive mill wastewater treatment by integrated membrane process, Desalination and Water Treatment 53(5) (2015) 1254-1262.

[139] R. Jarboui, F. Sellami, A. Kharroubi, N. Gharsallah, E. Ammar, Olive mill wastewater stabilization in open-air ponds: Impact on clay–sandy soil, Bioresource Technology 99(16) (2008) 7699-7708.

[140] R. Jarboui, M. Chtourou, C. Azri, N. Gharsallah, E. Ammar, Time-dependent evolution of olive mill wastewater sludge organic and inorganic components and resident microbiota in multi-pond evaporation system, Bioresource Technology 101(15) (2010) 5749-5758.

[141] J.M. Ochando-Pulido, M.D. Victor-Ortega, G. Hodaifa, A. Martinez-Ferez, Physicochemical analysis and adequation of olive oil mill wastewater after advanced oxidation process for reclamation by pressure-driven membrane technology, Science of the Total Environment 503 (2015) 113-121.

[142] I. Karaouzas, N.T. Skoulikidis, U. Giannakou, T.A. Albanis, Spatial and temporal effects of olive mill wastewaters to stream macroinvertebrates and aquatic ecosystems status, Water Research 45(19) (2011) 6334-6346.

[143] M. Asfi, G. Ouzounidou, S. Panajiotidis, I. Therios, M. Moustakas, Toxicity effects of olive-mill wastewater on growth, photosynthesis and pollen morphology of spinach plants, Ecotoxicology and Environmental Safety 80 (2012) 69-75.

[144] D. Daassi, L. Belbahri, A. Vallat, S. Woodward, M. Nasri, T. Mechichi, Enhanced reduction of phenol content and toxicity in olive mill wastewaters by a newly isolated strain of Coriolopsis gallica, Environmental Science and Pollution Research 21(3) (2014) 1746-1758.

[145] B. Kiril Mert, T. Yonar, M. Yalili Kilic, K. Kestioglu, Pre-treatment studies on olive oil mill effluent using physicochemical, Fenton and Fenton-like oxidations processes, Journal of hazardous materials 174(1-3) (2010) 122-8.

[146] J.M. Ochando-Pulido, G. Hodaifa, A. Martinez-Ferez, Fouling inhibition upon Fenton-like oxidation pretreatment for olive mill wastewater reclamation by membrane process, Chemical Engineering and Processing 62 (2012) 89-98.

[147] Y. Esfandyari, Y. Mahdavi, M. Seyedsalehi, M. Hoseini, G.H. Safari, M.G. Ghozikali, H. Kamani, J. Jaafari, Degradation and biodegradability improvement of the olive mill wastewater by

peroxi-electrocoagulation/electrooxidation-electroflotation process with bipolar aluminum electrodes, Environmental Science and Pollution Research 22(8) (2015) 6288-6297.

[148] A. Ginos, T. Manios, D. Mantzavinos, Treatment of olive mill effluents by coagulation-flocculation-hydrogen peroxide oxidation and effect on phytotoxicity, Journal of Hazardous Materials 133(1-3) (2006) 135-142.

[149] S. Khoufi, F. Feki, S. Sayadi, Detoxification of olive mill wastewater by electrocoagulation and sedimentation processes, Journal of Hazardous Materials 142(1-2) (2007) 58-67.

[150] A. Zirehpour, M. Jahanshahi, A. Rahimpour, Unique membrane process integration for olive oil mill wastewater purification, Separation and Purification Technology 96 (2012) 124-131.

[151] D.P. Zagklis, E.C. Arvaniti, V.P. Papadakis, C.A. Paraskeva, Sustainability analysis and benchmarking of olive mill wastewater treatment methods, Journal of Chemical Technology and Biotechnology 88(5) (2013) 742-750.

[152] K.S. Ashaghi, M. Ebrahimi, P. Czermak, Ceramic ultra- and nanofiltration membranes for oilfield produced water treatment: A mini review, The Open Environmental Journal 1 (2007) 1-8.

[153] C. Russo, A new membrane process for the selective fractionation and total recovery of polyphenols, water and organic substances from vegetation waters (VW), Journal of Membrane Science 288(1-2) (2007) 239-246.

[154] N. Kalogerakis, M. Politi, S. Foteinis, E. Chatzisymeon, D. Mantzavinos, Recovery of antioxidants from olive mill wastewaters: A viable solution that promotes their overall sustainable management, Journal of Environmental Management 128 (2013) 749-758.

[155] M.L.d.M. Ponte , N. da, J.L.C.d. Santos , A.A.F. Matias , A.V.M.M. Nunes , Crespo , J.P.S. Goulão, C.M.M. Duarte Method of obtaining a natural hydroxytyrosol-rich concentrate from olive tree residues and subproducts using clean technologies, 2008. Patent US8066881B2

[156] C. Russo, A new membrane process for the selective fractionation and total recovery of polyphenols, water and organic substances from vegetation waters (VW), Journal of Membrane Science 288(1–2) (2007) 239-246.

[157] T. Coskun, E. Debik, N.M. Demir, Treatment of olive mill wastewaters by nanofiltration and reverse osmosis membranes, Desalination 259(1-3) (2010) 65-70.

[158] M. Stoller, Effective fouling inhibition by critical flux based optimization methods on a NF membrane module for olive mill wastewater treatment, Chemical Engineering Journal 168(3) (2011) 1140-1148.

[159] M. Ebrahimi, D. Willershausen, K.S. Ashaghi, L. Engel, L. Placido, P. Mund, P. Bolduan, P. Czermak, Investigations on the use of different ceramic membranes for efficient oil-field produced water treatment, Desalination 250(3) (2010) 991-996.

[160] M. Cakmakci, N. Kayaalp, I. Koyuncu, Desalination of produced water from oil production fields by membrane processes, Desalination 222(1-3) (2008) 176-186.

[161] R. Tomczak-Wandzel , M. Fraga, S. Sanches, V. Pereira, E. Vik, J. Crespo, P. Wilinski, An integrated membrane process for oily wastewater treatment, water reuse and valuable by-products recovery – DAF Nikuni unit presentation, 23rd International Fair of Machines and Facilities for Water Supply and Sewage Systems WOD-KAN 2015, Bydgoszcz, Poland, 26-28 May 2015.

[162] J.D. Box, Investigation of the Folin—Ciocalteu phenol reagent for the determination of polyphenolic substances in natural waters, Water Research 17(5) (1983) 511-525.

[163] C. Fersi, L. Gzara, M. Dhahbi, Treatment of textile effluents by membrane technologies, Desalination 185(1–3) (2005) 399-409.

[164] I. Leouifoudi, A. Zyad, A. Amechrouq, M.A. Oukerrou, H.A. Mouse, M. Mbarki, Identification and characterisation of phenolic compounds extracted from Moroccan olive mill wastewater, Food Science and Technology 34 (2014) 249-257.

[165] J.M.O. Pulido, A.M. Ferez, Impacts of operating conditions on nanofiltration of secondary-treated two-phase olive mill wastewater, Journal of Environmental Management 161 (2015) 219-227.

[166] H.Y. Ng, M. Elimelech, Influence of colloidal fouling on rejection of trace organic contaminants by reverse osmosis, Journal of Membrane Science 244(1–2) (2004) 215-226.

[167] L.D. Nghiem, A.I. Schäfer, M. Elimelech, Removal of Natural Hormones by Nanofiltration Membranes: Measurement, Modeling, and Mechanisms, Environmental Science & Technology 38(6) (2004) 1888-1896.

[168] K. Kestioglu, T. Yonar, N. Azbar, Feasibility of physico-chemical treatment and Advanced Oxidation Processes (AOPs) as a means of pretreatment of olive mill effluent (OME), Process Biochemistry 40(7) (2005) 2409-2416.

[169] 91/271/EEC, Council Directive of 21 May 1991concernig urban waste water treatment (91/271/EEC).

[170] C.M. Kalua, M.S. Allen, D.R. Bedgood, Jr., A.G. Bishop, P.D. Prenzler, K. Robards, Olive oil volatile compounds, flavour development and quality: A critical review, Food Chemistry 100(1) (2007) 273-286.

[171] F. Angerosa, Influence of volatile compounds on virgin olive oil quality evaluated by analytical approaches and sensor panels, European Journal of Lipid Science and Technology 104(9-10) (2002) 639-660.

[172] S. Kesen, H. Kelebek, S. Selli, Characterization of the Volatile, Phenolic and Antioxidant Properties of Monovarietal Olive Oil Obtained from cv. Halhali, Journal of the American Oil Chemists Society 90(11) (2013) 1685-1696.

[173] S.A. Vekiari, V. Oreopoulou, Y. Kourkoutas, N. Kamoun, M. Msallem, V. Psimouli, D. Arapoglou, Characterization and seasonal variation of the quality of virgin olive oil of the Throu mbolia and Koroneiki varieties from Southern Greece, Grasas Y aceites, 2010, pp. 221-231.

[174] R.C. Martins, A.M.T. Silva, S. Castro-Silva, P. Garcao-Nunes, R.M. Quinta-Ferreira, Adopting strategies to improve the efficiency of ozonation in the real-scale treatment of olive oil mill wastewaters, Environmental Technology 31(13) (2010) 1459-1469.

[175] J.M. Ochando-Pulido, G. Hodaifa, M.D. Victor-Ortega, S. Rodriguez-Vives, A. Martinez-Ferez, Reuse of olive mill effluents from two-phase extraction process by integrated advanced oxidation and reverse osmosis treatment, Journal of Hazardous Materials 263 (2013) 158-167.

[176]Eurostat,http://ec.europa.eu/eurostat/tgm/table.do?tab=table&init=1&plugin=1&pcode=ten00117&language=en.

[177] ASAJA-Jaén, https://www.asajajaen.com/urgente/nuevas-tablas-salariales-parala-campana-2015-2016., 2016.

[178] M. Molinos-Senante, F. Hernandez-Sancho, R. Sala-Garrido, Cost modeling for sludge and waste management from wastewater treatment plants: an empirical approach for Spain, Desalination and Water Treatment 51(28-30) (2013) 5414-5420.

[179] R.P. Schwarzenbach, T. Egli, T.B. Hofstetter, U. von Gunten, B. Wehrli, Global Water Pollution and Human Health, Annual Review of Environment and Resources 35(1) (2010) 109-136.

[180] A. Pal, K.Y.-H. Gin, A.Y.-C. Lin, M. Reinhard, Impacts of emerging organic contaminants on freshwater resources: Review of recent occurrences, sources, fate and effects, Science of The Total Environment 408(24) (2010) 6062-6069.

[181] W.F. Jardim, C.C. Montagner, I.C. Pescara, G.A. Umbuzeiro, A.M. Di Dea Bergamasco, M.L. Eldridge, F.F. Sodré, An integrated approach to evaluate emerging contaminants in drinking water, Separation and Purification Technology 84 (2012) 3-8.

[182] H. Choi, S.R. Al-Abed, D.D. Dionysiou, E. Stathatos, P. Lianos, Chapter 8 TiO2-Based Advanced Oxidation Nanotechnologies for Water Purification and Reuse, in: I.C. Escobar, A.I. Schäfer (Eds.), Sustainability Science and Engineering, Elsevier2010, pp. 229-254.

[183] Y. Zhou, M. Fukushima, H. Miyazaki, Y.-i. Yoshizawa, K. Hirao, Y. Iwamoto, K. Sato, Preparation and characterization of tubular porous silicon carbide membrane supports, Journal of Membrane Science 369(1–2) (2011) 112-118.

[184] R.S. Faibish, Y. Cohen, Fouling and rejection behavior of ceramic and polymer-modified ceramic membranes for ultrafiltration of oil-in-water emulsions and microemulsions, Colloids and Surfaces A: Physicochemical and Engineering Aspects 191(1–2) (2001) 27-40.

[185] A. Lee, J.W. Elam, S.B. Darling, Membrane materials for water purification: design, development, and application, Environmental Science: Water Research & Technology 2(1) (2016) 17-42.

[186] P. de Wit, E.J. Kappert, T. Lohaus, M. Wessling, A. Nijmeijer, N.E. Benes, Highly permeable and mechanically robust silicon carbide hollow fiber membranes, Journal of Membrane Science 475 (2015) 480-487.

[187] M. Facciotti, V. Boffa, G. Magnacca, L.B. Jørgensen, P.K. Kristensen, A. Farsi, K. König, M.L. Christensen, Y. Yue, Deposition of thin ultrafiltration membranes on commercial SiC microfiltration tubes, Ceramics International 40(2) (2014) 3277-3285.

[188] A. Alem, H. Sarpoolaky, M. Keshmiri, Sol–gel preparation of titania multilayer membrane for photocatalytic applications, Ceramics International 35(5) (2009) 1837-1843.

[189] A. Alem, H. Sarpoolaky, M. Keshmiri, Titania ultrafiltration membrane: Preparation, characterization and photocatalytic activity, Journal of the European Ceramic Society 29(4) (2009) 629-635.

[190] L. Djafer, A. Ayral, A. Ouagued, Robust synthesis and performance of a titania-based ultrafiltration membrane with photocatalytic properties, Separation and Purification Technology 75(2) (2010) 198-203.

[191] H. Zhang, X. Quan, S. Chen, H. Zhao, Y. Zhao, Fabrication of photocatalytic membrane and evaluation its efficiency in removal of organic pollutants from water, Separation and Purification Technology 50(2) (2006) 147-155.

[192] N. Ma, X. Quan, Y. Zhang, S. Chen, H. Zhao, Integration of separation and photocatalysis using an inorganic membrane modified with Si-doped TiO2 for water purification, Journal of Membrane Science 335(1–2) (2009) 58-67.

[193] V.S. Smitha, K.A. Manjumol, K.V. Baiju, S. Ghosh, P. Perumal, K.G.K. Warrier, Sol–gel route to synthesize titania-silica nano precursors for photoactive particulates and coatings, Journal of Sol-Gel Science and Technology 54(2) (2010) 203-211.

[194] R. Fateh, R. Dillert, D. Bahnemann, Preparation and Characterization of Transparent Hydrophilic Photocatalytic TiO2/SiO2 Thin Films on Polycarbonate, Langmuir 29(11) (2013) 3730-3739.

[195] K. Guan, Relationship between photocatalytic activity, hydrophilicity and self-cleaning effect of TiO2/SiO2 films, Surface and Coatings Technology 191(2–3) (2005) 155-160.

[196] H. Choi, E. Stathatos, D.D. Dionysiou, Sol–gel preparation of mesoporous photocatalytic TiO2 films and TiO2/Al2O3 composite membranes for environmental applications, Applied Catalysis B: Environmental 63(1–2) (2006) 60-67.

[197] H. Choi, A.C. Sofranko, D.D. Dionysiou, Nanocrystalline TiO2 Photocatalytic Membranes with a Hierarchical Mesoporous Multilayer Structure: Synthesis, Characterization, and Multifunction, Advanced Functional Materials 16(8) (2006) 1067-1074.

[198] V. Gitis, G. Rothenberg, V.C.H. Wiley, Ceramic Membranes New Opportunities and Practical Applications, 2016.

[199] L.Y. W. Zhou, Y. Wang, Y. Zhang, SiC nanowires: A photocatalytic nanomaterial, Appl. Phys. Lett. 89 (2006) 1-3.

[200] M.D. Abramoff, Magalhaes, P.J., Ram, S.J., Image Processing with ImageJ, Biophotonics International 11(7) (2004) 36-42.

[201] I. Masselin, L. Durand-Bourlier, J.-M. Laine, P.-Y. Sizaret, X. Chasseray, D. Lemordant, Membrane characterization using microscopic image analysis, Journal of Membrane Science 186(1) (2001) 85-96.

[202] L.Y. W. Zhou, Y. Wang, Y. Zhang, SiC nanowires: A photocatalytic nanomaterial, Appl. Phys. Lett. 89 (2006) 1-3.

[203] C. Gómez-Solís, I. Juárez-Ramírez, E. Moctezuma, L.M. Torres-Martínez, Photodegradation of indigo carmine and methylene blue dyes in aqueous solution by SiC–TiO2 catalysts prepared by sol–gel, Journal of Hazardous Materials 217–218 (2012) 194-199.

[204] L. Andronic, D. Perniu, A. Duta, Synergistic effect between TiO2 sol–gel and Degussa P25 in dye photodegradation, Journal of Sol-Gel Science and Technology 66(3) (2013) 472-480.

[205] L. Zhou, S. Yan, B. Tian, J. Zhang, M. Anpo, Preparation of TiO2–SiO2 film with high photocatalytic activity on PET substrate, Materials Letters 60(3) (2006) 396-399.

[206] K. Fischer, M. Grimm, J. Meyers, C. Dietrich, R. Gläser, A. Schulze, Photoactive microfiltration membranes via directed synthesis of TiO2 nanoparticles on the polymer surface for removal of drugs from water, Journal of Membrane Science 478 (2015) 49-57.

[207] L.F.F. T. G. Cooney, Processing of sol-gel derived PZT coatings on non-planar substrates, J. Micromech. Microeng 6 (1996) 291–300.

[208] L. Liu, D.K. Wang, D.L. Martens, S. Smart, J.C. Diniz da Costa, Interlayer-free microporous cobalt oxide silica membranes via silica seeding sol–gel technique, Journal of Membrane Science 492 (2015) 1-8.

[209] C. Vladuta, L. Andronic, M. Visa, A. Duta, Ceramic interface properties evaluation based on contact angle measurement, Surface and Coatings Technology 202(11) (2008) 2448-2452.

[210] J.M. Ochando-Pulido, S. Pimentel-Moral, V. Verardo, A. Martinez-Ferez, A focus on advanced physico-chemical processes for olive mill wastewater treatment, Separation and Purification Technology 179 (2017) 161-174.

[211] C.M. Fraga, S. Sanches, G.J. Crespo, J.V. Pereira, Assessment of a New Silicon Carbide Tubular Honeycomb Membrane for Treatment of Olive Mill Wastewaters, Membranes 7(1) (2017).

[212] Y. Chen, B.Z. Dong, N.Y. Gao, J.C. Fan, Effect of coagulation pretreatment on fouling of an ultrafiltration membrane, Desalination 204(1) (2007) 181-188.

[213] S.S. Yoo, K.H. Chu, I.-H. Choi, J.S. Mang, K.B. Ko, Operating cost reduction of UF membrane filtration process for drinking water treatment attributed to chemical cleaning optimization, Journal of Environmental Management 206 (2018) 1126-1134.

[214] I. Kovács, G. Veréb, S. Kertész, C. Hodúr, Z. László, Fouling mitigation and cleanability of TiO2 photocatalyst-modified PVDF membranes during ultrafiltration of model oily wastewater with different salt contents, Environmental Science and Pollution Research (2017).

[215] A. Wold, Photocatalytic properties of titanium dioxide (TiO2), Chemistry of Materials 5(3) (1993) 280-283.

[216] R.A. Damodar, S.-J. You, S.-H. Ou, Coupling of membrane separation with photocatalytic slurry reactor for advanced dye wastewater treatment, Separation and Purification Technology 76(1) (2010) 64-71.

[217] R.M. Huertas, M.C. Fraga, J.G. Crespo, V.J. Pereira, Sol-gel membrane modification for enhanced photocatalytic activity, Separation and Purification Technology 180 (2017) 69-81.

[218] V.L. Singleton, R. Orthofer, R.M. Lamuela-Raventós, Analysis of total phenols and other oxidation substrates and antioxidants by means of folin-ciocalteu reagent, Methods in Enzymology, Academic Press1999, pp. 152-178.

[219] F. Angerosa, Influence of volatile compounds on virgin olive oil quality evaluated by analytical approaches and sensor panels, European Journal of Lipid Science and Technology 104(9-10) (2002) 639-660.

[220] N. Sabatini, V. Marsilio, Volatile compounds in table olives (Olea Europaea L., Nocellara del Belice cultivar), Food Chemistry 107(4) (2008) 1522-1528.

[221] S.B. Kim, S.C. Hong, Kinetic study for photocatalytic degradation of volatile organic compounds in air using thin film TiO2 photocatalyst, Applied Catalysis B: Environmental 35(4) (2002) 305-315.

[222] D.S. Selishchev, N.S. Kolobov, A.A. Pershin, D.V. Kozlov, TiO2 mediated photocatalytic oxidation of volatile organic compounds: Formation of CO as a harmful by-product, Applied Catalysis B: Environmental 200 (2017) 503-513.

[223] R.M. Huertas, M.C. Fraga, D. Nunes, E. Fortunato, J.G. Crespo, P.V. J., Environmental Friendly Production of Ceramic Membranes with Photocatalytic Activity, Submited to Journal of the European Ceramic Society (2018).

A1 SUPPORTING INFORMATION

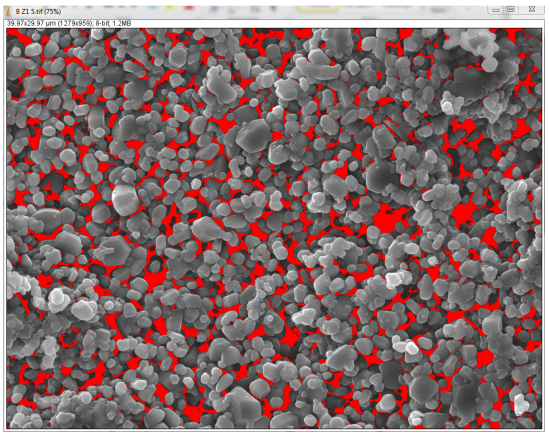

Figure A1.1 *Image J analysis of SEM for top view of control membrane and zone 1 (Z_1) – (×3000 magnification) and threshold 35 (defined cut off point); Porosity 10.1%*

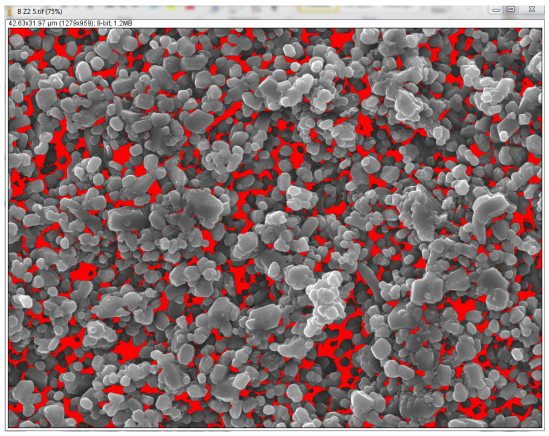

Figure A1.2 *Image J analysis of SEM for top view of control membrane and zone 2 (Z_2) – (×3000 magnification), Threshold 35; Porosity 11.0%*

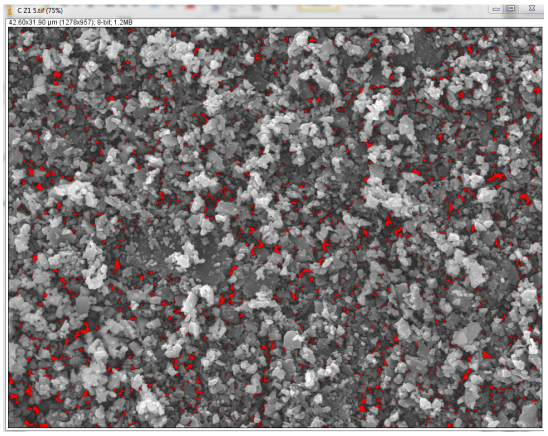

Figure A1.3 *Image J analysis of SEM for top view of SiC/Control membrane and zone 1 (Z_1) – (×3000 magnification), Threshold 35; Porosity 2.4%.*

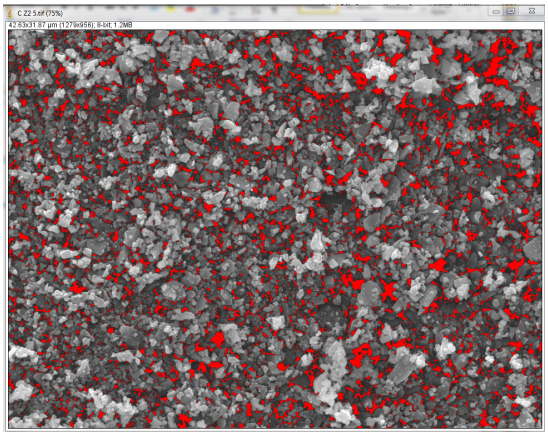

Figure A1.4 *Image J analysis of SEM for top view of SiC/Control membrane and zone 2 (Z_2) – (×3000 magnification), Threshold 35; Porosity 9.4%.*

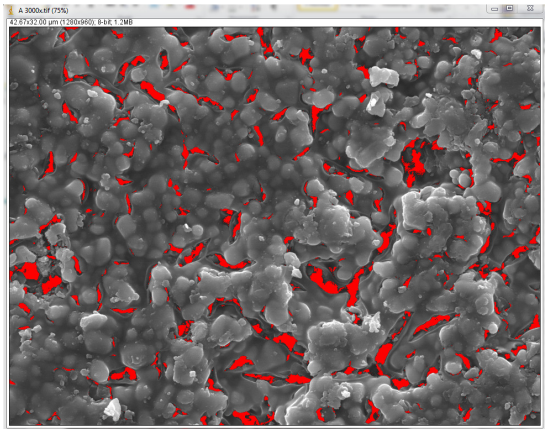

Figure A1.5 *Image J analysis of SEM for top view of SGTi 1.5 (L_3) membrane and zone 1 (Z_1) – (×3000 magnification), Threshold 35; Porosity 4.8%.*

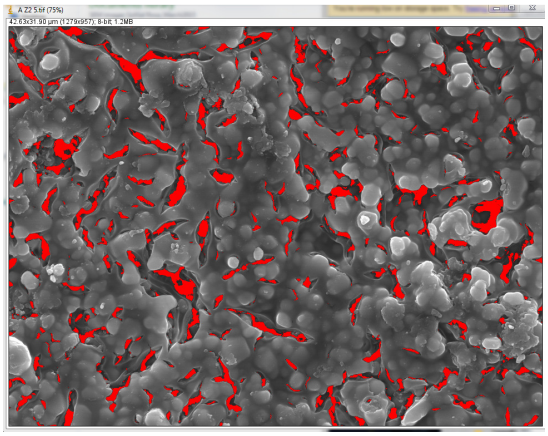

Figure A1.6 *Image J analysis of SEM for top view of SGTi 1.5 (L_3) membrane and zone 2 (Z_2) (×3000 magnification), Threshold 35; Porosity 6.5%.*

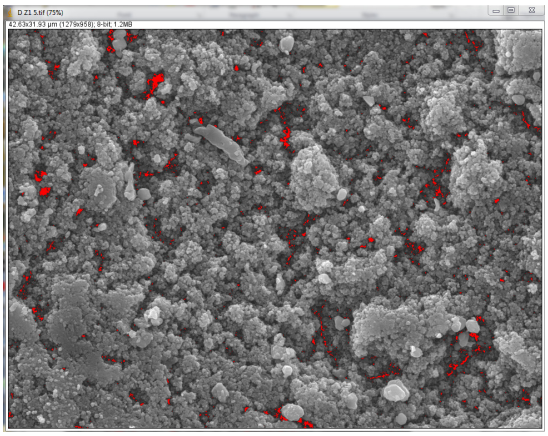

Figure A1.7 *Image J analysis of SEM for top view of SiC/SGTi 0.5-D1 (L_3) membrane and zone 1 (Z_1) (×3000 magnification), Threshold 35; Porosity 0.9%*

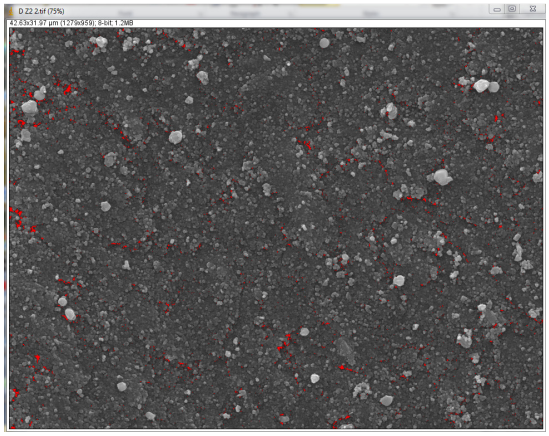

Figure A1.8 *Image J analysis of SEM for top view of SiC/SGTi 0.5-D1 (L_3) membrane and zone 2 (Z_2) (×3000 magnification), Threshold 35; Porosity 0.7%.*

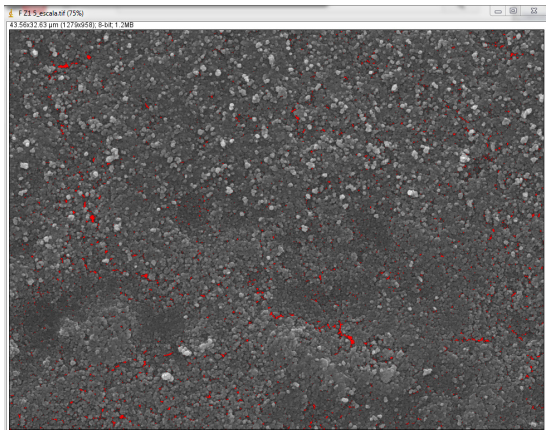

Figure A1.9 *Image J analysis of SEM for top view of SGSi-D (L_3) membrane and zone 1 (Z_1) (×3000 magnification), Threshold 35; Porosity0.9%*

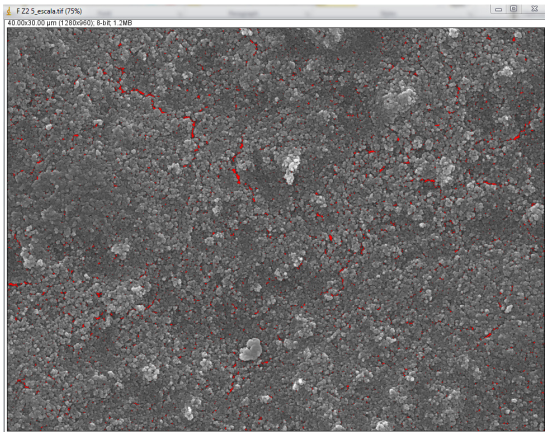

Figure A1.10 *Image J analysis of SEM for top view of SGSi-D(L_3) membrane and zone 2 (Z_2) (×3000 magnification)F – Z_2 – ×3000, Threshold 35; Porosity0.9%*

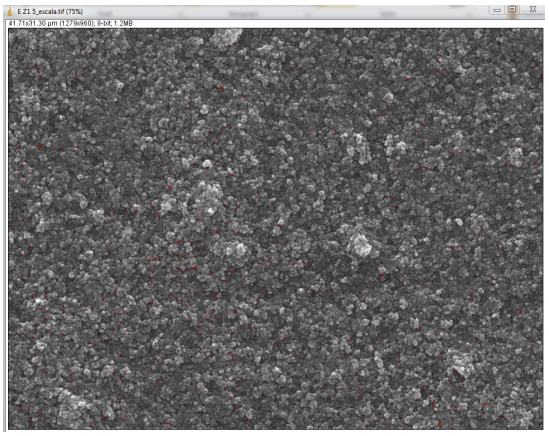

Figure A1.11 *Image J analysis of SEM for top view of SGTi 0.5-D1 (L_3) membrane and zone 1 (Z_1) (×3000 magnification); Threshold 35; Porosity0.3%.*

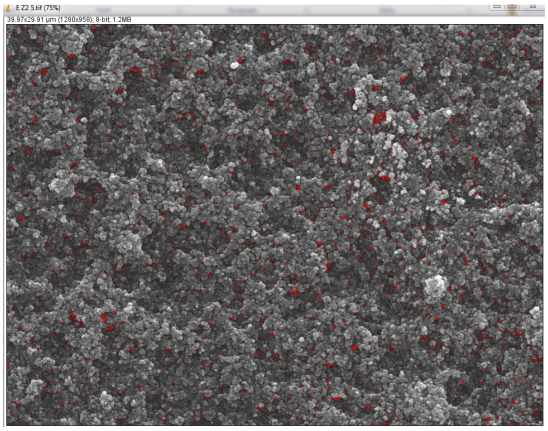

Figure A1.12 *Image J analysis of SEM for top view of SGTi 0.5-D1(L_3) membrane and zone 2 (Z_2) (×3000 magnification),Threshold 35; Porosity1.2%.*

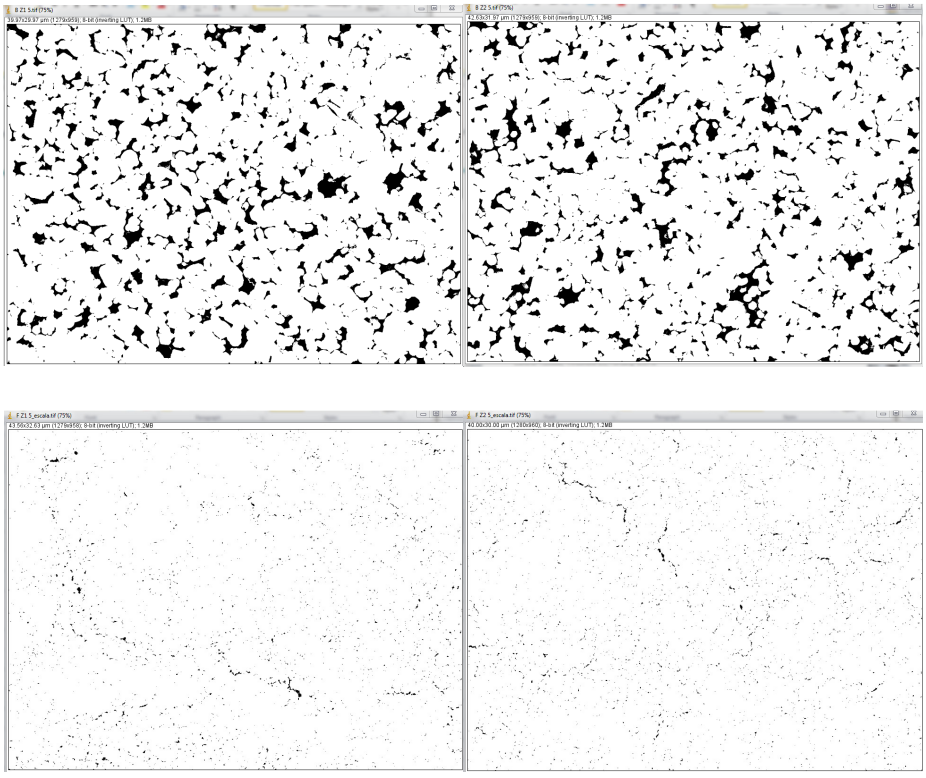

Figure A1.*13 Binary images using Image J analysis of zone1 (left) and zone 2 (right) for control (up) versus SGSi-D(L3)(down) membranes.*

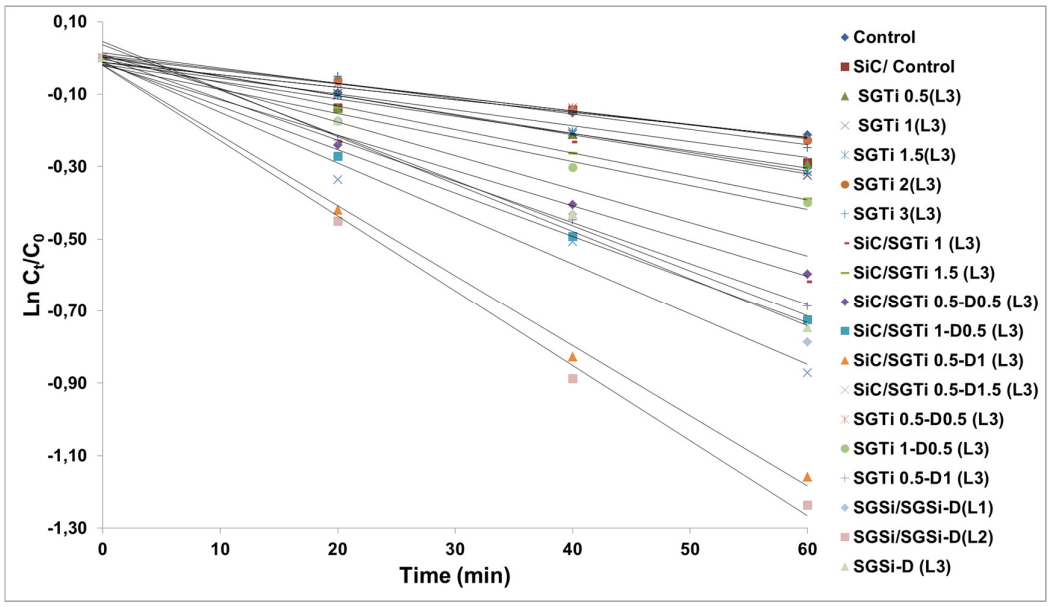

Figure A1.14. *Pseudo-first-order kinetics for the degradation of methylene blue.*

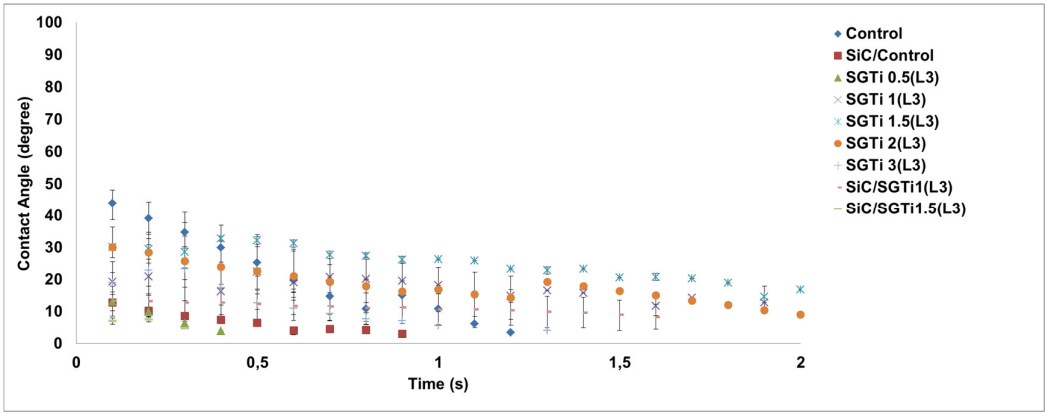

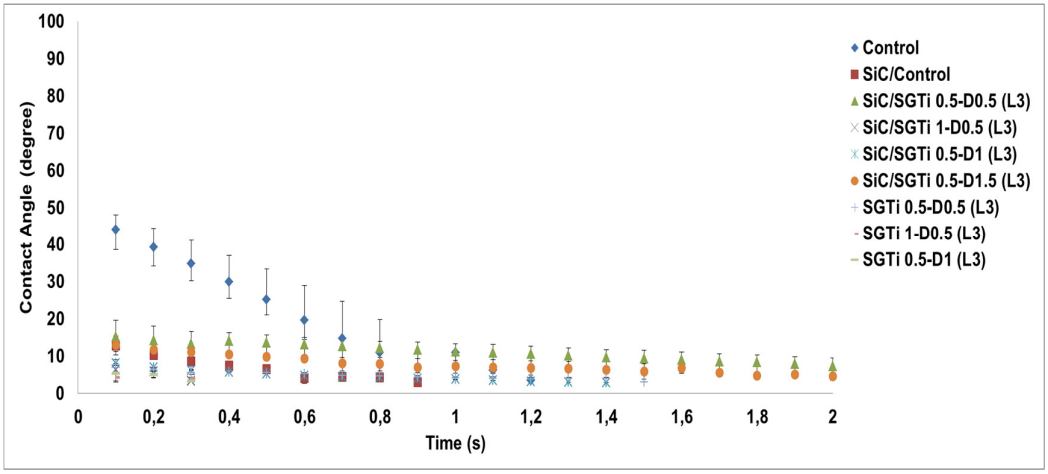

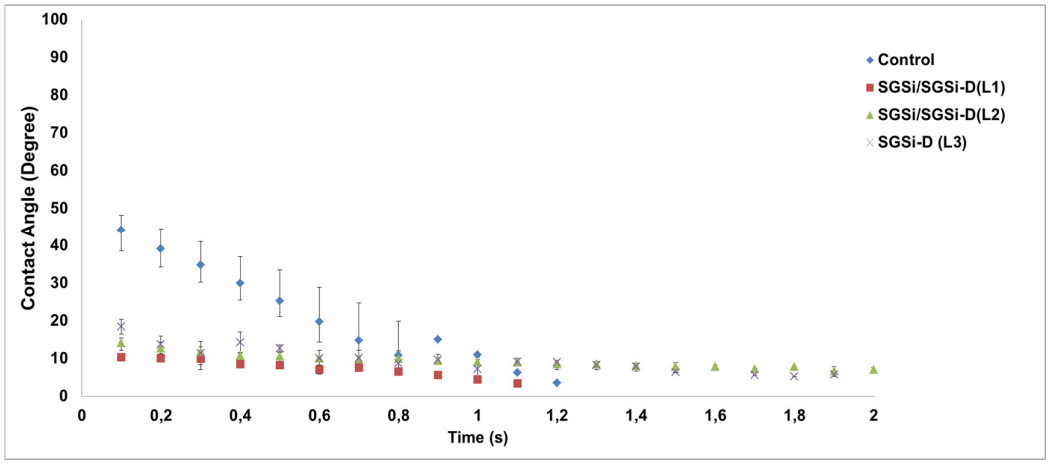

Figure A1.15 *Comparison of the time course of water contact angle for control and modified substrates.*

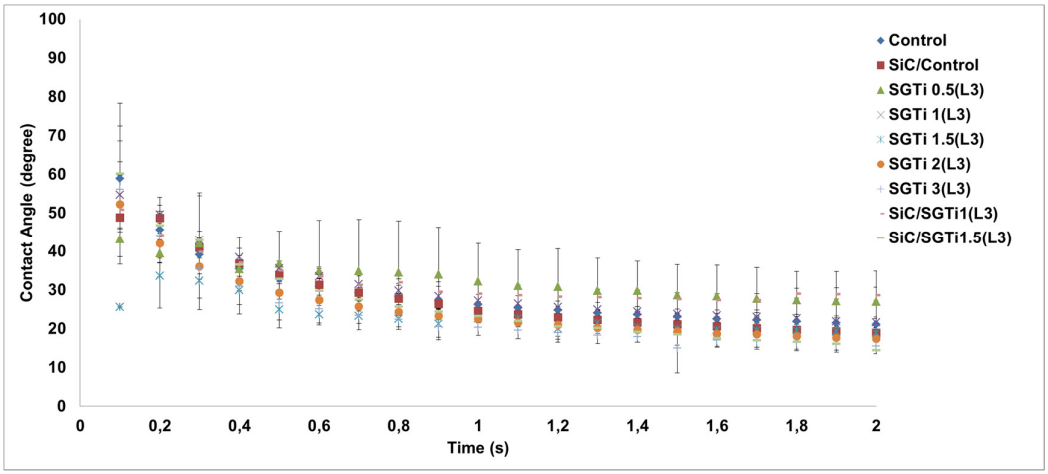
Contact Angle (degree)
Time (s)
Control
SiC/Control
SGTi 0.5(L3)
SGTi 1(L3)
SGTi 1.5(L3)
SGTi 2(L3)
SGTi 3(L3)
SiC/SGTi1(L3)
SiC/SGTi1.5(L3)

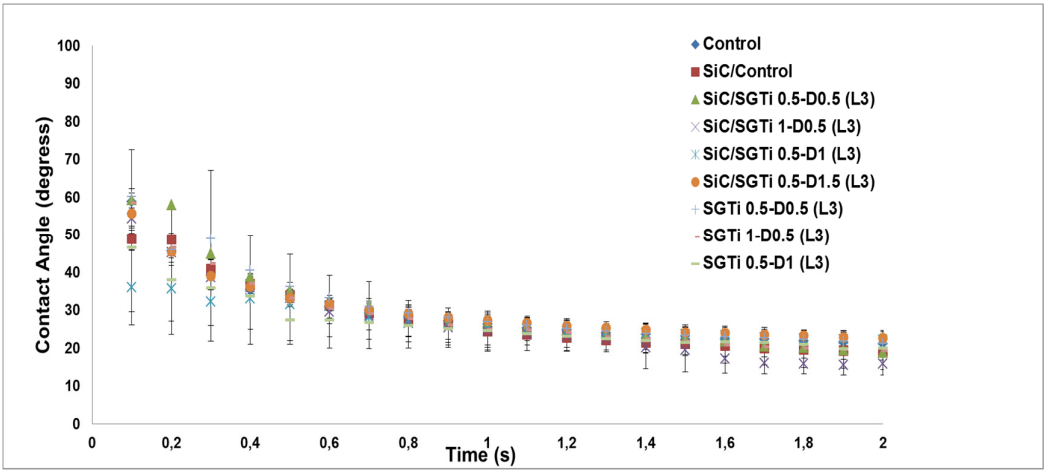
Contact Angle (degress)
Time (s)
Control
SiC/Control
SiC/SGTi 0.5-D0.5 (L3)
SiC/SGTi 1-D0.5 (L3)
SiC/SGTi 0.5-D1 (L3)
SiC/SGTi 0.5-D1.5 (L3)
SGTi 0.5-D0.5 (L3)
SGTi 1-D0.5 (L3)
SGTi 0.5-D1 (L3)

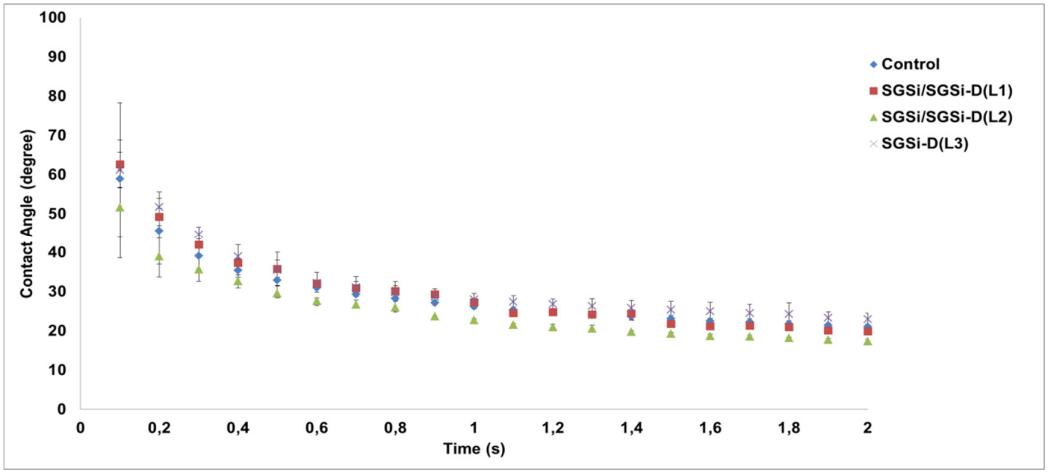

Figure A1.16 *Comparison of the time course of rapeseed oil contact angle for control and modified substrates.*